HYDRATION OF BINARY AND TERTIARY FLY ASH AND QUICKLIME BLENDED CEMENT PASTE SYSTEM

by

Akpovona Maurice Ojaruega

A thesis submitted to the faculty of
The University of North Carolina at Charlotte
in partial fulfillment of the requirements
for the degree of Master of Science in
Civil and Environmental Engineering

Charlotte

2018

Approved by:

_____
Dr. Vincent Ogunro

_____
Dr. Brett Tempest

_____
Dr. Tara Cavalline

ABSTRACT

AKPOVONA MAURICE OJARUEGA. Hydration of Binary and Tertiary Fly ash
and Quicklime Blended Cement Paste System (Under the direction of
DR. VINCENT OGUNRO)

The hydration kinetics in blended cementitious systems with fly ash are quite different from those in conventional cementitious systems. The pozzolanic nature of fly ash not only reduces the rate of hydration in cement-fly ash blends, but also reacts with hydrates from cement hydration to form additional calcium silicate/aluminate hydrates. Depending on the cement content and the reactivity level of the fly ash, the pozzolanic reaction could be a fairly slow process compared to straight Portland cementitious systems.

This study investigates the hydration kinetics of cement-fly ash-quicklime blended paste at 3 distinct fly ash replacement levels of 20%, 40% and 95% to determine their suitability for engineering applications. Two sets of cement-fly ash blends were studied in this work, one set of cement-fly ash blended pastes with quicklime and the second set without quicklime. Since the siliceous minerals in fly ash react with the $Ca(OH)_2$ produced during hydration of cement, the inclusion of quicklime was to provide this additional $Ca(OH)_2$ to aid the fly ash pozzolanic hydration reactions. Additional water was also used in two sets of fly ash replacement of 20% and 95% to account for moisture consumed during hydration of quicklime (CaO to $Ca(OH)_2$) reaction and to test the effect of quicklime slaking on hydration in cement-fly ash blended paste with moderate and high fly ash replacement levels. The thermogravimetric analysis (TGA) was used in assessing the degree of hydration for all paste mixes in this study at curing intervals of 3,7, 28 and 180 days.

TGA results indicated an additional increase in hydration for all cement-fly ash blended pastes with quicklime compared to those without quicklime, at the end of the 180-day curing period with the effect of quicklime being most significant in mixes with high fly ash replacement levels. Although for the high-volume fly ash of 95% replacement cement blended paste, the effect of additional water increased the overall hydration by an additional 40% in the slaked mix, indicating the potential of quicklime slaking as a technique for increasing pozzolanic hydration reactions in applications where high fly ash contents are desired. However, TGA measurements also indicate that increased weight which correlates degree of hydration in fly ash cement blended paste could be as a result of the formation of AFm and AFt phases and not necessarily hydration products like calcium silicate/aluminate hydrates. Pearson ANOVA analysis showed a correlation of 0.718 between the calcium silicate/aluminate hydrates and the compressive strength for cement-fly ash blended paste with fly ash replacement of 0%, 20% and 40%. The ANOVA analysis resulted in a correlation of 0.8049 between compressive strength and DTG peak. The DTG peak values for most of the paste values were established at temperatures within 90 to 100 $^{\circ}$C. Which were slightly less than the initial decomposition temperature of 105°C for calcium silicate and aluminate hydrates. It is possible that this correlation was established due to a portion of the calcium silicate and aluminate hydrate mineral phases decomposing at temperatures lower than 105°C.

ACKNOWLEDGEMENT

I would like to acknowledge several individuals for their contributions to this work. I am very thankful to my advisor and friend Dr. Vincent Ogunro for his patience, support and mentorship throughout my studies. My gratitude goes to other members of my committee Dr. Brett Tempest P.E. and Dr. Tara Cavalline, P.E. for their understanding, guidance and constant support during the course of this work. I would like to thank Dr. Katherine Weaver for all her help during the TGA experiments at the Energy Prodcution and Infrastructure Center (EPIC) Material Characterization Laboratory (MCL). I would also like to thank the Electric Power Research Institute (EPRI) for providing partial funding for my research and special thanks to Kirk Ellison, Technical leader, Generation, EPRI for his assistance throughout the duration of this project.

My sincere appreciation to thank Abhishek Manikonda for always listening to me rant and for always being there to lend a helping hand whenever I needed one. Special thanks to the Wolves of EPIC, Livingstone Dumenu, Manohar Seetharamu, Vivek Francis and Rui He for making the past two years full of fun and good memories.

I would like to thank my parents and my siblings for all their gentle encouragement over the years and for always believing in me. A special thank you to Dr. Tanure Ojaide NNOM, for his steadfast support.

TABLE OF CONTENTS

LIST OF TABLES

LIST OF FIGURES

CHAPTER 1 INTRODUCTION

1.1 Background and Significance

With millions of tons of fly ash currently in storage and about 111.3 million tons being produced in the United States in 2017 only from energy generation by coal combustion, proper and sustainable management of this waste material has remained a challenging issue. Despite significant efforts and resources invested in the beneficial use of fly ash in construction industry, fly ash beneficial reuse still does not match its generation. Fly ash is generally used as a partial replacement for ordinary Portland cement (OPC) in concrete production to improve targeted characteristics of the concrete for which it was designed. However, use of high volumes of fly ash in concrete has both the potential to slow the rate and limit the attainment of strength gained hence replacement levels of fly ash are usually restricted in construction. Compared to ordinary Portland cement concrete, blended cements, like those containing fly ash and other additives in the right proportions, have proven to be more resistant to sulphate attack due to decreased permeability, increased water to cement (w/c) ratio and lower calcium hydroxide content (Moffatt et al. (2017).

Hydration kinetics in straight cementitious systems (not containing fly ash or other supplemental cementitious materials) are well characterized with simple and accurate standard methods being used to correlate early microscopic characteristics of cement paste hydrations to its macro properties. Enabling the prediction of characteristics and suitability of straight cement concrete for the purpose it is intended. The rate of hydration could either be monitored directly by microscopic analysis of the hydrated minerals or by thermogravimetric measurements in straight cementitious systems and can serve as an indicator of engineering properties such as strength and permeability. However, unlike

conventional cement system the hydration kinetics for blended cement mixes are quite different and require further characterization to better understand the relationship between microscopic characteristics and its engineering applications especially in fly ash blended cementitious systems. For fly ash blended cement systems, the pozzolanic reaction between fly ash and calcium hydroxide is responsible for the formation of additional hydration products. Pozzolanic reactions are quite slow and reduce the rate of hydration as the fly ash replacement levels are increased and require adequate moisture to continue hydration reactions. This study supplements previous studies conducted by NCDOT researchers at the University of North Carolina at Charlotte (UNC Charlotte) on the use of internal curing aggregates which supply internal moisture for hydration goal of improving the mechanical properties of bridge deck concretes containing moderate fly ash replacements.

With adequate understanding of hydration kinetics in wide range of fly ash replacement paste matrixes, the microscopic characteristics of the hydrating system can possibly be correlated to engineering properties and mineral solubility constants used in design of structural components and containments encapsulation potential. The goal of this study is to generate data contributing to better understanding the hydration process in cementitious systems of fly ash blended cement paste containing various fly ash replacement levels and investigate changes in hydration phases. The idea is to extend studies of hydration process typical in blended cement concrete to high volume fly ash cement or quicklime paste. Possible application of this high-volume cementitious paste hydration study to include sequestration of flue gas desulphurized waste water in fly ash and quicklime paste that is pump-able, easy to handle and capable of gaining adequate strength and produce sTable mineral phases with time. It is important to properly

characterize hydration kinetics using accepted methods, hence the approach adopted by this study is to properly understand the hydration kinetics using the well-known system of cement/fly ash paste blends and determine if these standard methods for characterizing hydration kinetics are applicable to these quicklime blended paste systems.

1.2 Objectives and Scope

This research aims to provide a better understanding of the hydration kinetics in normal and high-volume replacement ranges of fly ash in cement paste blends in the presence of quicklime (CaO) cured under sealed conditions. Sealed curing conditions were adopted in this study to properly understand the effect of internal curing on hydration and also maintain an enclosed system preventing desiccation. This study will provide useful information from experiments on both the rate of hydration due to the pozzolanic reaction of fly ash at different replacement levels, effect of additional water on hydration, the effect of quicklime amended paste and the effect of both slaked lime and non-slaked quicklime while testing thermogravimetric analysis as a suiTable hydration monitoring technique for these sets of cementitious systems. The thermogravimetric (TGA) technique used as the major hydration monitoring technique for these experiments has been previously established by other researchers to be a very dependable method by which hydration kinetic rates can be monitored (Bhatty, 1986; Monteagudo et al., 2014; Scrivener, 2004; Vedalakshmi et al., 2003). Apart from being very reliable method of monitoring hydration, the TGA technique is cost effective, relatively fast and does not require high skill level to operate, or interpret its results.

Additional experiments were performed to assess and evaluate the effectiveness of certain hydration halting techniques immediately after hydration is stopped and after

prolonged period of storage, this was done to validate the use of these hydration halting methods for future studies. Hydration was halted using a microwave oven to remove moisture and freezing at -80°C, TGA measurements were taken 30, 60 and 90 days after hydration was halted for the selected samples.

1.3 Organization of Contents

This document was arranged to provide information in logical manner as follows: Chapter 1 includes a brief introduction of the blended cement systems and objectives of this research. Chapter 2 provides a review of relevant literature with a detailed background of TGA measurements as a hydration monitoring method, as well as a summary of previous findings by other researchers. Chapter 3 provides information on limited study of internal light weight aggregates on hydration as measured by TGA and discussed lessons learned. Chapter 4 documents the material characterization, methodology and experimental approach including paste design, mixing and testing procedures. In Chapter 5, the results are analyzed, and findings of this research are presented. Chapter 6 includes the research conclusions and recommendations for future research. Limited and most relevant supplemental information for Chapters 3, 4 and 5 are included in the appendix.

CHAPTER 2 LITERATURE REVIEW

2.1 An Overview of Hydration

Hydration kinetic reactions in cementitious systems are quite complex and interdependent, making it difficult to offer detailed explanations for hydration kinetic rates. However, rigorous research by academia and industry has continually strived to improve the understanding of hydration mechanism in cementitious materials. Hydration is a combination of both physical and chemical processes. These processes occur at rates governed by the composition of the individual materials in the system, nature of that process and the state of the system at a given instant or time.

At present, an exceptionally vast amount of studies has been conducted on the hydration kinetics of cement. These studies have provided a handful of insights to the seemingly complex reactions of cement hydration. These reactions are typically categorized into one of the following processes: dissolution/dissociation, diffusion, growth, nucleation or complexation. The above-mentioned processes may occur in series, parallel or in random complicated forms. The inability to effectively isolate and study these processes makes it difficult to fully understand hydration kinetics. Just like most chemical reactions in series, the products of the above processes become the reactants for the next process and most times (but not always the case), one of these processes has a significantly slower rate compared to the others in the hydration sequence. The process with the slowest rate becomes the controlling step of the hydration kinetics (Ioannidou et al., 2015)

2.2 Hydration Kinetics of Portland Cement

Portland cement pastes, mortars and concretes remain the most widely studied cementitious systems in construction engineering. The major products of Portland cement

hydration process are $Ca(OH)_2$ (Portlandite) and C-S-H gels (calcium silicate hydrates). Hydration studies on Portland cement are mainly focused on the dominant and the hydrating strength producing components, tricalcium silicate (C_3S) also known as alite and tricalcium aluminate C_3A. Alite is known to constitute about 50% to 70% of PC by mass. This has restricted attention to the study of cement hydration to understanding the hydration kinetics of alite in other to provide a less complex and more feasible understanding of Portland cement hydration. Obviously C_3S is the single most important component contributing to formation of calcium silicate hydrate gels (C-S-H), the mineral to which strength gain in straight Portland cementitious system is attributed, hence hydration studies are majorly focused on the reaction kinetics of C_3S.

Rigorous analysis of the C_3S hydration kinetics/rate has led researchers to divide hydration progress over time into four distinct phases. These phases were interpreted from calorimetry plots of hydration with time by Bullard et al. (2011) to include: initial reaction, period of slow reaction, acceleration period and deceleration period. Although the exact start and finish points on the hydration plots are not fully known, this phase differentiation gives an overview of the current state of PC hydration studies. The first phase often termed as the initial reaction, involves the dissolution/dissociation and the rapid reaction between alite and water which begins upon contact of the cement with water. This reaction is highly exothermic and contributes significantly to isothermal calorimetry signals as hydration progresses during calorimetry analysis. Careful analysis of the initial reaction phase by Taylor et al. (1984) in their study, showed that C_3S dissolves in a harmonious and rapid manner in the first few seconds after wetting and continues to do so until the system reaches an equilibrium of calcium and silicate concentrations in solution. At equilibrium, this

dissolution of C$_3$S rate rapidly decelerates as the saturation levels of calcium and silicate in the system is reached.

The period of slow reaction is characterized by the gradual deceleration in the dissolution of calcium and silicate ions as the solution reaches saturation. Stein and Stevels (1964), and Jennings and Pratt (1979), proposed a hypothesis for the cause of this period of slow reaction to be the continuous formation of a thin *metastable* layer of C-S-H gels which covers solid surfaces, restricting the unreacted C$_3$S access to water and preventing the further dissolution of ions from the unreacted C$_3$S surfaces. A major challenge of the *metastable* hypothesis has been a lack of adequate experimental evidence to support its existence.

Acceleration period refers to the nucleation and growth (commonly referred in literature as N+G) phase of C-S-H hydration. This comes after the so called "*metastable*" phase mentioned earlier, several mechanisms have been proposed by Gartner et al. (2002) to explain the N+G phase of C$_3$S hydration, these include the exposure of the high soluble C$_3$S as the *metastable* layer formed at the end of the slow reaction period becomes chemically unstable. Another possible explanation provided is a rupture of the initial semipermeable metastable C-S-H barrier due to osmotic pressure from the unreacted C$_3$S underlying the metastable layer. Another N+G explanation is buttressed by the growth and nucleation of portlandite Ca(OH)$_2$, this becomes the rate controlling process, which indirectly controls the growth rate of C-S-H. Lastly N+G phenomenon is associated with the exponential growth by nuclei of the already formed C-S-H from the metastable phase.

The fourth distinct period interpreted from the calorimetry plots is termed the deceleration period. This is the concluding phase of the hydration progress, i.e. the post

hydration peak period, an understanding of this period in C_3S hydration kinetics provides an insight to the slower strength gain period of PC cementitious systems. Literature proposes that the rate of this deceleration period is typically controlled by diffusion, however other factors considered to affect this phase include studies of the hydration reactions and microstructure of cement-fly ash pastes, the finer reactive particles being exhausted leaving larger and less reactive particles, lack of space to allow continual C-S-H growth or expansion and lastly lack of water (Taylor et al., 1984). Lack of water is singularly the most controllable of these factors. Scrivener and Pratt (1983) studied the effect of cement particle sizes on the rate of hydration. With the typical particle size of cement ranging from 60μm to 1μm, the study showed that particles less than 7μm were consumed within 24hours and particles less than 3μm consumed within 10 hours.

Based on aforementioned four phases of the hydration kinetics of neat Portland cement systems, the governing factors affecting hydration kinetics can be summarized as dissolution of cement minerals, transport and diffusion of the reactants to accessible sites where hydration occurs and lastly the formation and growth the first C-S-H products. Additional studies have also been conducted on blended cement system, with the most common mineral admixtures being fly ash (Fourmentin et al. (2015), blast furnace slag (BFS) and silica fume (SF) (Mehta and Gjørv, 1982).

2.3 Hydration Kinetics of Pozzolans in Cementitious Systems

Partial replacement of PC with SF and pozzolans like fly ash has become a common practice in concrete industry. The addition of these admixtures to PC cementitious systems indirectly reduces CO_2 emission and other greenhouse gasses associated with the production of Portland cement due to a lesser amount of cement being consumed (Rivera

et al., 2001). Plus, pozzolans like fly ash are readily available and they provide desirable characteristics of the hardened cementitious systems when added in the right proportions. Pozzolans which are rich in silicate oxides (SiO_2) and aluminum oxides (Al_2O_3), when added to Portland cementitious systems react with the portlandite $Ca(OH)_2$, a by-product of C_3S hydration from cement, to form additional C-S-H hydrates (Bouzoubaa et al, 2001: Ramenzanianpour and Malhotra, 1995). Exceptional results have been reported in concrete performance when fly ash is included in cement-fly ash blended concretes, even in blends where the fly ash exceeded the cement content (Zhang and Canmet, 1995). The hydration kinetics rate of the cementitious system is not only impacted by the addition of pozzolans but strongly dependent on the reactivity these pozzolans. Hydration kinetics can either be accelerated or retarded by the addition of pozzolans as shown by Ghose and Pratt (1981) in a study where fly ash with different reactivity levels were incorporated into concrete production. Fly ashes containing high calcium (class C fly ash) mainly composed of glassy and crystalline phase minerals like $CaSO_4$, MgO, C_4A_3S, C_2S, C_3A and CaO, possessing self-hardening properties, are more reactive and therefore accelerated the hydration kinetics. Although the hydration kinetics of C_2S and C_3A in high calcium fly ash are similar to that of cement, the formation of C-S-H from the glassy phase mineral is slower when compared to cement, while fly ash with low calcium content (class F fly ash) with no self-hardening properties can only hydrate in the presence of alkalis or when $Ca(OH)_2$ is added. Uchikawa and Furuta (1981) reported that in the presence of $Ca(OH)_2$, low calcium fly ash forms hydration products such as C-S-H, C_4AH_{13} and C_2ASH_8. Bouzoubaâ et al. (2001) showed that irrespective of the reactivity levels of the amorphous siliceous content of pozzolans, it reacts with the $Ca(OH)_2$ to form additional C-S-H, which is the major

purpose for which fly ash is included in cement concrete mixes. Studies have also showed the inclusion of fly ash in PC cementitious system improves the overall long-term hydration compared to straight PC systems.

2.4 Effects of Fly ash on Cement Hydration

According to Lawrence et al. (2003), the effect of admixtures on cement hydration kinetics are divided into the dilution effect and the heterogeneous nucleation effect. The dilution effect is attributed to the increase in water to binder ratio due to the lesser density of fly ash compared to cement when fly ash replacement is volume-based mix design, the dilution effect also considers that the inclusion of admixture replacements reduces the actual cement content which in turn decreases the cement hydration products. The heterogeneous nucleation effect describes the additional surface area provided by new admixtures which act as nucleation sites providing extra favorable surfaces for hydration reactions. The hydration kinetics is quite different in the presence of fly ash as discussed in section 2.3, the same can also be reported for the hydration products in cement-fly ash systems. Studies by Pietersen and Bijen (1994), indicated that fly ash particles serve as precipitation and nucleation sites for the C-S-H and $Ca(OH)_2$ minerals in the early stages of cement hydration.

Sakai et al. (2005) also studied the hydration of fly ash cement blends by varying Portland cement replacement with fly ash from 20% to 60% using two different kinds of fly ash. Their findings showed that irrespective of the glass/amorphous content, or the composition of the fly ash, the fly ash in the paste did not react until about 7 days. This reiterates the slow nature of fly ash pozzolanic reaction and its effect on rate of Portland cement hydration. Results of studies conducted by Langan et al. (2002) on fly ash-cement

blended pastes also showed that when fly ash is incorporated in cement paste mixtures, it slows down the rate of hydration experienced in the acceleration period by almost 2 hours when compared to straight cement paste mixes.

ASTM C593 (2011) "Standard Specification for Fly Ash and Other Pozzolans for Use With Lime for Soil Stabilization" specifies the silica, alumina and iron content for fly ash to be used in cement blended systems. While high fraction of silica and alumina present in fly ash are typically in the amorphous phase and easily contribute towards the Pozzolanic reaction of fly ash, other minerals like mullite and quartz present in crystalline phases are non-reactive, hence do not contribute towards hydration. Ramezanianpour (2013) showed that the chemical composition and mineralogical composition of fly ash as well its crystalline and glass/amorphous contents all play important roles in the formation of additional hydration products and rate at which these products are formed in fly ash blended cement systems. The author also reported that glass/amorphous content of fly ash may vary between 50 - 90% and will only contribute towards hydration after it is broken down. This time dependent process involving the glass phase has been termed the incubation period and requires that pore water should attain a minimum pH of 13.3 at room temperature (approximately $20^{o}C$) to activate the glass phase of fly ash. For high calcium fly ash- cement system (class C fly ash), the CaO present in the fly ash, as well as the dissolution of Na^{+} and K^{+} increases the pH which may result in the activation of hydration. While in low calcium fly ash (class F fly ash) the introduction of calcium hydroxide typically increases the pH of the pore water to about 12.5. Apart from increasing the OH^{-}, the dissolution of Na^{+} and K^{+} from the fly ash into the pore water also results in a the breaking down of the Si and Al rich amorphous layer on the surface of the fly ash from

which these Na^+ and K^+ ions dissociate, therefore creating suitable nucleation sites for the formation of hydrates like C-S-H and C_2ASH_8.

2.5 Hydration Kinetics of $Ca(OH)_2$ and Pozzolans

The free $Ca(OH)_2$ content available as hydration progresses indicates the degree of hydration at that given instant for straight Portland cement systems (Vedalakshmi et al., 2003). Hence in cementitious systems without pozzolans, the $Ca(OH)_2$ content continually increases as hydration progresses. However, since pozzolans react with the available $Ca(OH)_2$ to further form C-S-H hydrate gels, the free $Ca(OH)_2$ content at all ages of hydration is expected to reduce due to the dilution effect of cement by pozzolans as well as the consumption of $Ca(OH)_2$ in the formation of additional C-S-H. This reaction is quite slow, and the formation of additional C-S-H is dependent upon the $Ca(OH)_2$ available for the pozzolanic reaction with fly ash. High fly ash replacements in cement fly ash blends results in less cement hydration products which implies that reduction in the amount of $Ca(OH)_2$ available for additional C-S-H formation. This relatively slow hydration rate experienced in fly ash-cement blends have led various researchers to explore activation techniques to improve fly ash-$Ca(OH)_2$ reactivity. One of such study was conducted by Antiohos et al. (2003), where they investigated the activation of fly ash hydration in the presence of quicklime in other to improve the pozzolan reactivity and also speed up hydration rate for two kinds of fly ash. One blend had a high calcium content and the other contained a moderate calcium fly ash. The addition of quicklime (CaO), increased compressive strength and the non-evaporable water for the high calcium fly ash-cementitious system and its effect was not easily detected for the moderate calcium fly ash cement blends.

In the second part of the study conducted by Antiohos et al. (2006), apart from hydrates like portlandite, ettringite, calcium sulfoaluminate ($CaO.3Al_2O_3.SO_3$), other minerals like gehlenite ($Ca_2Al_2SiO_7.8H_2O$) shortened as C_2ASH_8 were also formed in the early stages of hydration. C_2ASH_8 minerals was the main hydration product detected for these quicklime activated paste and was due to the reaction between the hydrated lime and SO_3. Results from this study also indicates that the activation effect of quicklime is short-termed as a reduction in porosity was only noticed in early stages of hydration and slightly increased at later age. This conforms to the theory that quicklime hydration and reactions are expansive in the presence of high SO_3 content. Microscopic images by Antiohos et al. (2006) also confirmed the formation of additional C-S-H crystals around the fly ash particles, however, excessive amounts of portlandite were noticed around fly ash particles in which the lime replacements were increased, therefore acting as inhibitors not enabling the fly ash to further react.

Even in the presence of $Ca(OH)_2$, the pozzolanic reaction of fly ash is not easily activated at room temperatures. Huang et al. (1986) showed that in fly ash – $(Ca(OH)_2$ pastes only about 1.5% to 3% of hydration occurs after a period of 7 days at room temperature. This is because the glassy phase of fly ash requires a higher pH to break it down and allow it to react with the available $Ca(OH)_2$. Hence when fly ash with a low calcium content is used, only small amounts of C-S-H gels are formed. For reasons mentioned earlier, researchers have employed the use of activators to increase the pH of the pore solution to help accelerate the breakdown of glassy structure of fly ash. Shi and Day (1995) used Na_2SO_4 and $CaCl_2$ as activators for hydrated lime-fly ash pastes produced from low and high calcium subbituminous coals. These pastes made of 80% fly ash and

20% hydrated lime indicated that the inclusion of Na_2SO_4 and $CaCl_2$ in small amounts increased the pozzolanic reaction between the fly ash and lime, with most noticeable significant effect in the early days of hydration. It was concluded that these activators when added in the right dosage can greatly influence strength gain and hydration rate of fly ash –lime pastes. Li et al. (2000) also confirm that the use of Na_2SO_4 as an activator in low calcium content fly ash-$Ca(OH)_2$ system enhances hydration in addition to production of more stable hydrates.

2.6 CaO Hydration

Several methods have been adopted in activating the CaO contained in high calcium fly ash systems, for such systems additional CaO in the form of quicklime may not be required due to its self-hardening characteristics. Quicklime is produced from limestone by heating it above 900°C, at this temperature the limestone $CaCO_3$ decomposes into quicklime (CaO) and Carbon dioxide (CO_2). The quality and reactivity of the quicklime produced from this process among other characteristics depend on the calcining process as heating over long period of time or extremely high temperatures produces lime with low reactivity. Quicklime properties like particle size, pore volume and BET surface area are all strong indictors of its reactivity.

CaO is highly unstable in the presence of water or CO_2, the reaction between quicklime and water to become hydrated lime is not only exothermic but also quite expansive. Although quicklime is commonly used for geotechnical purposes such as in wet soil subgrade drying and soil modification, its use in concrete components remains unpopular. When quicklime is included in cement mortars or concrete, the expansive nature of quicklime hydration causes them to swell, this had limited its use in concrete. Hydrated

lime has a volume apparently twice that of quicklime. When quicklime is included in cement fly ash blends, a certain amount of the mix water is consumed in hydrating the quicklime, thereby reducing the actual water going towards the cement-fly ash hydration reaction and effective water to binder ratio in the system. The equations 2.1 to 2.4 describe the typical reaction between common reactants in cementitious systems in the formation of hydrates.

$$CaO + H_2O \rightarrow Ca(OH)_2 + Heat \qquad (2.1)$$

$$Ca(OH)_2 \rightarrow Ca^{++} + 2(OH) \qquad (2.2)$$

$$Ca^{++} + 2(OH) + SiO_2 \rightarrow \text{calcium silicate hydrate (C-S-H)} \qquad (2.3)$$

$$(SiO_2 \text{ from fly ash})$$

$$Ca^{++} + 2(OH) + Al_2O_3 \rightarrow \text{calcium aluminate hydrate (C-A-H)} \quad (2.4)$$
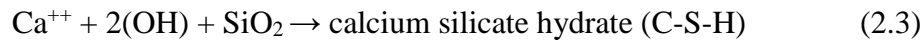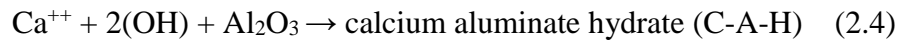
$$(Al_2O_3 \text{ from fly ash})$$

In blended cement systems, pozzolans react with the available $Ca(OH)_2$ to further form C-S-H hydrate gels. This reduces the free $Ca(OH)_2$ content as pozzolanic hydration reaction progresses due to the consumption of $Ca(OH)_2$ in the formation of additional C-S-H. The above equations provides a balanced chemical hydration equation of quicklime as well as a breakdown of the reaction between hydrated lime and the amorphous components of fly ash. From basic stoichiometry, 0.32 gram of water is required to completely hydrate 1 gram of CaO and will produce 1.32 grams of $Ca(OH)_2$.

2.7 Hydration Monitoring in Cementitious Systems

Although hydration reactions in cementitious systems are highly complex and heterogeneous, the microstructure of the cementitious system can provide an adequate information of the level of hydration at a giving time. Identifying and quantifying the hydrating mineral phase serves as an indication of the degree of hydration within the

cementitious system. Richardson et al (2002) established patterns typical in the microstructural development of hydration reactions for straight cement systems. However, rapidly identifying these different mineral phases still remains a problem in hydration studies. Several approaches have been employed in the microstructural analysis of cementitious systems, these include thermogravimetric analysis (Zeng et al., 2012) and (Deboucha et al., 2017), XRD/Rietveld analysis (Scrivener, 2004), nuclear magnetic resonance (NMR) and scanning electronic images (SEM) (Scrivener, 2004). All of the above-mentioned methods have proven quite reliable in monitoring the microstructural development of cementitious systems.

Scrivener (2004) monitored hydration progress for Portland cement paste using XRD/Rietveld analysis to quantify mineral phases and then compared these results with other independent methods like backscattered electron images (BSE/IA) and thermogravimetric analysis (TGA). The XRD/Rietveld technique basically compares the diffractive patterns from XRD measurements with an extensive database of anhydrous cementitious materials whose actual phase compositions have been determined by Walenta and Füllmann (2004). This method relies on the fact that every crystalline material has a unique pattern, these patterns are compared with simulated patterns of known crystalline phases and the generated database of these known crystalline phases serve as control files. Rietveld analysis quantitatively determines the sum of these known crystalline phases present in the cementitious system normalized to a 100%. The most difficult aspect of employing XRD/Rietveld analysis remains the development of these control files.

Scrivener, (2004) aslo successfully monitored hydration progress using SEM. Although back scattered electron microscopy image analysis only provides a two-

dimensional observation of the cementitious microstructure sections it has proven to be an adequate method of monitoring the morphology of hydrated phases like C-S-H, ettringite and other hydration by products.

The thermogravimetric analysis (TGA) remains one of the most widely used techniques for monitoring hydration in cementitious systems. In TGA, hydration progress is typically measured as a function of the amount of chemically bound water. The TGA identifies hydrates like C-S-H and aluminum hydroxide (AH_3) and is often but not always the case used complimentarily with the XRD technique. (Deboucha et al., 2017) compared the weight loss from TGA with XRD confirming the presence of mineral phases such as C-S-H, $Ca(OH)_2$ and $CaCO_3$ among other mineral phases. Thermogravimetric analysis basically measures the changes in weight as a function of increasing temperatures. It is a common practice to heat up known sample weight from room temperature up to about a 1000 degrees Celsius at a constant rate after which the recorded change in weight, both differential weight (DTA) and differential scanning calorimetry (DSC) data are collected and analyzed. While derivative thermogravimetric or differential thermal analysis (DTA) provides information on the consecutive weight loss, differential scanning calorimetry (DSC) describes the change in heat as the common mineral phases in cementitious systems undergo reactions like dehydration, dehyroxylation and decarbonation. These reactions could be endothermic or exothermic. (Bhatty, 1986), Pane et al. (2005) and Monteagudo, (2014) have all proposed methods for interpreting hydration from TGA measurements.

2.8 Factors Affecting TGA Measurements

A couple of factors have been identified to influence thermogravimetric measurements, these include heating rate, gas flow and type of heating vessels. It is

established that higher heating rates leads to better defined peaks in the DSC curves from TGA experiments (Paulik et al., 1992). The sample weight is another factor affecting TGA measurements, as higher quantity of a particular phase in the test sample might affect the position of the decomposition peaks (Paulik et al. (1992). Pretreatment technique utilized to halt sample hydration before TGA testing is a very important factor affecting the TGA measurements especially for samples which testing are not performed immediately. Diluting cementitious samples with organic solvents like ethanol or isopropanol or freeze-drying are some of the most common pretreatment techniques that have been employed in the past. Studies have shown that these methods can greatly affect the TGA measurements especially as seen in samples pretreated with organic solvents. Day (1981) showed that alcohol (isopropanol) adsorbs onto the hydrates, displaces water and prevents further hydration reaction. However prolonged treatment with alcohol can also lead to the dehydration of the monosulfate ($C_4A_SH_{12}$) from 12 to 10 H_2O ($C_4A_SH_{10}$), and also increases the weight loss in the carbonate decomposition region of hydrated cementitious systems due to a reaction of liberated organic solvents at temperatures greater than 600 degrees C. The typical approach employed in halting hydration with the use of organic solvents like alcohol involves crushing the hardened cementitious paste into small pulverized particles, then soaking them in alcohol for about 24 hours, after which it is oven dried for another 24 hours. Soaking crushed paste particles in alcohol displaces the pore water, thereby preventing moisture for further hydration ((Monteagudo et al., 2014). However, previous findings by Day (1981) showing that the use of alcohol affects the TGA measurements led to an attempt by Deschner et al. (2012) to mitigate the effect of solvents like isopropanol

on the TGA measurements in blended pastes by using less polar solvents like diethyl ether to replace isopropanol.

Other hydration halting techniques like quenching the samples with liquid nitrogen in combination with freeze drying have been recommended, studies have shown that this method is less likely to affect the TGA measurements (Zhang and Scherer, 2011). Another factor that affects TGA measurements in cementitious systems is carbonation during storage. For samples that are stored and TGA not performed immediately at specific curing intervals, there is a possibility of carbonation of the stored samples if they are not properly sealed.

Table 2.1 provides a summary of typical solid phases in cementitious systems and the decomposition temperature associated with these phases. While Figure 2.1 shows a typical DTG curve associated with distinct peaks of solid phases at for a straight cement paste tested at 3, 7 and 31 days.

Table 2.1 TGA weight for solids typically observed in cementitious systems

Solid Mineral Phases	Temperature Range (^{o}C)	Source
Ettringite	130	K. Scrivener et al. 2016
Gypsum	140 - 150	
AFt Phases	260	
Magnesium silicate hydrates, M-S-H and Hydrotalcite	270	Nied et al. 2015
Calcium silicate hydrates, C-S-H	50 - 600	Mayers et al. 2015, Mistuda and Taylor 1978, Muller et al. 2013
Calcium aluminium hydrates, C-A-H	260 - 320	Nied et al. 2015, Muller et al. 2013
AFm Phases	60 - 200, 250 - 350	K. Scrivener et al. 2016
Brucite, Mg(OH)	420	Goto et al. 1995
Calcite, CaCO3	600 - 800	Goto et al. 1995
Portlandite, Ca(OH)2	460	Goto et al. 1995
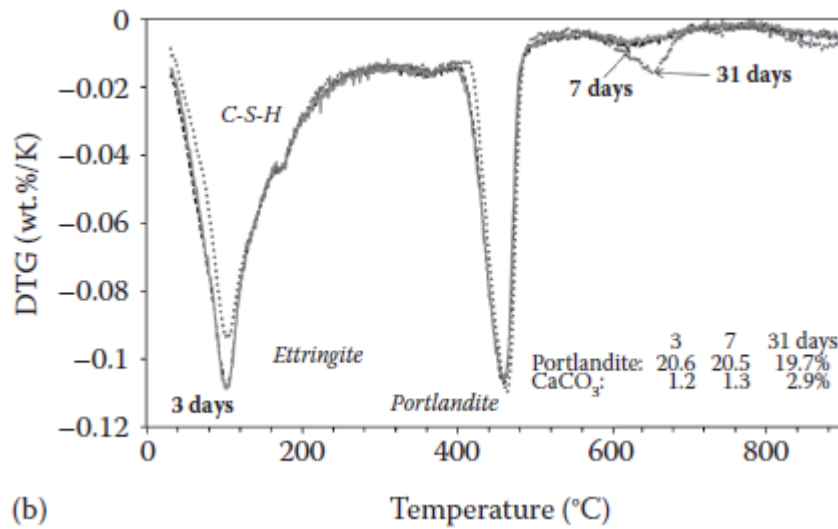
Figure 2.1 DTG vs temperature for OPC paste (Scrivener et al. 2016)

Table 2.2 provides the typical decomposition ranges associated with weight loses due to the formation of hydration products interpreted from TGA measurements by Bhatty (1986), Pane et al. (2005) and Monteagudo et al. (2014). The dehydration zone (Ldh) refers to the weight loss due to decomposition of the C-S-H minerals, the dehydroxylation (Ldx) represents weight loss as a result of the decomposition of the $Ca(OH)_2$, while the decarbonation (Ldc) accounts for the decomposition of calcium carbonate, $CaCO_3$ minerals present in the hydrating paste.

Table 2.2 Temperature ranges for different phases

Region	Methods		
	Temperature range (ºC)		
	Bhatty(1986)	Pane et al.(2005)	Monteagudo et al. (2014)
Dehydration (Ldh)	105 - 440	140 - 440	105 - 430
Dehydroxylation (Ldx)	440 - 580	440 - 520	430 - 530
Decarbonation (Ldc)	580 - 1000	520 - 1100	530 - 1100

2.9 Curing and Storage of Paste Samples

Although it is a common practice to cure demolded cement pastes, mortars or concrete samples in water after 24 hours or relative humidity chambers under different

temperatures, depending of the purpose for which they are made (Thomas et al., 2018), (Song et al., 2018), and Tonelli et al. (2017). In the past, cementitious samples prepared for TGA measurements are either cured under controlled temperature surroundings (Deboucha et al., 2017), Scrivener et al. (2004) or under controlled relative humidity (Shafiq, 2011). Studies conducted by Shafiq (2011) on the degree of hydration for both normal and blended cement paste systems cured under various relative humidity showed that reduced relative humidity results in the drying of the cementitious systems. This drying reduces the water available for hydration and affects the overall hydration for both the normal and blended cement paste systems. The study concluded that at a relative humidity of about 75%, the overall degree of hydration straight cement system was reduced by 7%, while for the blended cement systems, overall hydration was reduced by 28% and 30% for fly ash replacement rates of 40% and 50%, respectively. Palou et al. (2016) studied the effect of curing temperature on the hydration of two binary Portland cement systems, one with metakaolin (MK) and the other with blast furnace slag. The early hydration was monitored using DSC/TGA measurements for both blended systems cured at 30, 40, 50 and 60°C and the results showed that higher curing temperatures accelerated the initial hydration reactions. This study will employ sealed curing conditions so as to avoid desiccation and moisture loss while studying the effect of lime hydration reaction on water available for cement fly ash pozzolanic reaction.

CHAPTER 3 EXPLORATORY-LIMITED STUDY ON INTERNAL CURING

3.1 Introduction to Internal Curing

Internal curing is defined by the American Concrete Institute as "supplying water throughout a freshly placed cementitious mixture using reservoirs, via pre-wetted lightweight aggregates, that readily release water as needed for hydration or to replace moisture lost through evaporation or self-desiccation" (ACI 2010). Internal curing (IC) uses the principle of internal reservoirs to supply water to aid hydration in contrast to conventional curing approach. These internal reservoirs are highly porous light weight aggregates (LWA) capable of storing water in their highly connected pores and releasing moisture as the demand for water increases due to either hydration or drying. Internal curing is achieved in concrete by replacing a portion of the fine aggregates (sand) with pre-wetted LWA during concrete batching. Fully saturated LWA are capable of providing enough water to fully hydrate cementitious systems and also mitigate the effect of shrinkage associated with cement hydration. Internally cured concrete (ICC) can potentially mitigate issues of cracking caused by shrinkage in concrete due to hydration reactions, as lesser pore volume of concrete is occupied by hydration products compared to the individual reactants (Henkensiefken et al., 2009).

3.2 Literature on Internal Curing

ACI specifies that internal curing aggregates could either be made of pre-wetted crushed stone fines, superabsorbent polymers, absorbent limestone aggregates and or pre-wetted wood fibers (ACI 2013). Figure 3.1 shows a comparison between the mechanisms of external and internal curing.
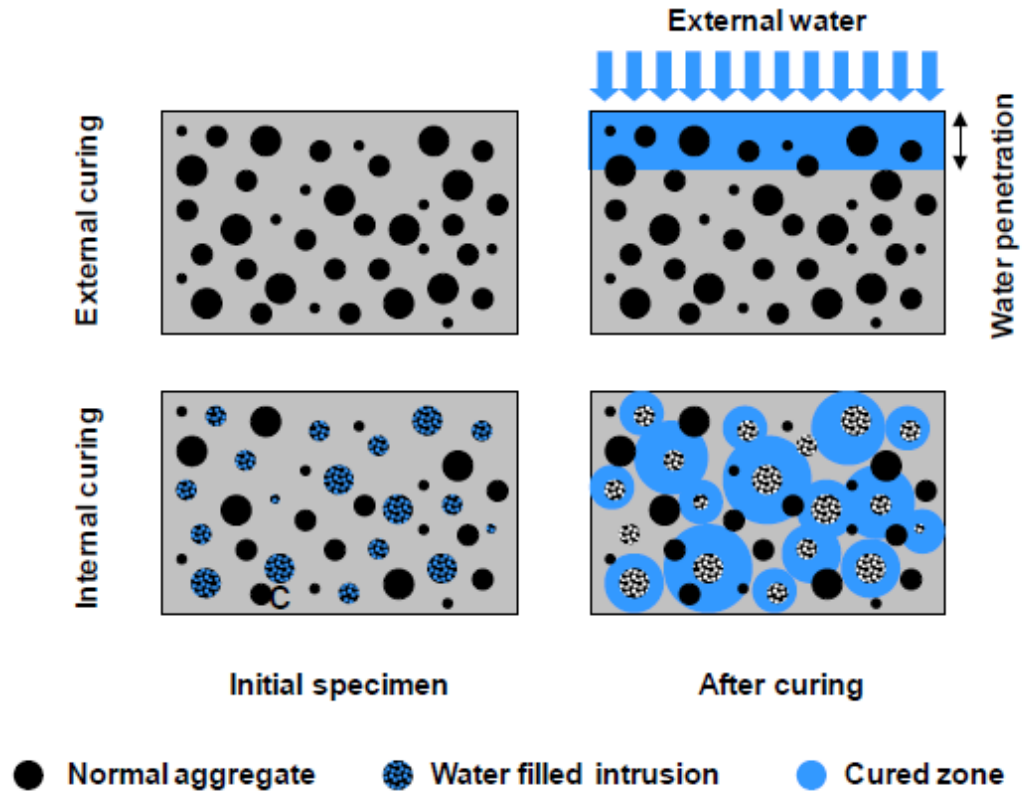
Figure 3.1 External versus internal curing (Castro et al. 2011)

To successfully implement internal curing, it is important to properly estimate the amount of required for curing. This is dependent of factors like the adsorption capacity, desorption isotherms, evaporation and degree of saturation of the LWA (Castro et al. 2011). An evaluation of internal curing as a potential strategy in minimizing the reductions in early day strength in mixtures with high volume fly ash by reducing the w/c ratio in other to improve its mechanical properties was performed by De la Varga et al. (2012). The mixtures in this study were internally cured to mitigate self-desiccation and autogenous shrinkage. The result of this study showed that the inclusion of LWA produced does not significantly alter the rate of early hydration in high volume fly ash mixes, but an increased degree of hydration was noticed after 7 days as measured by heat of hydration.

Properly characterizing LWA properties in other to accurately estimate the desorption capacity of water from the pores of the LWA to the hydrated phases is a crucial part of internal curing. Bentz et al. (2005) proposed an equation for estimating the required LWA replacement level in concrete based on the adsorption capacity of the LWA, level of saturation of the LWA, the batching w/c ratio and the expected chemical shrinkage of the cement paste. Equation 3.1 was proposed by Bentz et al. (2005) for proportioning mixtures with internal light weight aggregates

$$Cf * CS * \alpha max = S * \Phi_{LWA} * M_{LWA} \tag{3.1}$$

Where;

M_{LW} = mass of (dry) IC-LWA needed per unit volume of concrete (kg/m^3 or lb/yd^3)

Cf = cement factor (content) for concrete mixture (kg/m^3 or lb/yd^3)

CS = chemical shrinkage of cement (g of water/g or cement lb/lb)

αmax = maximum expected degree of hydration of cement

S = degree of saturation of aggregate (0 to 1) must be great than zero

Φ_{LWA} = absorption of lightweight aggregate (kg water/kg dry LWA or lb/lb)

Laboratory tests on concrete mixtures containing internal curing aggregates performed by Wei and Hansen (2008) using w/c ratios of 0.35 and 0.45 containing of 20% and 40% sand replacement by LWA showed that the tensile stresses associated with autogenous shrinkage was significantly reduced by internal curing especially for 0.35 w/c mixtures. The study concluded that pre-wetted LWA can effectively reduce and even possibly eliminate autogenous shrinkage in concretes with *w/c* ranging from 0.35 to 0.45.

A more recent study on the use of LWA for internally curing bridge deck and pavement concrete containing moderate fly ash replacement was performed at UNC Charlotte. This was a collaborative effort between NCDOT and researchers at UNC Charlotte to understand the benefit of internal curing on reduced early age shrinkage in

bridge deck and pavement concrete in other to produce more durable highway infrastructures. In this study two sets of pre-wetted LWA were used to replace sand in different quantities and the performance of the internally cured concrete were compared with conventionally cured concrete. Internally cured and conventionally cured concrete and mortar mixtures were tested for strength, autogenous shrinkage and modulus of elasticity. Results showed that internally cured concrete indicated reduced autogenous shrinkage of up to 56% compared to conventional mixes in addition to averagely lower modulus of elasticity (20%). The coefficient of thermal expansion (CTE) associated with cement hydration was also reduced by 11% for internally cured concrete compared to the control mixes which indicates the beneficial use of internal curing in improving concretes' thermal performance. As for mechanical properties, although both internally and conventionally cured mixtures met the NCDOT required 28-day compressive strength of 4500psi, the internally cured concrete had slightly lower strength values. The strength results also showed that internally cured mixtures with fly ash had higher compressive strength between 28 and 90 days compared to internally cured mixtures without fly ash (Leach 2017). This result was consistent with previous findings by Zhang and Canmet, (1995) which showed that moderate fly ash additions benefit hydration in later ages in cement-fly ash concrete blends.

3.3 Exploratory Study on the Hydration of Internally Cured Mortars

To characterize the hydration benefits of internal curing on cement-fly ash mixtures in the laboratory, a brief study was performed to monitor hydration using TGA technique. This study was intended to complement work previously done by UNC Charlotte by correlating overall hydration from this study to the improved characteristics recorded in

the previous study on internally cured bridge deck and pavement concrete mixtures by Leach (2017)

3.3.1 Material and Method for Mortars

Table 3.1 provides summary of the cement, fly ash, sand and internal curing aggregates (IC-LWA) characteristics used for this study. Supplemental information pertaining to material characterization for this exploratory study such particle size distribution, adsorption capacity and density are included in Appendix A of this document. The IC-LWA used was an expanded lightweight slate produced in North Carolina, while the sand was natural silica sand from the Piedmont region of North Carolina. Type I/II ordinary Portland cement was sourced from South Carolina and class F fly ash from a power plant in Belews creek North Carolina was used as binders in this study.

Table 3.1 Material Properties for IC-LWA mortars

Properties	IC-LWA	Sand	Cement	Flyash
Fineness Modulus	-	2.72		-
Specific gravity	1.69	2.44	3.15	2.53
Adsorption (%)	13.33	-	-	-
Bulk Density (kg/m^3)	1041	1557		-

A total of 12 mortar mixtures were prepared for this study, with set of cement-fly ash mortars containing IC-LWA and another set without which served as control mixes to quantify effect of internal curing on hydration. Both sets of mortars contained fly ash replacement of 0%, 20%, 40% and 60%. Table 3.2 provides the percentage proportioning for mortars in this study. The amount of IC-LWA for each mix was calculated based on

the desorption capacity of the IC-LWA using Equation 3.1, and equal amount of sand was replaced with the calculated IC-LWA for each mixture.

Table 3.2 Percentage mix proportion of raw materials

| Mixture | Binder (OPC + CFA) 26% | | Water | Sand + IC-LWA |
	Cement (%)	Flyash (%)	%	%
1A	100	0	24	50
2A	80	20	24	50
3A	60	40	24	50
4A	40	60	24	50
1B	100	0	24	50
2B	80	20	24	50
3B	60	40	24	50
4B	40	60	24	50
2B-i	80	20	24	50
2B-ii	80	20	24	50
4B-i	40	60	24	50
4B-ii	40	60	24	50

Sample 1A through 4A contains only sand as aggregates while samples 1B through 4B-ii contain both calculated IC-LWA required to prevent autogenous shrinkage and sand. Table 3.3 provides mass of individual material for each mix. The additional water expected to desorb from the pre-wetted IC-LWA for each mix was calculated and added to the batching water. The dry IC-LWA was soaked in for 24 hours in the batching + additional water for internal curing for a period of 24 hours prior to batching each mortar mixture. All mortars prepared in this study were tested for compressive strength and degree of hydration using unconfined compressive strength tests and thermogravimetric analysis respectively at curing intervals of 3, 7 ,14 and 28 days.

Table 3.3 Mix Design for Mortars

Mixture	Cement	Fly ash	Water	Add. water from IC-LWA	Fine agg	IC-LWA
	grams	grams	grams	grams	grams	grams
1A	4114	-	1234	-	6192	-
2A-20%CFA	3289	635	1234	-	6192	-
3A-40%CFA	2468	1347	1234	-	6192	-
4A-60% CFA	1647	2150	1234	-	6192	-
1B	4114	-	1234	240	4395	1801
2B-20%CFA	3289	635	1234	240	4395	1801
3B-40% CFA	2468	1347	1234	240	4395	1801
4B-60% CFA	1647	2150	1234	240	4395	1801
2B-I 20% CFA	3289	635	1234	191	4754	1442
2B-ii-20% CFA	3289	635	1234	286	4032	2159
4B-i-60% CFA	1647	2150	1234	191	4754	1442
4B-ii-60% CFA	1647	2150	1234	286	4032	2159

Freshly prepared mortars were casted in 50 mm cube molds and covered for 24 hrs before they were demolded and cured under sealed curing conditions by tightly wrapping the mortar cubes in saran plastic wraps before storing in the laboratory where the surrounding relative humidity and temperature of the room was monitored. The sealed curing approach was used employed in order to properly characterize any change in hydration or strength gain resulting from the additional water being supplied by the IC-LWA. At the selected curing intervals hydration was halted by first crushing the mortars and sieving through US sieve No. 10 and then soaking the portion passing sieve No.10 in isopropanol for 24 hours to displace any moisture left in the system. After soaking in isopropanol, crushed samples were then oven dried at 60ºC for another 24 hours to remove any absorbed isopropanol before TGA measurements were taken.

3.3.2 Testing of Mortars

In addition to 50 mm mortar cubes, 50 x 101mm cylinders were also cast to measure compressive strength. The TestMark CM-4000 device was used to perform unconfined

compressive strength testing in accordance with ASTM C39/C39M. The unconfined compression test was performed on three specimens for each mortar mix after 3, 7, 14 and 28 days and the average values are presented in Table 3.4.

Duplicate TGA measurements were taken for the mortars using the after the hydration halting process was completed. Changes in the known weight of a specimen is monitored as it either cooled or heated at a controlled rate. For this study the SDT Q600 manufactured by TA instruments was used for thermogravimetric measurements. The SDT Q600 furnace has a heating capacity of up to $1500^{O}C$ and can measure differential heat flow also known as DSC. The samples in study were heated from room temperature to about $1000^{o}C$ and the change in weight corresponding to increasing temperature is recorded.

3.3.3 Result and Conclusion

The (Bhatty, 1986) equation was used to correlate the chemically bound water at all ages to the degree of hydration from TGA measurements. Results from hydration are summarized in Table 3.4, while compressive strength data are presented in Table 3.5. Figures 3.2 and 3.3 also provide bar charts indicating the compressive strength and degree of hydration respectively with time.

Table 3.4 Summary of hydration results from TGA

Degree of Hydration				
Sample	3 Days	7 Days	14 Days	28 Days
1A	46.92	44.54	47.56	45.88
2A	46.44	47.77	48.33	48.07
3A	42.58	47.96	48.04	49.75
4A	32.80	36.53	40.11	35.87
1B	40.72	39.67	39.68	41.91
2B	42.21	44.20	43.59	41.40
3B	38.66	42.68	42.42	40.77
4B	26.42	34.43	36.32	35.41
2B-i	38.82	41.39	40.76	40.07
2B-ii	42.71	43.62	40.88	43.10
4B-i	30.22	36.04	35.80	33.72
4B-ii	30.07	35.47	35.18	35.55

Table 3.5 Summary of compressive strength test

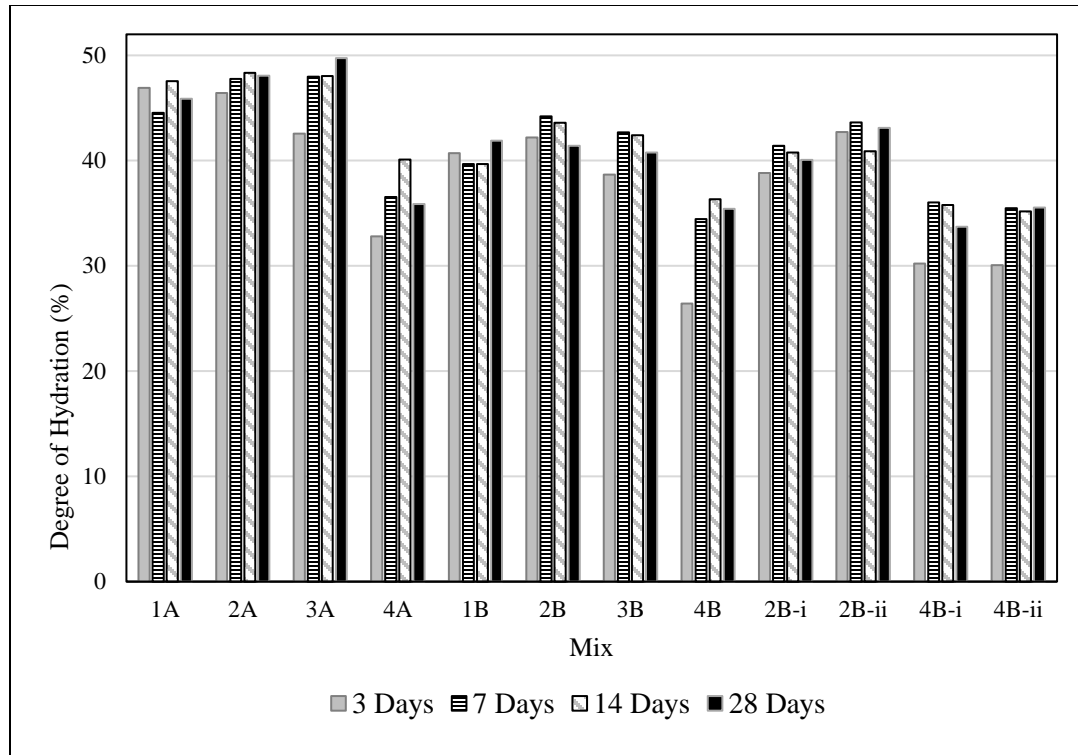| Compressive Strength (psi)				
Sample	3 Days	7 Days	14 Days	28 days
1A	9981	10987	12335	12832
2A	7043	8284	9289	10804
3A	5283	7772	8717	8885
4A	4299	4615	5750	5980
1B	8768	9259	8042	8950
2B	7924	7989	9618	10241
3B	4147	6201	7882	8669
4B	3271	4771	4876	5448
2B-i	7151	7334	7983	8382
2B-ii	6774	6962	8865	9308
4B-i	3255	4600	4809	5049
4B-ii	3013	4019	4220	4431

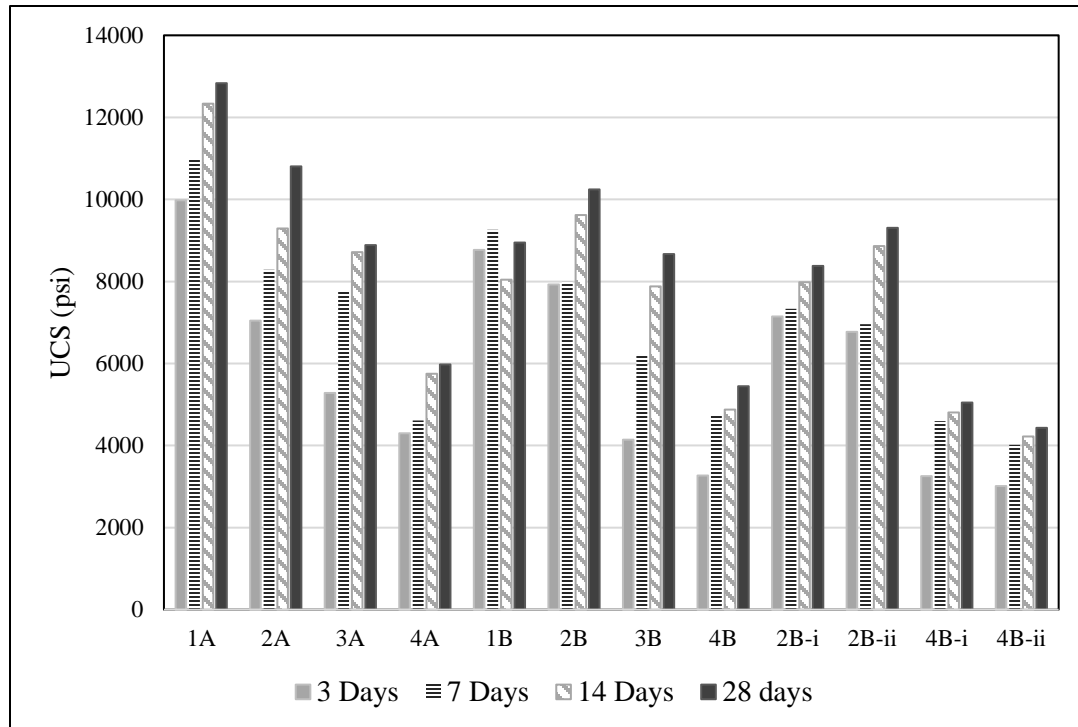Figure 3.2 Degree of hydration for IC-LWA mortars using Bhatty 1986 method

Figure 3.3 Compressive strength for IC-LWA mortars

As shown in Table 3.4 and Figure 3.2, hydration data did not follow any definitive trend. Results were expected to show a decrease in the rate of hydration as fly ash content in the mortars increases for mixes without IC-LWA. Mortars with fly ash replacement levels of 20% and 40% show relatively the same level of hydration across all ages. While Mix 4A showed slight increase in hydration between 3 and 14 days but decreases at 28 days. Also comparing mortars with similar fly ash and cement contents with and without IC-LWA showed that the mixes with IC-LWA had reduced level of hydration when compared with the control mixes at all ages. This could either be due to the fact the IC-LWA was not fully saturated prior to batching, therefore absorbing moisture required to hydrate the paste or the presence of fines from the IC-LWA in TGA samples affected weight loss at the various decomposition ranges. It is also possible hydration halting technique used in this study might have affected TGA measurements. Previous research by Day (1981), and Zhang, et al. (2011) have shown that solvents like methanol and isopropanol affects the hydrating phases of cementitious systems by increasing weight loss in the carbonate and portlandite decomposition regions and also damage the microstructure of ettringite and monosulfate phases.

Compressive strength followed the expected trend; as compressive strength values decreased with increasing replacement levels of fly ash as shown in Table 3.5 for mortars without IC-LWA. A similar trend was also noticed for mortars containing IC-LWA, however 2B (20% fly ash replacement) showed higher strength gain compared to mix 1B (0% fly ash replacement) after 14 days. Comparing mortars with similar fly ash and cement contents with and without IC-LWA showed that the presence of IC-LWA caused a slight reduction in compressive strength values. A possible explanation for this is the highly

porous and weak nature of the IC-LWA, reducing the strength of the mortar matrix when compared mortars with only sand as aggregate.

SAS analysis was also performed using ANOVA on the data set from both TGA and compressive strength experiments in an attempt to establish a correlation between strength and TGA results. The ANOVA resulted in a correlation of 0.5461, which was considered inadequate to reach a definite conclusion correlating strength and TGA results in this study. With these challenges, a new experimental design was established to look at the hydration of cement-fly ash-quicklime blended pastes to eliminate the possibility of TGA measurement errors caused by the addition of aggregates. In this new design blended pastes were tested immediately after crushing without undergoing hydration halting to effectively capture the hydrating phases at the selected curing intervals.

CHAPTER 4 MATERIALS AND METHODS FOR BLENDED PASTE

This chapter of the study focuses on the laboratory experimentation of the hydration of blended cement paste mixes with fly ash and quicklime under sealed curing conditions at room temperature and ambient humidity. Material characterization including physical properties and chemical characteristics of the raw materials is key to the success of this study. This section will discuss the materials used for this study the experimental methods, the mix proportions for the paste batches, and the justifications for the selected test methods

4.1 Materials

4.1.1 Ordinary portland cement (OPC)

The Portland cement used for this study is a Type I/II cement and it meets the requirements of ASTM C150, "Standard Specification of Portland Cement." The cement was manufactured by a plant in Holly Hill, South Carolina, and has a relative density (specific gravity) of 3.15 and a Blaine fineness of 393 m^2/kg as provided by the manufacturer in the mill report attached in appendix B

4.1.2 Fly ash

Ten of the twelve paste mixes prepared in this study contained fly ash replacements by mass. The fly ash chosen was a class F fly ash (low calcium fly ash) sourced from a power station in the southeast of the U.S. Specific gravity was measured in the lab in accordance with ASTM D584 to be 2.53 by dispersing the fly ash in de-aired water using a pycnometer. The particle size distribution measured using a laser diffraction particle size analyzer, showed that the fly ash had a mean particle diameter of 26 µm, with 100% (by volume) finer than 257 µm as shown in Figure 4.1. The laser diffraction method of particle size analysis determines particle size distribution by measuring the angular variation and

intensity of the dispersed particles as light passes through it. The particles are usually dispersed in water, air or any other wetting medium depending on the nature of the material. Although the XRD analysis to determine the key mineralogical compositions of the fly ash was not performed on the batch of fly ash used in this study, however, the results from the XRD analysis performed by RJ Lee Group Incorporated on more recent fly ash from the same power plant can be assumed to closely represent the fly ash used in this study. Previous XRF analysis on fly ash sourced from this power plant has relatively remained the same over the past 5 years, (Table 4.1) this is mainly attributed to little or no change in coal combustion techniques employed at the plant. Some of the major chemical compositions present in the fly ash as measured by X-ray fluorescence (XRF) are Fe_2O_3, Al_2O_3, and SiO_2. When combined, these oxides constitute about 97% of the fly ash composition while the unburnt carbon measured as loss on ignition (LOI) makes up only about 2%.
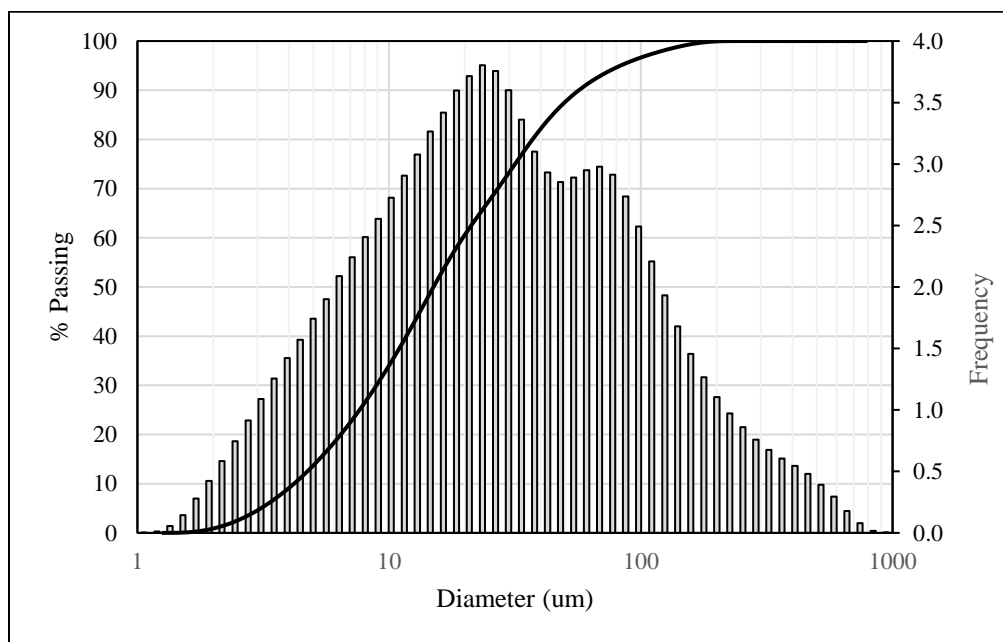

Figure 4.1 PSD curve for fly ash

Table 4.1 Chemical composition of fly ash over time

Element Oxide (%)	March* 2017	April 2017	June 2017	July 2017	June 2013
	(%)	(%)	(%)	(%)	(%)
Total Carbon	NA	NA	NA	NA	NA
Total Sulphur	0.24	0.20	0.11	0.20	NA
Al_2O_3	27.70	28.60	29.50	28.30	29.48
BaO	NA	NA	NA	NA	NA
CaO	1.31	1.44	1.26	1.50	1.49
Cr_2O_3	1.54	NA	NA	NA	NA
Fe_2O_3	8.39	6.85	6.96	8.70	6.21
Na_2O_e*	1.20	1.28	2.11	0.59	0.59
K_2O	0.50	0.49	2.76	2.45	NA
MgO	1.54	1.57	1.06	0.89	0.87
MnO	NA	NA	NA	NA	NA
Na_2O	0.87	0.96	0.29	0.36	NA
P_2O_5	0.19	0.18	0.15	0.20	NA
SiO_2	55.80	55.10	55.30	52.90	55.17
TiO_2	2.44	2.62	1.24	1.41	NA
SrO	NA	NA	NA	NA	NA
V_2O_5	NA	NA	NA	NA	NA
LOI	NA	NA	NA	NA	1.92
SO_3*	0.59	0.50	0.28	0.49	0.39
Total	99.33	98.31	98.79	97.20	NA
$SiO_2 + Al_2O_3 + Fe_2O_3$	91.89 (>70)	90.55 (>70)	91.40 (>70)	89.90 (>70)	90.86 (>70)

*used for this study

The XRD analysis of the minerals in the fly ash shows that mullite, quartz and magnetite were the predominant phases present in the fly ash. The glassy/amorphous phases were also identified but not quantified.

4.1.3 Quicklime (CaO)

Quicklime used for this study is commercially available and was provided by Lhiost North America. The inclusion of quicklime in the mix was to provide additional portlandite ($Ca(OH)_2$) to aid the pozzolanic nature of fly ash cementitious reactions. Physical and

chemical characteristics of the quicklime were provided by RJ Lee Group Inc. The quicklime had a mean particle size of approximately 20 μm with about 50% of its particles having a diameter of 8.6 μm as measured by a laser diffraction particle size analyzer with 100% (by volume) finer than 262 μm. The full particle size distribution and frequency curve of the quicklime is included in the Appendix. Isopropyl alcohol was used as the dispersant for this analysis for the particle size analysis. The specific gravity for this quicklime was determined to be 3.297 in accordance with ASTM D5550 "Standard Test Methods for Specific Gravity of Soil Solids by Gas Pycnometer."

A breakdown of the elemental oxide composition for the lime as measured by XRF showed that this quicklime contained 95.0% CaO, about 0.97% SiO_2, 0.77% MgO, while other oxides such as Fe_2O_3, Al_2O_3, K_2O and SO_3 when combined make up about 2%. The loss on ignition (LOI) of 2.52 was measured for the quicklime at 650°C. The mineral composition of the lime as measured by XRD is presented in Table 4.2. Quantitative analysis of the mineral composition measured by XRD-Rietveld analysis shows that 90% and 7% of the total composition of the lime are CaO and portlandite respectively

Table 4.2 XRD/Rietveld mineral composition of lime

Phase	Composition	Concentration (weight %)
Lime	CaO	90
Portlandite	$Ca(OH)_2$	7
Calcite	$CaCO_3$	1
Magnetite	Fe_3O_4	1
Periclase	MgO	1
Brucite	$Mg(OH)_2$	<1
Quartz	SiO_2	<1
Unkown(s)	-	Trace

4.2 Experimental Design

Understanding the hydration kinetics of blended cement paste with different fly ash or quicklime replacement levels will serve as basis for future hydration studies involving more complex parameters. In addition to hydration studies being related to the performance of structural components, of interest to industry is the rate and kinetics of hydration in cement-fly ash or quicklime pastes and their effect on the formation of stable mineral phases responsible for encapsulation process. Several parameters such as quicklime replacement and water to binder ratio were held constant throughout in paste mixes in other to properly interpret hydration results and thoroughly characterize the hydration differences as fly ash replacement is increased. Since there are currently no ASTM standards stipulating mix parameters in pastes for hydration studies, paste mixes were prepared using ASTM C305 (2014) "Standard Practice for Mechanical Mixing of Hydraulic Cement Pastes" and ASTM C1738 (2018) "Standard Practice for High-Shear Mixing of Hydraulic Cement Pastes" as guidelines.

A water/binder (w/b) ratio of 0.4 was selected for the base mixes to ensure adequate moisture was maintained for continuous hydration within the paste matrixes. Also, to keep paste mixes as consistent and comparable as possible, the lime replacement level for all mixes was kept constant at 5%. For this study "binder" refers to the combined quantity or amount of cement, fly ash and quicklime in the paste mix.

As discussed in Chapter 2, the hydration kinetics for cement-fly ash paste blends are quite different when compared to straight cement paste, due to the dilution effect from fly ash as well as the consumption of the portlandite $Ca(OH)_2$ when forming additional C-S-H minerals during the pozzolanic reaction of fly ash, according to Sakai et al. (2005). To

confirm and investigate this effect of fly ash replacement in the paste hydration, the first four paste mixes contained fly ash replacement levels of 0%, 20%, 40%, and 95%. Fly ash replacement of cement by mass was used implying an equal amount of cement corresponding to the desired percentage replacement was substituted by fly ash, while maintaining the same total mass of each mix. This method was adopted due to the different densities (specific gravities) of the solids (cement, fly ash and quicklime). A replacement by volume will result in a reduction of the total mass of each mix with increase in fly ash replacement thereby altering the w/b ratio for each mix.

Quicklime was added to the next four mixes, the fly ash replacement levels for these four mixes were the same as the initial four mixes, however, the inclusion of lime in these mixes was achieved by further replacing 5% of the cement mass in each mix. A constant 5% replacement of cement by quicklime was maintained for all the paste mixes containing lime.

The last set of mixes assessed in this study considered the effect of additional water required to hydrate the quicklime as discussed in the literature section (Chapter 2). Based on the total mass of each mix, the preselected w/b ratio, the amount of quicklime in each mix and the stoichiometry of quicklime hydration, a new w/b ratio of 0.42 was selected for the last four set of mixes. The new selected w/b ratio ensures adequate water for the hydration of CaO to $Ca(OH)_2$ while maintaining the required moisture within the paste matrix for the continuous formation of expected hydrates. Table 4.3 provides a list and description of the full experimental design of the paste mixes.

Table 4.3 Identification for each paste mix

Mixture ID	Paste Mixture Description
P[1]	Conventional cement paste
P20FA[1]	20% of cement mass replaced w/flyash
P40FA[1]	40% of cement mass replaced w/flyash
P95FA[1]	95% of cement mass replaced w/flyash
P-QL[1]	5% of cement replaced with quicklime
P20FA-QL[1]	20% and 5% of cement mass replaced w/flyash and quicklime respectively
P40FA-QL[1]	40% and 5% of cement mass replaced w/flyash and quicklime respectively
P95FA-QL[1]	95% and 5% of cement mass replaced w/flyash and quicklime respectively
P20FA-QL-EM[2]	20% and 5% of cement mass replaced w/flyash and quicklime respectively + additional water for quicklime hydration
P95FA-QL-EM[2]	95% and 5% of cement mass replaced w/flyash and quicklime respectively + additional water for quicklime hydration
P20FA-QL-EM-SL[2]	20% and 5% of cement mass replaced w/flyash and quicklime respectively + additional water for quicklime hydration (slaked)
P95FA-QL-EM-SL[2]	95% and 5% of cement mass replaced w/flyash and quicklime respectively + additional water for quicklime hydration (slaked)

[1] Water to binder (w/b) ratio of 0.40

[2] Water to binder (w/b) ratio of 0.42

4.3 Mixing and Curing Procedures

As mentioned earlier, the mixing and casting of paste prepared in this study closely conforms to those outlined in ASTM C305 "Standard Practice for Mechanical Mixing of Hydraulic Cement Pastes" and ASTM 1738 "Standard Practice for High-Shear Mixing of Hydraulic Cement Pastes". Although paste mixes were made in batches due to certain laboratory constraints such as limited volume of the mixer, handling of materials used for each batch was kept as consistent as possible.

Three sets of paste were made in this study, with each set containing four mixes bringing the total number of mixes prepared in this study to twelve (Table 4.3).

- Paste-I: these paste mixes contained fly ash replacements of 0%, 20%, 40% and 95% in the absence of quicklime, corresponding to P, P20FA, P40FA and P95FA, respectively and at w/b ratio of 0.4.

- Paste II: involved fly ash replacements of 0%, 20%, 40% and 95% in the presence of quicklime as P-QL, P20FA-QL, P40FA-QL and P95FA-QL, respectively. Quicklime inclusion was kept constant at 5% for all mixes and was achieved by replacing 5% of the cement with an equivalent mass of quicklime and at w/b ratio of 0.4.

- Paste III: examined two paste mixes each containing 20% fly ash and 5% quicklime replacement of cement and another pair of 95% fly ash and 5% quicklime and at w/b ratio of 0.42. As elaborated previously, the w/b for these for mixes was increased to account for the moisture required to hydrate CaO to $Ca(OH)_2$.

In addition to increasing the w/b for the mixes in Paste III, the mixing method adopted for two of the four mixes was slightly different than those employed for Paste I and Paste II mixes. For Paste III mixes, one of each of the 20% fly ash and 5% quicklime, and of 95% fly ash and 5% quicklime replacements, the quicklime was slaked by first dissolving it in the mixing water rather than adding it directly to the solids. This was done to investigate the effect of readily available hydroxide, in the form of dissolved Ca^{2+} in solution, on the hydration kinetics of cement-fly ash blended pastes for both low and high fly ash replacement levels

Table 4.4, summarizes the required amount of cement, fly ash and quicklime for each mix. A 20 quart Hobart legacy mixer was used as mixing device in accordance with ASTM C305 (2014) "Standard Practice for Mechanical Mixing of Hydraulic Cement Pastes". The measured fly ash, cement and quicklime were carefully emptied into the mixing bowl to

avoid loss of material and dusting. Before adding water, the contents of the mixing bowl were slowly stirred for 1 minute to homogenize the contents of the mixing bowl. Water was then added, and mixing was initiated at speed level 1 (lowest equipment speed 60 RPM) for one and the half minute, the mixing speed was then increased (intermediate equipment speed, 150 RPM) for 30 seconds.

After a total mixing time of approximately 2 minutes, the temperature, pH and specific gravity of the wet paste was then recorded. This mixing sequence was repeated for all mixes except those for which the quicklime was slaked.

Table 4.4 Paste proportioning for laboratory testing

Paste	Mixture	OPC grams (% solids)	Flyash grams (% solids)	QL grams (% solids)	Water grams	W/b (by mass)	Total grams	Water (g) for CaO
Paste I	P	7143 (100%)	0	0	2857	0.40	10000	0
	P20FA	5714 (80%)	1429 (20%)	0	2857	0.40	10000	0
	P40FA	4286 (60%)	2857 (40%)	0	2857	0.40	10000	0
	P95FA	357 (5%0	6786 (95%)	0	2857	0.40	10000	0
Paste II	P-QL	6786 (95%)	0	357 (5%)	2857	0.40	10000	0
	P20FA-QL	5357 (75%)	1429 (20%)	357 (5%)	2857	0.40	10000	0
	P40FA-QL	3923 (55%)	2857 (40%)	357 (5%)	2857	0.40	10000	0
	P95FA-QL	0	6786 (95%)	367 (5%)	2857	0.40	10000	0
Paste III	P20FA-QL-EM	5357 (75%)	1429 (20%)	357 (5%)	2857	0.42	10114	114
	P95FA-QL-EM	0	6786 (95%)	357 (5%)	2857	0.42	10114	114
	P20FA-QL-EM-SL	5357 (75%)	1429 (20%)	357 (5%)	2857	0.42	10114	114
	P95FA-QL-EM-SL	0	6786 (95%)	367 (5%)	2857	0.42	10114	114

For the two slaked quicklime mixes P20FA-QL-EM-SL and P95FA-QL-EM-SL (20% and 95% fly ash replacement respectively), the total mixing water was added to the measured quicklime and then stirred slowly and continuously until the quicklime is dissolved. The slaking processes is highly exothermic and upon hydration of CaO to $Ca(OH)_2$, the temperature of the solution increases rapidly and releases a significant amount of heat. As a precaution, the slaked quicklime solution was allowed to cool down to room temperature to avoid the heat of the slaked solution accelerating initial hydration reaction within the paste. Once the slaked solution was deemed cool enough (about $27^{o}C$), mixing was performed following the steps employed for non-slaked batches.

Unlike conventional concrete, mortar or paste curing practices, which includes curing in water baths, or in controlled atmospheric chambers, the paste samples prepared in this study were cured under sealed curing conditions in Ziploc bags at room temperature in the lab. The sealed curing approach was adopted to eliminate accidental introduction of external moisture in to the paste mixes during the curing process to accurately compare the effectiveness of the chosen w/b on the blended paste hydration. Since hydration measurements by thermogravimetric analysis correlates the degree of hydration by estimating chemically bound water within the paste matrix, curing paste samples in water baths will negate estimation of water balance of paste mixes. A sealed curing environment was created by casting the blended pastes in 50 x 100 mm HDPE cylinder containers with lids. Once the cylindrical molds were filled with freshly mixed paste and then covered, the weight was measured and recorded before placing them in Ziploc bags, the Ziploc bags were then sealed and placed on a shelf. The atmospheric conditions of the room were

monitored over time by taking both temperature and relative humidity using a HOBO UX100 device. Samples were tested after 3, 7, 28 and 180 days.

Figure 4.2 Sealed curing paste samples

4.4 Testing of Cement Blended Pastes

Tests performed on each fresh batch included specific gravity, pH and temperature measurements. While the thermogravimetric analysis was performed on hardened paste at selected curing intervals, compressive strength test was performed on paste samples after 180 days.

4.4.1 Specific gravity of fresh mixes

The measurement of specific gravity for freshly prepared paste doubles as both a quality control check method between each batch of paste and as a paste characterization technique dependent on the quantity of each material used for a given batch of paste. The specific gravity provides a quick means of interpreting volume/mass changes as certain mix materials are either increased or reduced from batch to batch. ASTM D4380 uses the

Mud balance instrument to measure density for slurries. This method measures the weight of a fixed volume (mud balance cup) by moving a counter weight along the graduated scale of the mud balance until the spirit level is centered. Once the spirit level was centered and the instrument was balanced, the density/ specific gravity was then read directly off the graduated scale. The mud balance was used because it is time saving and has proven to be a reliable method of measuring paste density in previous laboratory and field studies. Specific gravities of all the paste mixes were measured and recorded.

Figure 4.3 Mud balance

4.4.2 pH and temperature of fresh mixes

As mentioned in Chapter 2, the pH of the pore solution plays an important role in the early dissolution of minerals which triggers hydration processes. With the inclusion of quicklime in certain mixes, it was important to measure the pH value for all freshly mixed paste batches in order to better understand the effect of quicklime on the early hydration of paste mixtures.   The Hanna HI98195/10 multiparameter waterproof meter was used in

measuring properties of the fresh paste. Hanna HI98195 Multiparameter meter is equipped with electrical conductivity, temperature and pH probes, the procedure for measuring fresh paste parameters is a very simple and direct one. The multiparameter probes were first calibrated using the required calibration solution standards in accordance with the operating manual of the instrument. After a complete mixing time of approximately 2 minutes, the probes were carefully placed in the center of each batch of freshly mixed paste, pH and temperature readings were then taken once the digital display values became stable. Additional temperature measurements were also taken using an ASTM S15F (2014) "Non-Mercury Thermometer.
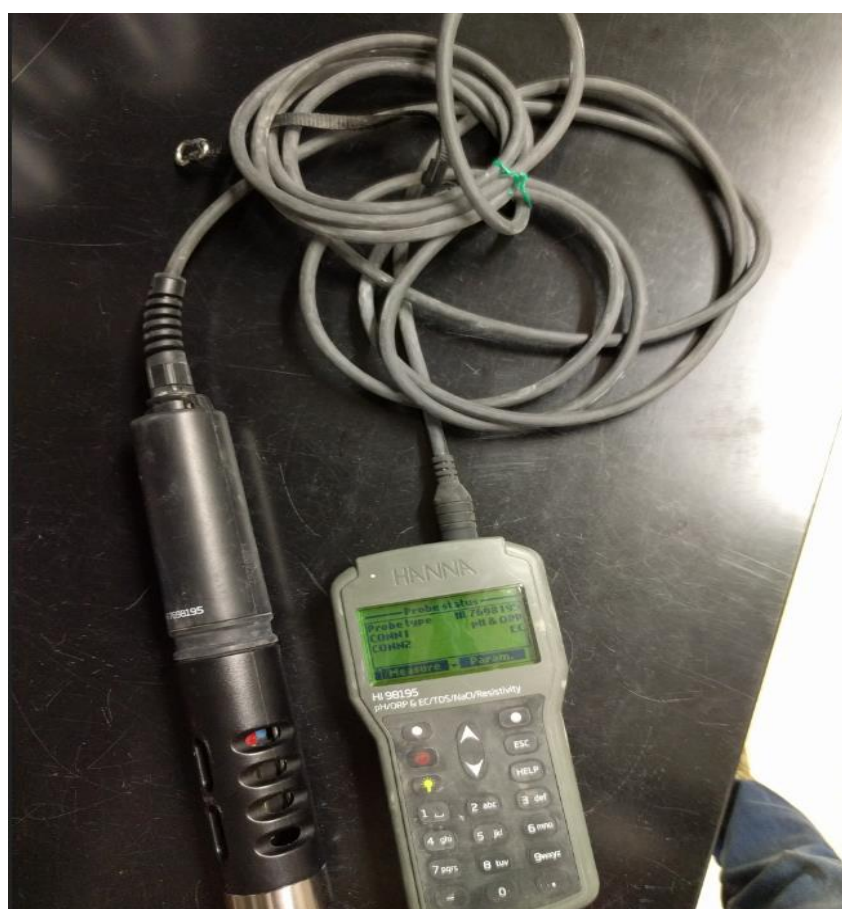

Figure 4.4 Hanna HI98195 multiparameter meter

4.4.3 Thermogravimetric analysis (TGA) of cured samples

Thermogravimetric analysis technique is one of the oldest and most reliable methods adopted in monitoring hydration rate and progress in cement chemistry. Apart from being a reliable method of monitoring hydration in cementitious systems, the TGA experiments are relatively cheaper compared to other hydration monitoring techniques and also does not require high technical skill to interpret the results from these tests. Changes in the known weight of a specimen is monitored as it either cooled or heated at a controlled rate. For this study the SDT Q600 manufactured by TA instruments was used for thermogravimetric measurements. The SDT Q600 furnace has a heating capacity of up to 1500^OC and can measure differential heat flow by differential scanning calorimetry (DSC).

At selected curing intervals of 3, 7, 28 and 180 days, thermogravimetric tests were performed on all mixes to assess the level of hydration at that given time. Samples were first crushed using the TestMark compressive strength machine, before breaking them further using a mortar and pestle to make the paste particles finer. TGA tests performed for all paste mixes were done on the exact day or $\pm$ 24 hours of the selected curing intervals mentioned above. For this study, an alumina crucible was used and about 20mg-30mg of the crushed paste was heated at a constant rate of 20^oC/min from room temperature to 1000^OC and then allowed to cool down with nitrogen as protective or purge gas.

4.4.4 Hydration halting and storage

Hydration halting techniques were only performed on all mixes at 28 curing days to assess the effectiveness of freezing crushed samples at $-80\ ^O\text{C}$ and microwaving samples to remove moisture and prevent further hydration. This was done to establish a suitable standard procedure for stopping hydration in cement-fly ash-quicklime blended pastes in

situations where hydration measurements are not taken at the desired time. At the selected curing interval 28 days, two separate portions of about 10-15 grams were taken from the crushed paste prepared for TGA measurement. A portion was kept in a freezer at -80°C to halt any further chemical reactions within the specimen. The second portion was microwaved at 2-minute intervals until there was no significant change in weight. The microwave technique was recommended by Saraya (2010) to be the most efficient method in halting hydration compared to both solvent and dry freezing. Both sets of halted samples were stored and tested by TGA after 30, 60 and 90 days after halting hydration. The results obtained from both of these hydration halting methods were compared with TGA measurements of samples tested at the 28-day curing interval and the results will be discussed in separately subsequent sections of this study.

4.4.5 Compressive strength

Compression strength test was performed on all samples except mix P95FA due to its fragile state at the time of this test. Duplicate 50 x 101 mm paste cylinder were crushed using the universal testing machine (UTM). Paste samples were demolded, before sulfur caps were placed at the top and bottom of the demolded cylinders and then centered on the base platen of the UTM. Once the sample was centered and the distance between the top platen and top sulfur cap was zeroed, the compression loading was initiated load until the sample failed. The compression test was performed in accordance with ASTM C39 (2018) "Standard Test Method for Compressive Strength of Cylindrical Concrete Specimens".

CHAPTER 5 RESULTS AND ANALYSIS

Prior to casting specimens for hydration and for engineering property studies, properties of freshly made paste mixes were tested under controlled laboratory conditions at UNC Charlotte in accordance with the ASTM standards governing these tests; ASTM D4380 (2012) and ASTM S18F (2014). Each batch of paste was prepared in accordance with the laboratory method practices to ensure uniformity between mixes.

5.1 Experimental Result for Fresh Paste

This section presents the pH, temperature and specific gravity measurements on freshly made paste batches. The results clearly show the specific gravity of each mix is dependent on the quantity of individual source materials in each mix. Table 5.1 shows that the specific gravity decreases with increase in fly ash content for all mixes with and without quicklime. Since the fly ash had a specific gravity of 2.53, while the cement and the quicklime had a specific gravity of 3.15 and 3.30, respectively, for a given mass of cement or lime replaced, more volume is occupied by the replacement mass of fly ash. An equivalent specific gravity for each paste mix was calculated using the specific gravities and the percentage amount of each individual material and was compared with experimental specific values

The addition of quicklime resulted in a marginal increase in pH values of the fresh pastes. As seen in Table 5.1, pH values measured for all mixes were within a range of 12.1 to 13.3, slightly skewed lower to the typical pH range 12.5 -13.3 for fresh cement paste specified by Bach et al. (2012). For paste batches containing additional water, slaking of quicklime resulted in a decrease in pH values compared to batches of similar mix ratios. While the temperature measured for pastes without quicklime were between $22^{O}C$ and

26^OC with an average temperature of 23.8^OC, slightly higher temperature values were measured for paste mixes with quicklime. This was expected, as the hydration of CaO to $Ca(OH)_2$ is highly exothermic (Fourmentin et al., 2015), and can contribute to the overall increased temperature of the paste mixes. Temperatures as high as 53^oC and 40^oC were recorded during and after slaking of quicklime respectively, though the temperatures after paste mixing were only slightly higher than equivalent un-slaked mixes.

Table 5.1 Fresh paste properties.

Mixture ID	Temperature (ºC)			S.G		pH
	During Slaking	After Slaking	After Mixing	Calculated	Experimental	
P	-	-	26	1.95	1.91	13.22
P20FA	-	-	22	1.91	1.87	13.08
P40FA	-	-	22	1.87	1.81	12.65
P95FA	-	-	25	1.77	1.68	12.10
P-QL	-	-	28	1.95	1.91	13.23
P20FA-QL	-	-	31	1.91	1.93	13.10
P40FA-QL	-	-	32	1.87	1.86	13.04
P95FA-QL	-	-	33	1.77	1.72	13.10
P20FA-QL-EM	-	-	30	1.92	1.90	13.15
P95FA-QL-EM	-	-	31	1.88	1.67	12.62
P20FA-QL-EM-SL	53	40	35	1.92	1.91	12.91
P95FA-QL-EM-SL	48	37	33	1.88	1.72	12.53

5.2 TGA Results

The TGA data shows the percentage weight loss versus temperature changes for the cement-fly ash-quicklime mixes. The differential thermogravimetric analysis method (DTG) is usually adopted in presenting the rate of weight loss measurements and identifying the temperature region of weight loss occurrence for TGA. The DTG shows the first order derivative of weight lost either as a function of temperature or time, this study presents DTG as a function of temperature. As mentioned earlier in Chapter 2, common solid mineral phases present in cementitious systems decompose at certain temperatures.

Although different researchers have varying opinions on the decomposition regions for certain solid mineral phases as TGA experiment results may vary depending on the measurement conditions, Table 2.1, provides a summary of these common solid mineral phases and the decomposition temperatures associated with them.

DTG curves generated from TGA measurements (% weight loss versus temperature) for all the paste mixes in this study mostly follow the typically established trends/patterns in literature for ordinary Portland cement and low volume fly ash blended cement pastes. As in the previous studies in the literature, the highest weight loss for many of the pastes in this study occurred within $25^{o}C$ to $120^{o}C$, the temperature zone commonly attributed to weight loss due to evaporation of free or chemically unbound water. A detailed examination of literature on DTG curves versus temperature for ordinary Portland cement paste reveals the occurrence of some solid mineral phases (most importantly ettringite) between $20^{o}C$ to $120^{o}C$. Ettringite, which is formed in Portland cement paste when there is a low ratio of calcium sulphate ($CaSO_4$) to tri-calcium aluminate (C_3A) is one of the minerals decomposed within temperature ranges designated for free or chemically unbound water. Although ettringite may have detrimental effects in concrete in the presence of excessive calcium sulphate, its production in right quantities has excellent affinity to sorb heavy metals. This a property highly attractive to environmental agencies and utility companies in the prevention of heavy metals from mobilizing and releasing to cause environmental contamination.

Despite the above discussion on the limitation of identifying the true temperature range for evaporation of free or chemically unbound water in cement and blended cement

pastes, the TGA measurement in this study will be analyzed by assuming weight loss occurring between 25°C to 120°C is due to free chemically unbound water.

Figures 5.1 and 5.2 presents the DTG curves of fly ash blended cement paste at 7 and 180 days for fly ash replacement of 0%, 20% and 40%. The DTG curves for these cement blended pastes agreed with patterns found by Scrivener et al. (2016), and Deboucha et al. (2017). As presented in the Figures, TGA measurements for the blended cement paste indicated that the major weight loses consistently occurred between 105°C to 405°C the temperature ranges identified as corresponding to the calcium silicate/aluminate hydrates, calcium hydroxide/portlandite and calcite phases.
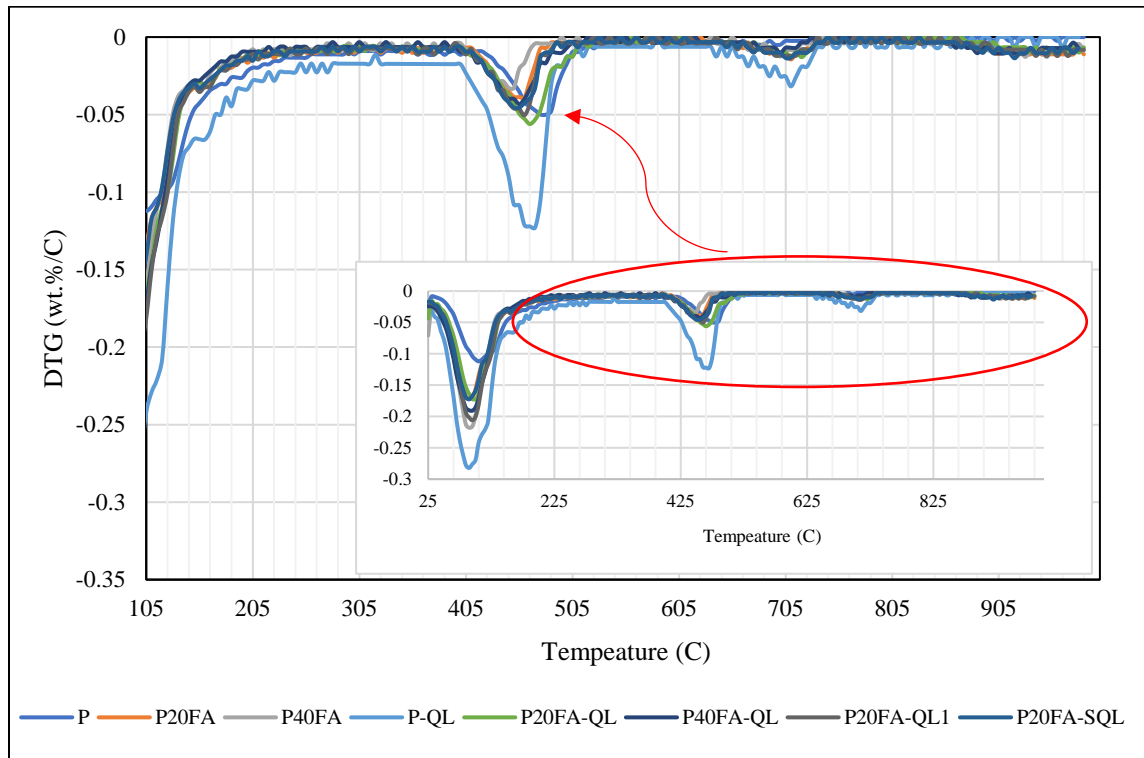
Figure 5.1 DTG curves for fly ash-cement-quicklime blended pastes at 7 days
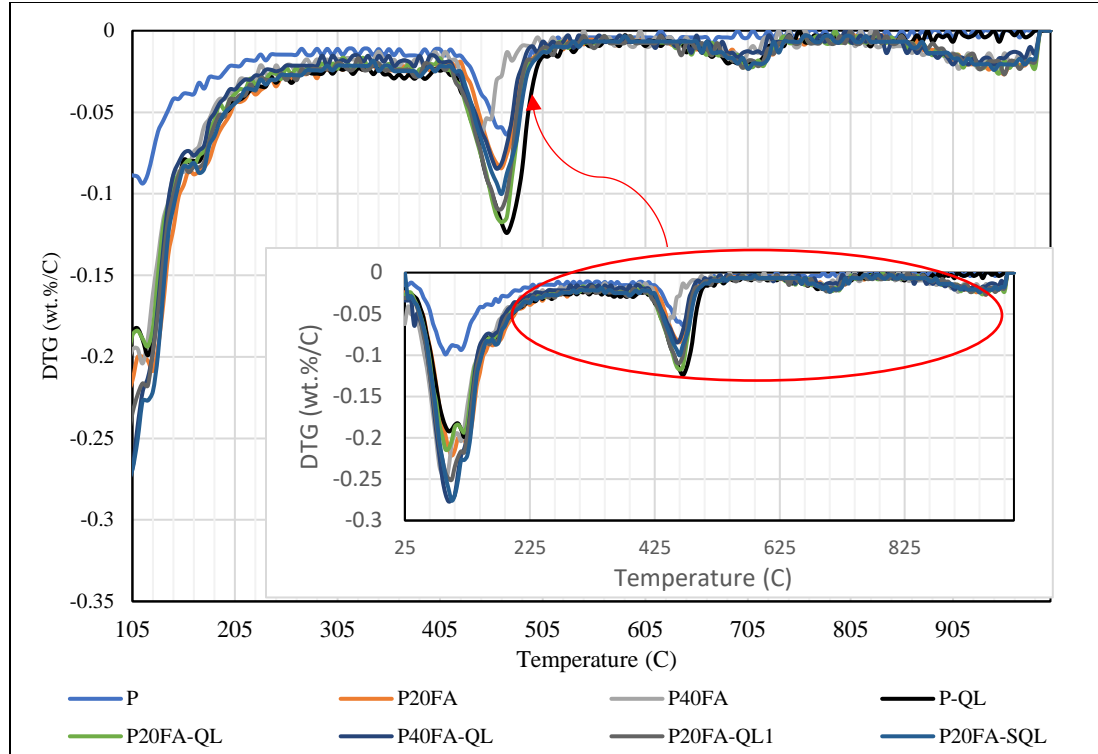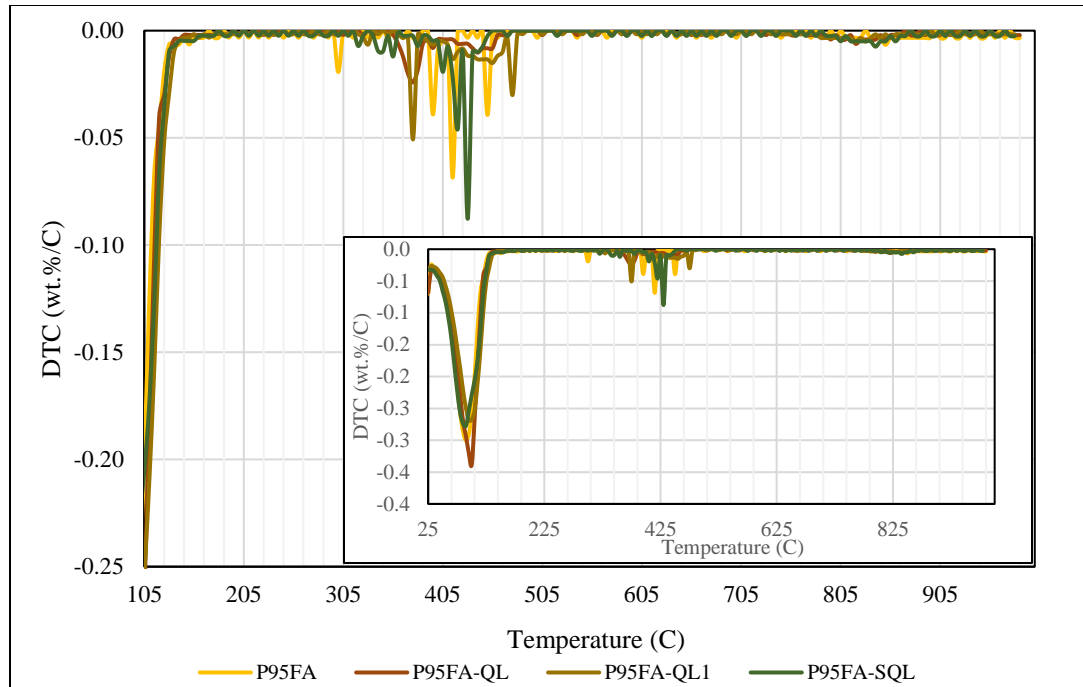(Inserted image: DTG curve over full temperature range of 25°C – 1000°C)

Figure 5.2 DTG curves for fly ash-cement-quicklime blended pastes at 180 days (Inserted image: DTG curve over full temperature range of $25^{\circ}C - 1000^{\circ}C$)

In Figures 5.3 and 5.4, although partly discernable patterns similar to those in Figures 5.1 and 5.2 are obtained for batches with 95% fly ash replacement with and without quicklime additions, other significant weight loses occurred within the $285^{\circ}C$ to $420^{\circ}C$ temperature range. These weight loses which generally fall within the range zoned as calcium silicate/aluminate hydrates merit further examination. It should be noted that Scrivener et al. (2016) have attributed the multiple weight loss between $200^{\circ}C$ to $350^{\circ}C$ to the presence of AFm (alumina, ferric oxide, monosulphate) and AFt (alumina, ferric oxide, trisulphate) mineral phases. Considering the high volume of fly ash in these batches, it is no surprise as AFm and AFt phases are typically associated with fly ash (rich in alumina and ferrioxide) and $Ca(OH)_2$ reaction in the presence of sulphate.

Figure 5.3 DTG curves for 95% fly ash-cement-quicklime blended pastes at 7 days
(Inserted image: DTG curve over full temperature range of 25ºC – 1000ºC)
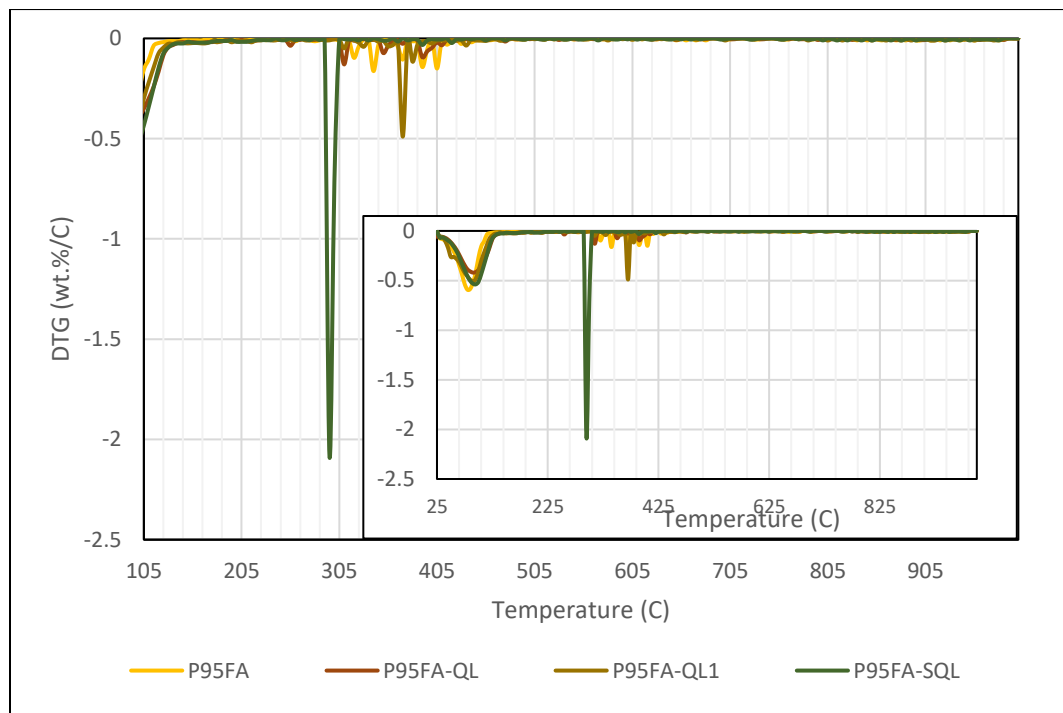

Figure 5.4 DTG curves for 95% fly ash-cement-quicklime blended pastes at 180 day
(Inserted image: DTG curve over full temperature range of 25ºC – 1000ºC)

Deschner et al. (2012) Performed hydration studies on two low calcium fly ash blended with portland cement over a period of 550 days. The XRD characterization of hydration products for these pastes showed AFm peaks due to partial replacement of OH^- by $SO4^{2-}$. These AFm phases comprises of octahedral layers and negatively charged layers with a general formula of $\{Ca^4Al^2(OH)_{12}\}^{2+}[A_{2/n}{}^{n-}.mH2O]^{2-}$, where "A" are usually mono or bivalent anions.

Based on the above DTG curves, it could be deducted P, P-QL, P20FA, P20FA-QL, P40FA, P40FA-QL are all good suitable for both structural components as well as environmental applications depending on production cost based of the formation of CSH and CAH phases and portlandite phases. Conversely P95FA and P95FA-QL and equivalent high fly ash volume mixes are only viable as paste technology for environmental applications because of the high formation of AFm and AFt phases

5.3 Degree of Hydration

Interpreting TGA measurements remains an issue for blended cement systems, however, certain equations have proven to successfully interpret these measurements. Some of the commonly used methods for interpreting hydration in cementitious systems include those proposed by Bhatty (1986), Monteagudo et al. (2014) and Pane and Hansen (2005). Table 2.3 in chapter 2 gives a breakdown of the various temperature ranges of different phases considered by these researchers. The dehydration zone (Ldh) refers to the weight loss due to decomposition of the C-S-H minerals, the dehydroxylation (Ldx) represents weight loss as a result of the decomposition of the $Ca(OH)_2$. while the decarbonation (Ldc) accounts for the decomposition of calcium carbonate, $CaCO_3$ minerals present in the hydrating paste.

On the basis of the DTG analysis and discussions in the preceding sections Figure 5.5, Figure 5.6 and Figure 5.7 are used to present the percentage weight loss versus temperature for cement-fly ash-quicklime pastes with 0%, 20% and 40% fly ash replacement after 180 days of curing for the various decomposition ranges identified by Bhatty (1986), Pane et al. (2005) and Monteagudo et al. (2014) respectively.

Applying the specified temperature ranges proposed by these 3 studies, the calculated weight loses within each zone are equivalent and the difference in values are negligible. In addition, experimental data is unavailable to use the equations proposed by Pane et al. (2005) and Monteagudo et al. (2014), analysis of the degree of hydration in this study is limited to the analysis method proposed by Bhatty (1986).

Figure 5.7 shows the percentage weight versus temperature for the 95% fly ash replacement for cement-fly ash-quicklime pastes after 180 days of curing for the decomposition ranges suggested by Bhatty (1986).

Use of the Bhatty (1986) equations has become one the most used and cited mathematical techniques for interpreting TGA measurements in cementitious systems. Equation 1 and 2 were proposed by Bhatty (1986) and was used to calculate the overall degree of hydration at each curing intervals of 3, 7, 28 and 280 days. Equation 1 represents % of chemically bound water (wb) in the system, while equation 2 calculates the degree of hydration (α)

$wb = Ldh + Ldx + 0.41 (Ldc)$ ....equation 1

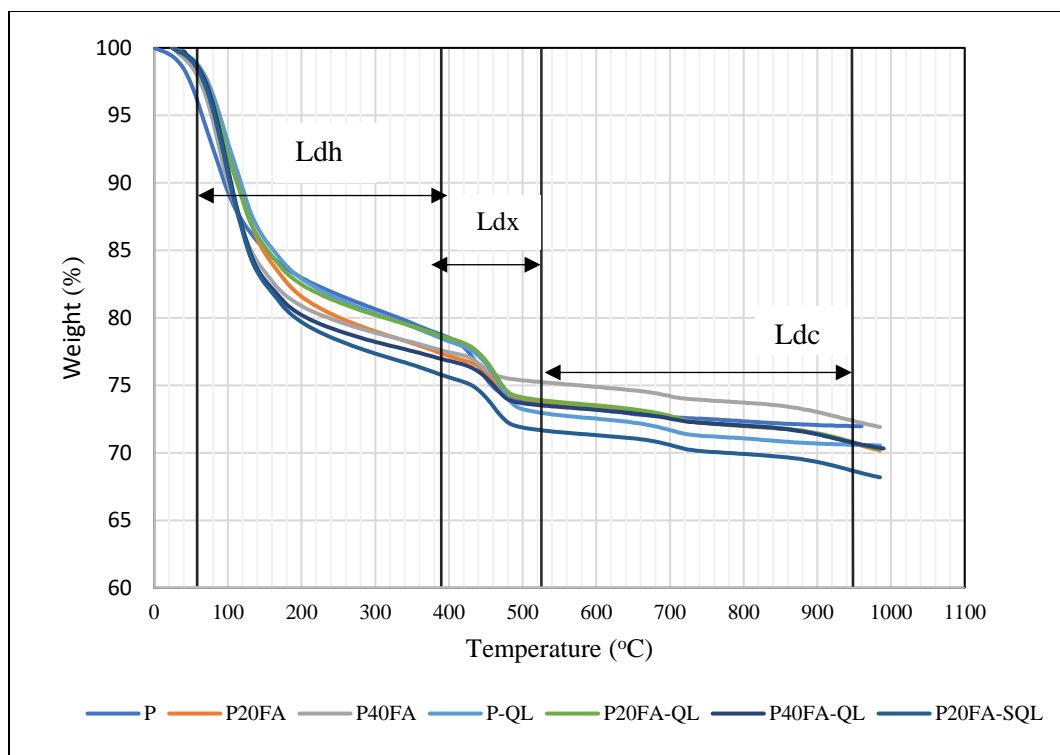$\alpha = wb/0.24$ ....equation 2

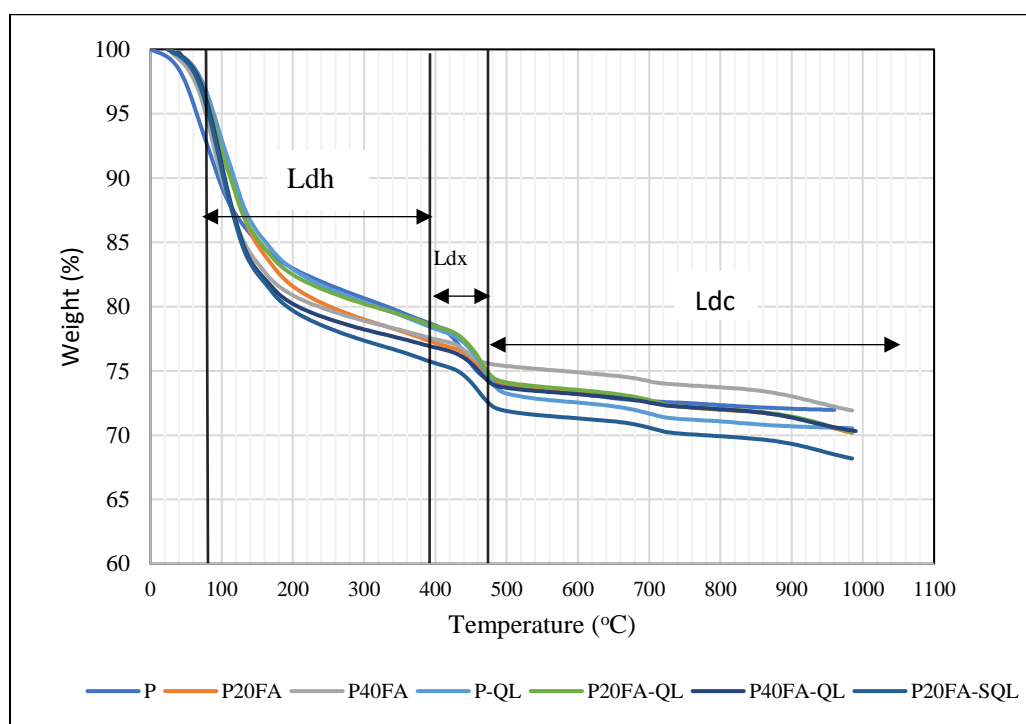Figure 5.5 Percentage weight vs temperature (Bhatty decomposition regions)

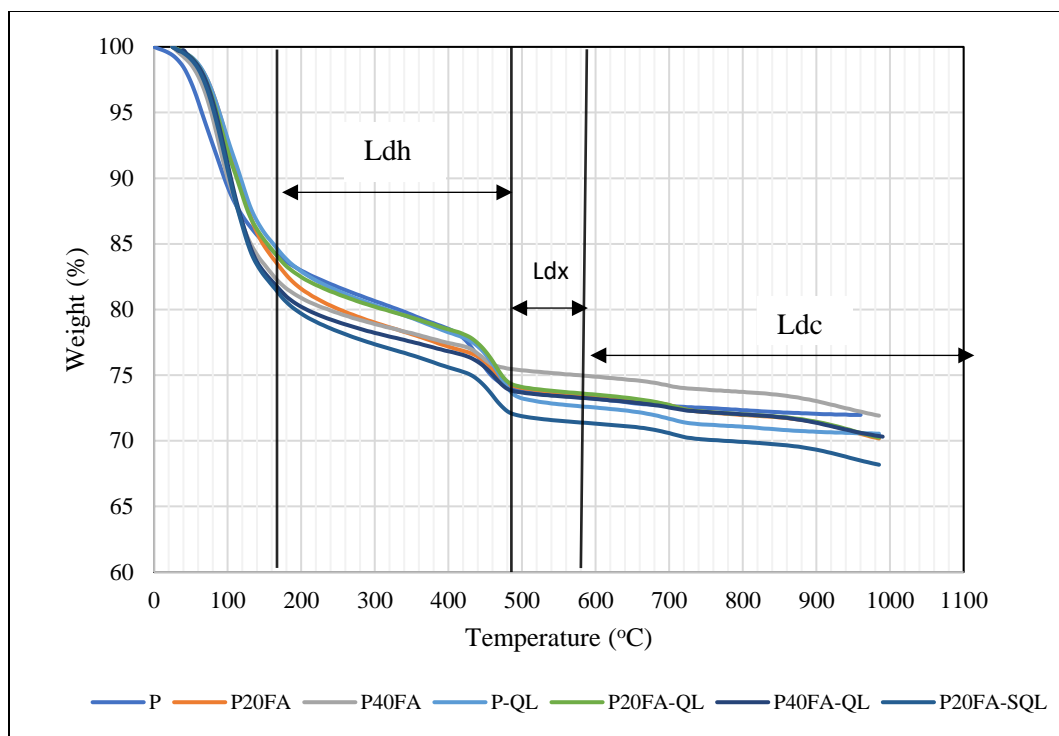Figure 5.6 Percentage weight vs temperature (Pane decomposition regions)

Figure 5.7 Percentage weight vs temperature (Monteagudo decomposition regions)
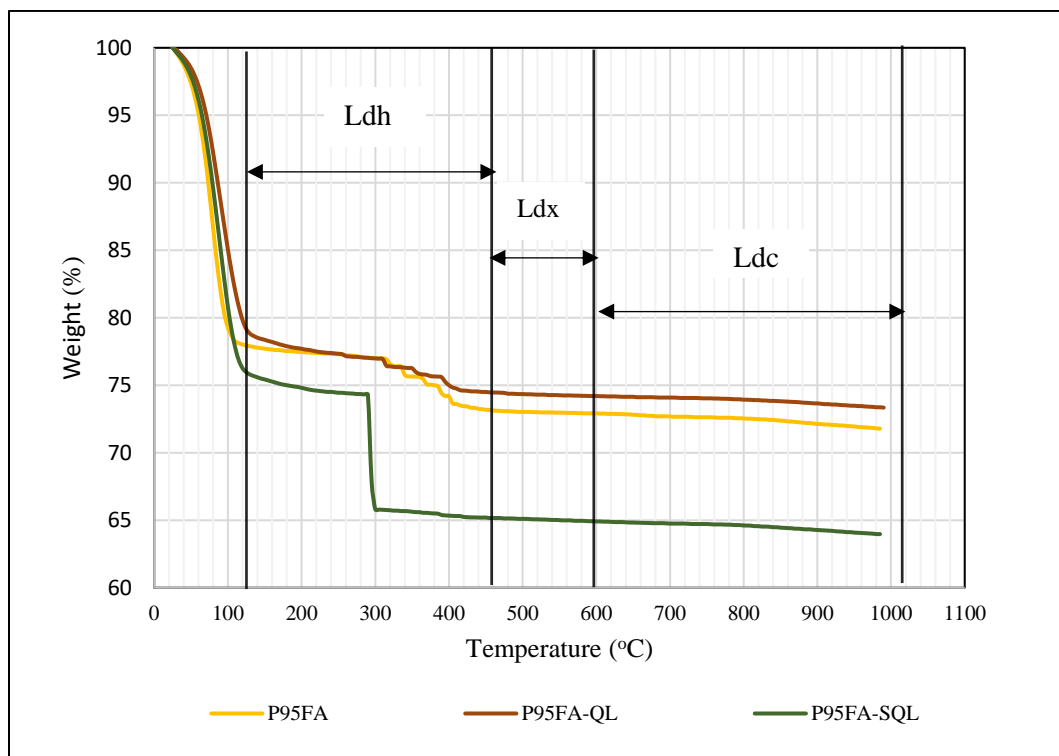

Figure 5.8 Percentage weight vs temperature (Bhatty decomposition regions)

Table 5.1 and Figure 5.9 summarize the degree of hydration over time calculated using equations 1 and 2 for all the mixes in this study.

Table 5.2 Overall degree of hydration vs time

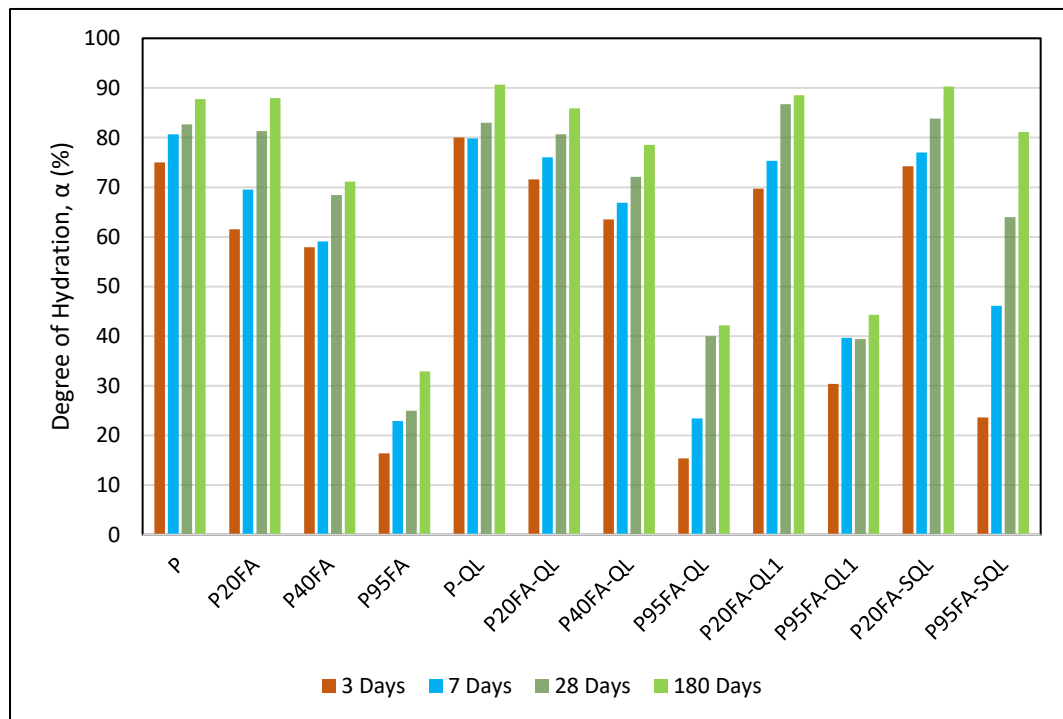| Sample	Degree of Hydration (%)			
	3 Days	7 Days	28 Days	180 Days
P	75	81	83	88
P20FA	62	70	81	88
P40FA	58	59	68	71
P95FA	16	23	25	33
P-QL	80	80	83	91
P20FA-QL	72	76	81	86
P40FA-QL	64	67	72	79
P95FA-QL	15	23	40	42
P20FA-QL-EM	70	75	84	89
P95FA-QL-EM	30	40	39	44
P20FA-QL-EM-SL	74	77	87	90
P95FA-QL-EM-SL	24	46	64	81

Figure 5.9 Degree of hydration vs time for cement-fly ash-quicklime blended pastes

5.3.1 Effect of fly ash replacement on hydration of blended cement paste

As shown in Table 2.3, the measured weight loss for the various mineral phases is an indicator of the state of hydration, with Ldh representing the amount of calcium silicate hydrate (CSH)/calcium aluminate hydrate (CASH), while Ldc and Ldx represent the measures the $Ca(OH)_2$ and $CaCO_3$. Increased amounts of Ldx (portlandite) can also be directly correlated to increased level of hydration Sakai et al. (2005) in straight Portland cement paste. As expected, weight loss corresponding to each mineral phase increases with increase in curing duration. The weight loses caused by the decomposition of the mineral phases in the straight mix (P) decrease as the corresponding temperature increases i.e. Ldh >Ldc > Ldx.

Table 5.3 TGA weight loss for cement-fly ash blended paste

Curing Time in Days		Weight Losses			Degree of Hydration (%)
		Ldh	Ldx	Ldc	
P	3	13.7	3.8	1.2	75
	7	14.6	4.2	1.3	81
	28	14.9	4.4	1.5	83
	180	15.3	5.1	1.6	88
P20FA	3	12.2	1.7	2.0	62
	7	12.9	2.3	3.4	70
	28	15.2	2.9	3.5	81
	180	16.4	3.2	3.7	88
P40FA	3	11.4	1.2	3.2	58
	7	11.4	1.5	3.3	59
	28	13.2	1.9	3.4	68
	180	13.8	1.9	3.5	71
P95FA	3	3.3	0.2	1.1	16
	7	4.7	0.3	1.2	23
	28	4.8	0.2	1.3	25
	180	6.9	0.4	1.5	33

Comparing the weight losses associated with mineral phases formed as hydration progresses at any instance shows that solid phases being formed decreases as fly ash replacement increases. This implies that with increased fly ash replacements, lesser hydration products are being formed. Deschner et al. (2012) attributed the decrease in the calcium silicate and aluminate hydrates measured (Ldh) to the dilution effect of fly ash which reduces the amount cement which contains C_3S silicate necessary in formation of calcium silicate/aluminate solid mineral phases. This dilution effect was only noticed in the early stages up to 7 days in the cement blended paste with 20% fly ash, and became less evident with time as the measured weight loss for Ldh increased and was relatively similar to mix P (0% fly ash) between 28 and 180 days. This can be attributed to commencement of the pozzolanic hydration reaction of the fly ash in mix P20FA. However, the dilution effect was greater for cement blended paste with fly ash replacement levels greater than 20% as seen in Table 5.3. The increasing weight loss measured for the portlandite (Ldx) solid mineral phases with time for all cement/fly ash blended pastes in Table 5.2 confirms that portlandite increases as hydration progresses (Sakai et al. (2005).

TGA analysis after 3 days indicates the degree of hydration as 75% for mix P (straight paste with no fly ash) with mixes P40FA and P95FA having hydration levels at 48% and 16%. Mix P20FA had a degree of hydration of 62%, 13% lower than straight mix P. At 28 days of curing, however, mixes P, P20FA, P40FA and P95FA had achieved degree of hydration of 83%, 81%, 68% and 25% respectively. After 180 days mix P20FA had achieved an equal degree of hydration of 88% with straight mix P, while mix P40FA and P95FA had achieved hydration of 71% and 33% respectively. The time dependent degree

of hydration of all the fly ash blended cement pastes (0%, 30%, 40% and 95%) are shown
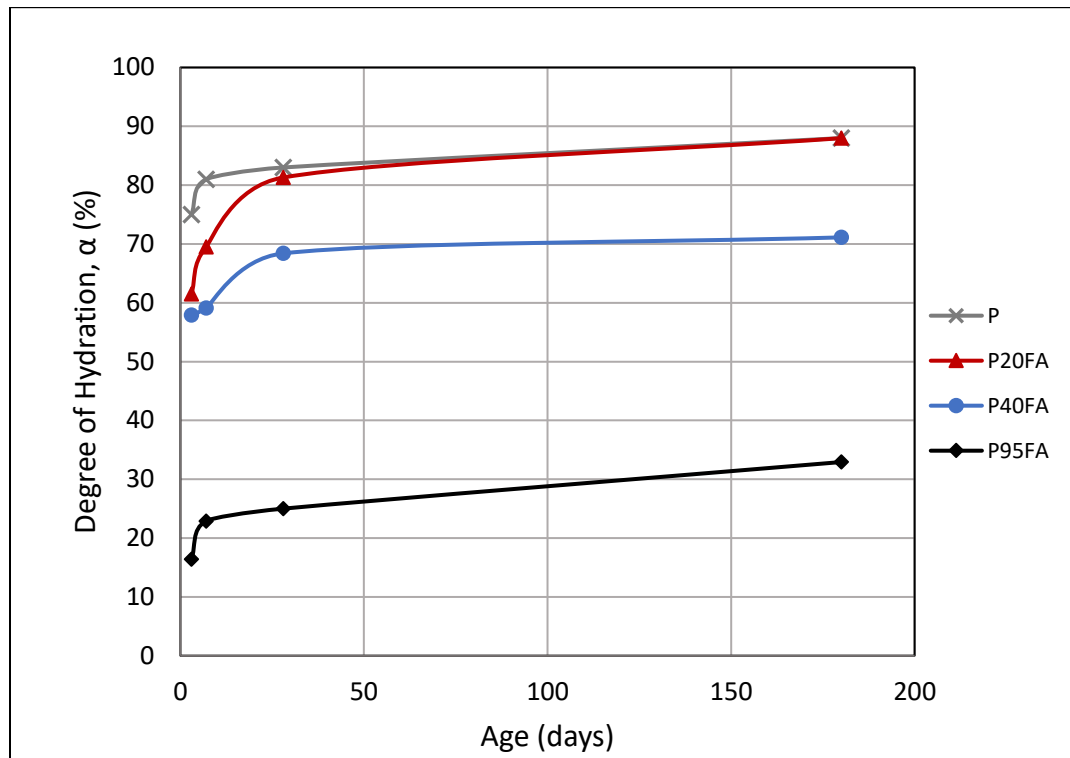
in Figure 5.10

Figure 5.10 Hydration vs time for blended paste with increasing fly ash replacement

As shown in Figure 5.10, up to curing age of 50 days, the degree of hydration

measured from TGA decreases with increasing fly ash replacement. After 50 days of curing

20% fly ash replacement achieved relatively the same degree of hydration with the straight

Portland cement paste. Blended mixes with fly ash replacement level greater than 20%

showed a lower degree of hydration compared with the straight mix. The lowest degree of

hydration seen in the bended paste occurs for cement-fly ash blended paste with fly ash

and cement content of 95% and 5% respectively. This confirms previous hydration studies

by Deboucha et al. (2017), Deschner et al. (2012) and Langan et al. (2002), showing that

both the heat of hydration and degree of hydration is affected by increasing replacement

levels of additives like fly ash, blast furnace slag and lime fillers. This has been attributed

to both the dilution effect and the pozzolanic reactive nature of additives like fly ash. The dilution effect appears viable for cement/fly ash blended cementitious systems with high fly ash volume at all stages of hydration considered in this study and only at early stages for low fly ash replacements blended systems. The gain in hydration after 28 days for the 20% fly ash replacement can be attributed to the dissolution and chemical reaction of the reactive pozzolans in the fly ash in agreement to the findings of Deschner et al., (2012).

5.3.2 Effect of quicklime on hydration of fly ash blended paste.

With established evidence that fly ash reacts with portlandite, $Ca(OH)_2$ in a pozzolanic reaction to form additional C-S-H minerals (Antiohos et al., 2006) , quicklime (CaO) was added to the fly ash blended paste to assess its effect on hydration.

Table 5.4 TGA weight loss for fly ash-cement-quicklime blended pastes

Curing Time in Days		Weight Losses			Degree of hydration (%)
		Ldh	Ldx	Ldc	
P-QL	3	14.0	4.3	2.0	80
	7	13.9	4.4	2.2	80
	28	14.4	4.6	2.3	83
	180	16.0	4.9	2.2	91
P20FA-QL	3	12.3	3.6	3.2	72
	7	13.3	3.6	3.2	76
	28	14.0	3.9	3.6	81
	180	14.9	4.2	3.7	86
P40FA-QL	3	11.6	2.3	3.2	64
	7	12.3	2.5	3.1	67
	28	12.7	3.3	3.3	72
	180	14.5	3.0	3.3	79
P95FA-QL	3	2.9	0.2	1.3	15
	7	4.5	0.6	1.2	23
	28	9.4	0.9	1.1	40
	180	9.1	0.4	1.6	42

Comparison of TGA measured weight loss at the various decomposition regions for these set mixes with those in Table 5.3, revealed greater weight loss in the Ldx region, a

clear indication of decomposition of the additional $Ca(OH)_2$ from quicklime. Slight to moderate additional (0.3% to 4.6%) weight loss measured for Ldh and Ldc across all these mixes.

As seen in Table 5.4, quicklime addition resulted in increased early hydration by approximately 3% - 15% in mixes P-QL, P20FA-QL and P40FA-QL, when compared with paste mixes with similar fly ash replacement without quicklime. Although P95FA-QL showed no significant increase in early (3 days and 7 days) hydration when compared with P95FA, an additional hydration of 15% was noticed after 28 days. This low early hydration could possibly be due to the slow reaction between quicklime and siliceous minerals present in the fly ash which are not readily available and may take more than 7 days for the pozzolanic reaction to initiate in fly ash according to Huang et al. (1986) and also due to the lack of C_3S and C_3A readily available in cement not being present in quicklime.

The increased hydration measured by TGA indicates that although increasing fly ash replacement level will subsequently lead to an increased demand for $Ca(OH)_2$ for fly ash pozzolanic reactions, the selected quicklime addition of 5% seemed to be sufficient for this increased demand for Ca(OH). As additional hydration ranging between 5% - 10% was measured for cement-fly ash blends with quicklime compared to fly ash cement blends without quicklime. This was most evident in mixes with higher fly ash replacement levels of 40% and 95%. A firm conclusion cannot be reached about the selected quicklime replacement level in this study, until hydration results of higher or lower replacement levels of quicklime are examined to understand its sensitivity on hydration for different fly ash contents in cement-fly ash blended paste
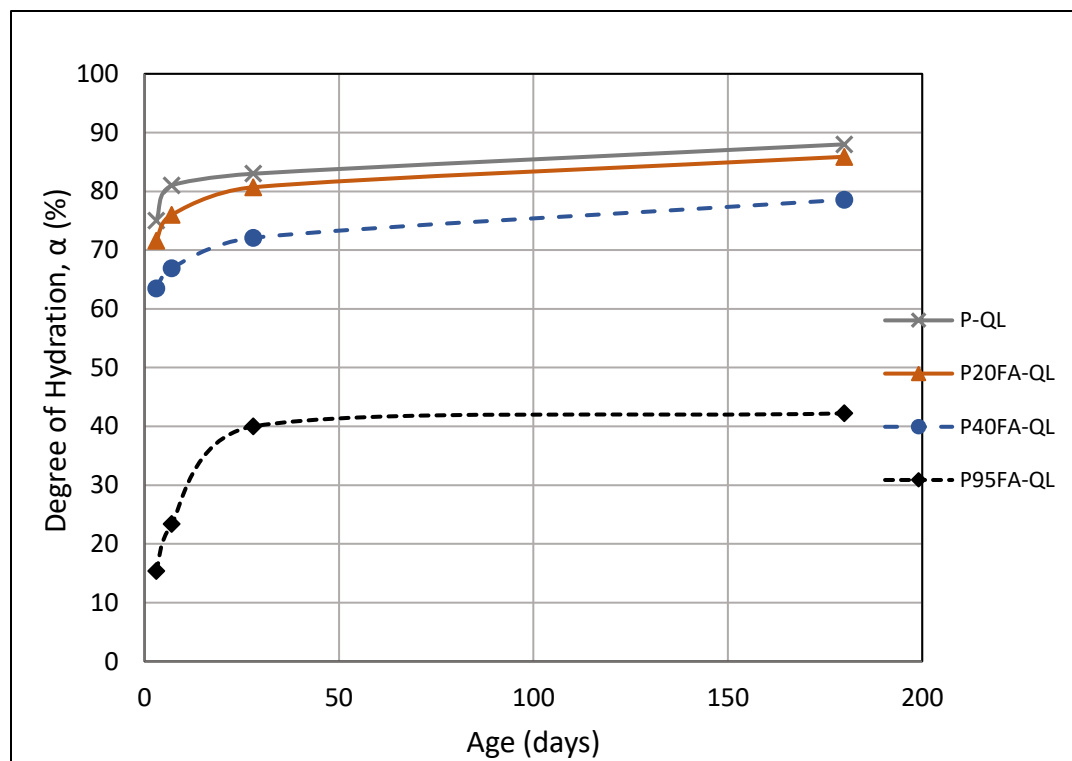
Figure 5.11 Hydration vs time for blended paste with increasing fly ash
replacement in the presence of quicklime

5.3.3 Effect of additional water and quicklime slaking on hydration

With the stoichiometric additional water required to first hydrate quicklime in the
paste solids to form Calcium hydroxide, TGA measurements of paste blends (P20FA-QL-
EM, P20FA-QL-EM-SL, P95FA-QL-EM and P95FA-QL-EM-SL) prepared with
additional amount are presented in Table 5.4.

Examination of the results from Table 5.5 reveals additional water had little to no
effect on the Ldx and Ldc weight losses for equivalent mixes (P20FA-QL-EM vs P20FA-
QL and 95FA-QL1 vs P95FA-QL-EM). However, the TGA results indicate that for mixes
containing quicklime with 20% fly ash replacement, the effect of additional water only
manifested after 28 days of curing as the weight loss measured for Ldh region increased
by an additional 2% for both slaked and un-slaked pastes (Table 5.5 and Figure 5.12). For

the mixes with 95% fly ash replacement (i.e 5% quicklime and 0% cement), the effect of additional water was significant. TGA results showed an additional weight loss of 3.5% and 5.7% for Ldh after 7 days for un-slaked and slaked mixes respectively. For the same mixes of 95% fly ash replacement, measured weight loss from TGA for the Ldh phases of the slaked mix showed an additional weight loss of almost 5.1% and 8.6% after 28 days and 180 days when compared to the un-slaked mix containing additional water. The little or no change in hydration experienced for the un-slaked mixes is an indicator that the initial w/b ratio was adequate to hydrate CaO to $Ca(OH)_2$ while leaving adequate moisture to continue paste hydration.

Table 5.5 TGA weight losses for blended pastes with additional water

Curing Time in days		Weight Losses			Degree of hydration (%)
		Ldh	Ldx	Ldc	
P20FA-QL-EM	3	12.5	3.0	3.1	70
	7	13.6	3.1	3.2	75
	28	15.7	3.7	3.6	84
	180	16.0	3.8	3.6	89
P95FA-QL-EM	3	6.3	0.6	1.2	30
	7	8.0	1.0	1.1	40
	28	8.3	0.6	1.4	39
	180	9.5	0.6	1.3	44
P95FA-QL-EM-SL	3	13.1	3.2	3.6	74
	7	13.0	3.1	3.6	77
	28	15.0	3.6	3.7	87
	180	16.5	3.6	3.6	90
P95FA-QL-EM-SL	3	4.9	0.3	1.3	24
	7	10.2	0.3	1.3	46
	28	14.5	0.4	1.2	64
	180	17.7	0.3	3.6	81

As evident in Figure 5.12, the additional water in mix P20FA-QL-EM makes no significant difference in early hydration (3 and 7 days) but slightly increase in later hydration (28 and 180 days) based on TGA measurements when compared to P20FA-QL. While the reverse is observed for P95FA-QL-EM, as the additional water seemed to have increased early hydration by almost twice the amount measured for P95FA-QL after 3 and 7 days. The effect of additional water slowly diminishes for both sets of paste blends as degree of hydration at later days for P20FA-QL-EM and P95FA-QL-EM were quite similar to degree of hydration measured for P20FA-QL and P95FA-QL respectively.
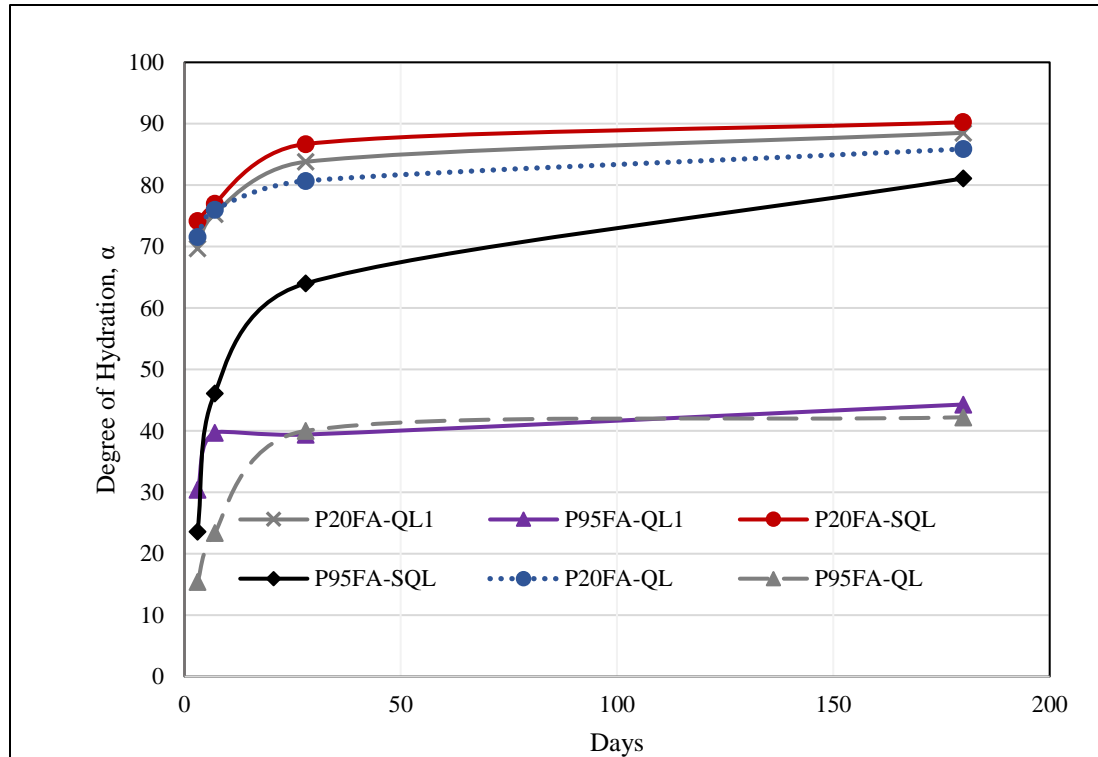
Figure 5.12 Hydration vs time for blended pastes with additional water

Comparing hydration TGA results for P20FA, P20FA-QL, P20FA-QL-EM and P20FA-QL-EM-SL (containing a minimum 75% cement content) presented in Table 5.6, the chemically bound water and degree of hydration do not differ significantly for all mixes with quicklime. However, mixes with 95% fly ash and 5% quicklime replacement of

cement content by generally result in slight increase in the degree of hydration compared

with P95FA without quicklime replacement (95% fly ash and 5% quicklime).

Table 5.6 Hydration vs time for 20% fly ash replacement blended pastes

Sample	Degree of Hydration (%)			
	3 Days	7 Days	28 Days	180 Days
P20FA	62	70	81	88
P20FA-QL	72	76	81	86
P20FA-QL-EM	70	75	87	89
P20FA-QL-EM-SL	74	77	84	90

Table 5.7 Hydration vs time for 95% fly ash replacement blended pastes

Sample	Degree of Hydration			
	3 Days	7 Days	28 Days	180 Days
P95FA	16	23	25	33
P95FA-QL	15	23	40	42
P95FA-QL-EM	30	40	39	44
P95FA-QL-EM-SL	24	46	64	81

Although mixes P95FA-QL and P95FA-QL-EM contained equal amounts of fly ash

and quicklime blends, the additional water in mix P95FA-QL-EM resulted in a noTable

increase in early hydration compared to P95FA-QL. Despite the slightly accelerated early

hydration (up to 7 days) obtained in P95FA-QL-EM due to the additional water, both sets

of mixes attained approximately the same level overall hydration after 180 days. The

increased hydration recorded for mix P95FA-QL-EM-SL when compared to P95FA-QL-

EM (same quantity of water) can be attributed to pre-hydrating CaO to Ca(OH)$_2$, rendering

dissolved Ca^{2+} readily available to react with siliceous mineral phases present in fly ash in

forming hydration products. Antiohos et al. (2006) explained in their study that the

incorporation of quicklime into fly ash blended pastes resulted in notable increase in

gel/space ratios measured by SEM and was attributed to the accelerating effect of

quicklime on the pozzolanic reaction of fly ash. This activation effect was clearly more

apparent for the slaked mix P95FA-QL-EM-SL. Porosity data was used by Antiohos et al.

(2006) to correlate and confirm this notable increase in C-S-H gel formation in the presence of quicklime.

The effect of eliminating cement by replacing the 5% cement in P95FA with quicklime in P95FA-QL, resulted in a marginal increase in hydration due to inclusion of quicklime only after 28 days. This could possibly be due to the in availability of the siliceous minerals (present in C_3S) in fly ash to react with hydroxide ions to initiate formation of stable calcium silicate/aluminate hydrates. As in Table 5.7, TGA results reveal higher weight lost in the Ldh region at 3 days and 7 days for mix P95FA compared to P95FA-QL. The measured weight loss in P95FA-QL is probably due to the formation of mainly AFm and AFt phases typical of fly ash cementitious systems induced by $Ca(OH)_2$ instead of forming more stable calcium silicate and aluminate hydrates. Further analysis by XRD method is needed to provide additional insight into which hydrated mineral phases are being formed compared to cement paste with no or lower fly ash replacement levels.

Table 5.8 Weight loss for 95% fly ash replacement pastes

Curing Time in days		Weight Losses			Degree of Hydration (%)
		Ldh	Ldx	Ldc	
P95FA	3	3.3	0.2	1.1	16
	7	4.7	0.3	1.2	23
	28	4.8	0.2	1.3	25
	180	6.9	0.4	1.5	33
P95FA-QL	3	2.9	0.2	1.3	15
	7	4.5	0.6	1.2	23
	28	9.4	0.9	1.1	40
	180	9.1	0.3	1.6	42

5.4 Effect of Hydration Halting Techniques and Storage by TGA Measurement

TGA halting techniques were tested in order to determine the most suitable method for halting hydration in cement-fly ash-quicklime blended paste, in cases where TGA

measurements are not take immediately. TGA measurements were taken on selected specimens halted after 30, 60 and 90 days of halting to assess the effectiveness of the selected halting techniques by freezing at 80ºC or by microwaving. Table 5.9 summarizes the result from this TGA measurements performed on these specimens. Comparing the degree of hydration at the time of halting (28 days) with both methods, it is evident that these methods are not the most efficient in halting hydration. The microwave technique seems to disintegrate the hydrates which reduces the chemically bound water as well as the degree of hydration. Although chemically bound water and overall hydration measured for the frozen samples are slightly closer to chemically bound water and hydration recorded at the time they were frozen for certain paste blends like P-QL, this method cannot be completely recommended for adoption due to As seen in Table 5.9, hydration measured after 30 days, 60 days and 90 days for samples that were frozen are not constant as Hydration seem to reduce with time for certain mixes, while it fluctuates for the others

Table 5.9 Halted hydration vs time

Mix	Degree of Hydration at Time of Halting	Measured Degree of Hydration After Hydration is Halted					
		30 Days After		60 Days After		90 Days After	
		Micro-wave	Freezer (-80C)	Micro-wave	Freezer (-80C)	Micro-wave	Freezer (-80C)
P95FA	23	7	33	10	35	14	34
P-QL	83	63	92	65	86	66	85
P95FA-QL	45	10	40	8	34	12	32
P95FA-QL-EM	39	13	36	15	49	9	35
P95FA-QL-EM-SL	64	12	43	11	39	11	16

5.5 Compressive Strength

Compressive strength test for all mixes after 180 days of curing was performed on 50 x 101 mm cylinders in accordance ASTM C39. Three specimens were crushed for each paste mix and the average values of are presented in Table 5.10 for all paste mixes except for P95FA which had not developed enough strength and crumbled after demolding. A linear correlation could not be established between hydration and compressive strength for the cement-fly ash-quicklime blended paste mixes in this study at 180 days, as compressive strength test are usually performed on concrete or mortars. This is due to the compressive strength being dependent on a combination of both the paste and aggregate materials in the cementitious matrix. In typical cement-fly ash blended concrete, early compressive strength decreases with fly ash inclusion but could also result in the development of additional long-term strength compared to straight concrete (Zhang, et al. 1995) depending on the fly ash replacement level. Table 5.10 shows that Mix P20FA had a significantly higher compressive strength after 180 days compared to the straight paste Mix P, despite both mixes relatively attaining the same level of hydration after 180 days. This could be as a result of a denser matrix caused by the unreactive portion of the fly ash, as fly ash is formed during a rapid cooling process after coal combusted resulting in fly ash particles having a dense crystalline core (unreactive) surrounded by the amorphous/glassy (reactive) minerals that are consumed in the pozzolanic hydration reactions (Ramezanianpour 2013). An ANOVA procedure using SAS was also performed to establish a statistical correlation between TGA hydration and compressive strength data.

Table 5.10 Compressive strength data for cement-fly ash-quicklime at 180 days

Mix	Maximum Load	Compressive stress at Maximum Load	Compressive extension at Maximum Load	Load at Break (Standard)	Modulus
	(lbf)	(psi)	(in)	(lbf)	(ksi)
P	12508	3982	0.09	11282	519
P20FA	18918	6022	0.16	17848	277
P40FA	11500	3660	0.14	10493	294
P95FA	-	-	-	-	-
P-QL	8865	2822	0.13	7865	244
P20FA-QL	5550	1767	0.13	5000	79
P40FA-QL	12433	3957	0.15	9757	287
P95FA-QL	1968	626	0.09	86	49
P20FA-QL-EM	10236	3258	0.12	9900	243
P95FA-QL-EM	807	257	0.13	197	13
P20FA-QL-EM-SL	13269	4224	0.07	12109	379
P95FA-QL-EM-SL	598	190	0.06	58	14

5.5.1 ANOVA statistical analysis

The ANOVA analysis performed with SAS used the Pearson correlation method to determine the interdependency of compressive strength on data from TGA measurements. A total of eight variables were uses to run the ANOVA model. Table 5.11 provides the ID and description of these variables.

The top value in each cell of Table 5.12 shows the correlation between two variables, with positive and negative signs indicating a positive or negative dependency between two variables. While the bottom cell value shows the likelihood of the correlation above it, with a value greater than 0.05 indicating that the correlation between two variables is mostly a coincidence. The results in Table 5.12 shows that degree of hydration (α) is strongly dependent on the formation of CSH/CAH mineral phases represented by Ldh as well as the other hydrating solid phases such as portlandite (Ldx) and calcite (Ldc). Trend from the Pearson correlation analysis indicates that compressive strength is most dependent on the

peak of the DTG curve which corresponds to the calcium silicate and aluminate hydrate decomposition regions for TGA measurements of the blended pastes. While the compressive strength was negatively dependent on weight loss due to free moisture as seen in Table 5.12.

Table 5.11 ANOVA variable description

ID	Variable Description
cs	Compressive strength
ldh	C-S-H/ C-A-H
ldx	$Ca(OH)_2$
ldc	$CaCO_3$
WtL	Weight loss due to free moisture (below 105°C)
α	Overall degree of hydration
peakDTG	Peak of DTG curve
std	Standard deviation

Table 5.12 ANOVA correlation results

Variables	cs	ldh	ldx	ldc	WtL	α	peakDTG	std
cs	1	0.7178 0.0086	0.6931 0.0125	0.5870 0.0448	-0.8432 0.0006	0.7034 0.0107	0.8048 0.0016	-0.8028 0.0017
ldh	0.7178 0.0086	1	0.7496 0.0050	0.7595 0.0042	-0.7657 0.0037	0.99375 <.0001	0.7457 0.0054	-0.6946 0.0122
ldx	0.69309 0.0125	0.7496 0.0050	1	0.3896 0.2106	-0.9155 <.0001	0.8041 0.0016	0.9198 <.0001	-0.9056 <.0001
ldc	0.5870 0.0448	0.7595 0.0042	0.3896 0.2106	1	-0.5516 0.0630	0.7386 0.0061	0.4472 0.1449	-0.4059 0.1904
WtL	-0.8432 0.0006	-0.7657 0.0037	-0.9154 <.0001	-0.5516 0.0630	1	-0.7890 0.0023	-0.9774 <.0001	0.9651 <.0001
α	0.7034 0.0107	0.9938 <.0001	0.8041 0.0016	0.7386 0.0061	-0.7890 0.0023	1	0.7707 0.0033	-0.7218 0.0080
peakDTG	0.8049 0.0016	0.7457 0.0054	0.9198 <.0001	0.4473 0.1449	-0.9774 <.0001	0.7708 0.0033	1	-0.9947 <.0001
std	-0.8028 0.0017	-0.6946 0.0122	-0.9056 <.0001	-0.4059 0.1904	0.9651 <.0001	-0.7218 0.0080	-0.9946 <.0001	1

5.6 Hydration – Strength Relationship

With limited compressive strength data (180 days only) for the fly ash-cement-quicklime blended paste due the presence of bleeding water after 28 days in the pastes of

curing, the ANOVA analysis performed on the strength and hydration data for 180 days showed positive correlation between the strength and Ldh and DTG peak from TGA measurements.

5.6.1 Strength - Hydration relationship for cement-fly ash paste

Although the established Pearson correlation from ANOVA, combined strength and hydration data for all cement-fly ash-quicklime blended paste in this study, a more detailed correlation can be established separately for cement-fly ash blended cement paste with and without quicklime. For cement-fly ash blended pastes without quicklime, Table 5.13 provides unconfined compressive strength, weight loss associated with Ldh, differential weight loss (DTG peak) from DTG curves and their corresponding temperatures. As seen in Table 5.13, an increase in calcium silicate/calcium aluminate hydrates (Ldh) corresponds to an increase in strength. It is also possible that part of the calcium silicate and aluminate hydrates are decomposing at temperatures lower than $105^{o}C$ delineated by Bhatty (1986) loss of free/chemically unbound moisture. The DTG peaks for these paste blends all fall between the $90^{o}C$ and $100^{o}C$ temperature ranges and literature has also shown that calcium silicate hydrates are decomposed over a wide range of temperature (50 to $600^{o}C$) (Mitsuda et al. 1978).

Figure 5.13 shows a regression correlation of 0.799 in support of this trend which is a close comparison to the Pearson correlation of 0.718 from the ANOVA analysis.

Table 5.13 Strength and TGA data for fly ash-cement blended paste

Mix	Ldh	DTG Peak	UCS (psi)	Temp (^{o}C)
P	15.3	-0.0991	3982	90
P20FA	16.4	-0.2215	6022	100
P40FA	13.8	-0.2545	3600	90
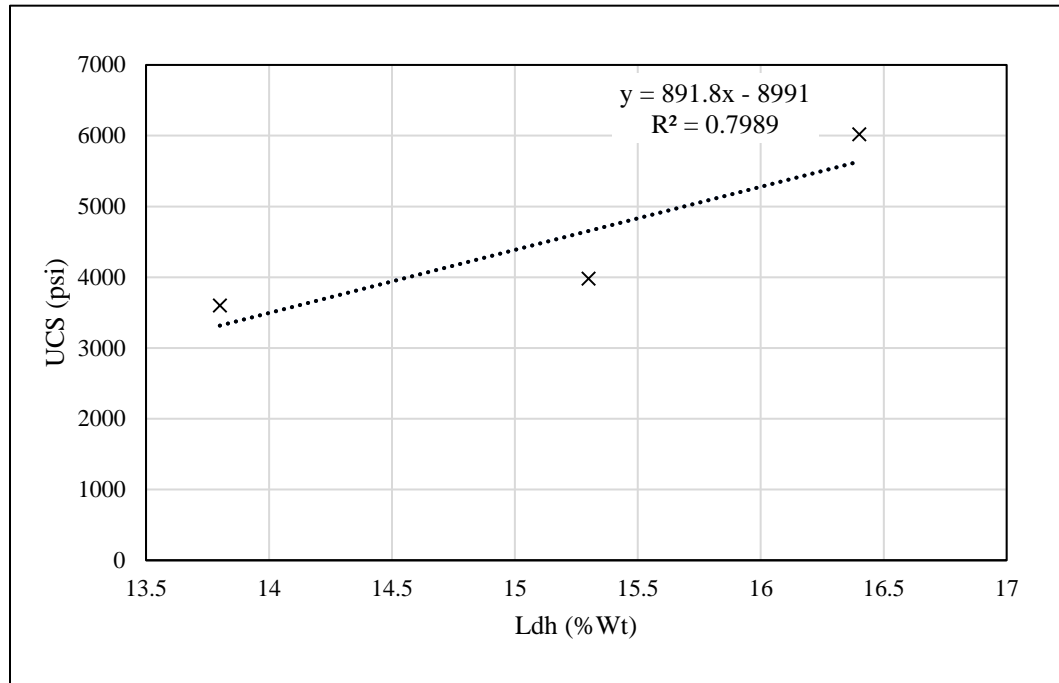
Figure 5.13 Compressive strength vs CSH/CAH for fly ash-cement pastes at 180 days.

An excel correlation of only 0.311 was established for strength versus Ldh for all blended paste prepared in this study which contradicted the ANOVA analysis. Hence the strength versus Ldh analysis was limited to just 0%, 20% and 40% fly ash replacement blended pastes without quicklime.

5.6.2 Strength - hydration relationship for cement-fly ash-quicklime paste

Comparing strength and the hydration data for the cement-fly ash-quicklime blended mixes, a regression correlation of 0.5999 between compressive strength and the peak differential weight loss (DTG peak) was established. While a direct correlation could not be established between compressive strength and calcium silicate and aluminate hydrates phases. Table 5.14 provides hydration and strength data for the cement-fly ash-quicklime blended pastes.

Table 5.14 Strength and TGA data for fly ash-cement-quicklime blended paste

Mix	Ldh	DTG Peak	UCS (psi)	Temp (ºC)
P-QL	16	-0.19906	2822	120
P20FA-QL	14.9	-0.21405	1767	90
P40FA-QL	14.5	-0.27700	3957	95
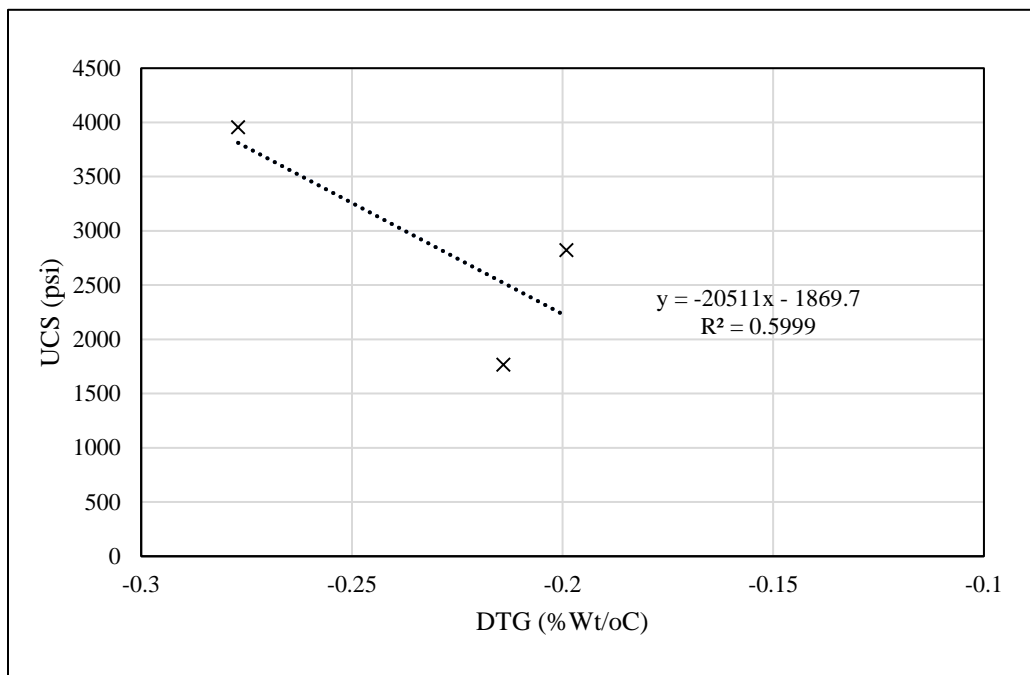
Figure 5.14 Compressive strength vs DTG peak for fly ash-cement-quicklime pastes
at 180 days

CHAPTER 6 CONCLUSIONS AND RECOMMENDATIONS

This work presents laboratory testing for hydration studies of cement-fly ash blended pastes using the thermogravimetric technique. The development of this study's mix design, and protocols for all experiments were also presented along with extensive literature forming the basis for this study. This section provides a summary of the findings of the study along with key considerations utilized in arriving at the conclusions as well as recommendations for future studies.

6.1 Findings and Conclusions

Thermogravimetric testing on the twelve cement-fly ash paste blends provided useful information supporting the use of thermogravimetric analysis as a reliable method of monitoring hydration. Key findings from this study are summarized in subsequent sections.

6.1.1 Cement-fly ash blended systems

• Results from this study confirms the dilution effect of fly ash on cement/fly ash blended systems resulting in reduction in rate of hydration for cementitious systems containing high volume fly ash replacement.

• The dilution effect of fly ash negatively affects hydration in high volume fly ash cement blends but can beneficial to cement-fly ash blended cementitious systems with moderate fly ash replacement (20% or less).

• The pozzolanic reaction of fly ash in cement/fly ash blended paste with fly ash replacement of 20% did not affect the degree of hydration until after 28 days. This resulted in the cement/fly ash blended paste with 20% fly ash achieving relatively the same degree of hydration with the straight cement paste at the end of the 180 day curing period.

6.1.2 Cement-fly ash-quicklime systems

- The inclusion of quicklime only had a slight effect on hydration for cement-fly ash blended paste when compared with cement-fly ash paste blends without quicklime. The increase in hydration due to addition of quicklime was most evident for cement/fly ash blended paste with 95% fly ash replacement.

- High fly ash replacement levels have been proven to cause bleeding (Gebler et al (2018), and this was noticed for cement-fly ash-quicklime blended mixes with high fly ash replacement of 95% (as shown in Figure 5.13). This potentially might have reduced the water available for hydration reactions.

- TGA measurements indicated additional hydration at all ages of hydration for cement-fly ash-quicklime blended paste prepared with slaked quicklime (20% and 95% fly ash replacements). However, the DTG curves shows that the increased hydration calculated for cement blended pastes with 95% fly ash replacement could be due to the formation of AFm and AFt minerals and not hydration minerals like C-S-H and C-A-S-H.

- The hydration results indicate the possible application of quicklime slaking to hydration reactions blended systems containing high volume fly ash replacements. As the hydrates measured for blended fly ash blended pastes increased with slaked quicklime.

- Although a sealed curing approach was used in this study, the mass balance performed on the cement-fly ash-quicklime blended pastes showed mass loss with time indicating possible desiccation. The average mass change for all blended mixes was between 0.45% - 2.77% at the end of the 180 day curing period.

- DTG curves for the cement-fly ash-quicklime blended paste showed that paste blends with fly ash replacement of 20% and 40% can possibly be considered for structural

applications, while paste blends with 95% can be explored for environmental and encapsulation technology.

6.1.3 Hydration halting

• The freezing and microwave hydration halting techniques used in this study did not yield favorable result as TGA measurements taken after hydration was halted using these methods still showed that hydration continued for as long 90 days after samples were halted.

It can be concluded from this study that quicklime slaking significantly affects the type of hydrating solid phases formed in high volume flyash blended cementitious systems as well as the rate at which these hydrated solid mineral phases are formed. While hydration halting techniques like microwaving or dry freezing have proven to be adequate for stopping hydration reactions in neat cement systems, this study shows that these hydration halting methods are not capable of doing the same for cement-fly ash-quicklime blended cementitious systems.

6.1.4 Compressive strength-hydration relationship

• ANOVA analysis showed that the compressive strength had a Pearson correlation of 0.718 with the calcium silicate/aluminate hydrates indicting a possibility of predicting strength from TGA measurements for specific cement-fly ash cementitious systems. This correlation seems to be most effective for cement-fly ash blended pastes without quicklime.

• The ANOVA correlation of 0.8049 between compressive strength and DTG peak. The DTG peak values for most of the paste values were established at temperatures within 90 to 100 $^{\circ}$C. Which were slightly less than the initial decomposition temperature for Ldh.

It is possible that this correlation was established due to a portion of the Ldh mineral phases decomposing at temperatures lower than 105°C.

6.2 Recommendations for Future Study

With the findings from the tests in the preceding sections the following are recommended for future work:

• Additional methods such as XRD/Rietveld analysis, Scanning Electron Microscope (SEM) imaging and compressive strength testing should be explored to support TGA hydration information for cement-fly ash-quicklime pastes.

• It will be beneficial to explore other fly ash replacement levels in cement-fly ash-quicklime paste blends to understand the effect of increased or reduced fly ash and quicklime replacement on TGA hydration measurements.

• A better sampling approach is required if TGA is to be used in characterizing hydration for internally cured mortars. The exploratory study on hydration of internally cured mortars (Chapter 3) showed that the presence of fines from IC-LWA possibly affected TGA measurements.

A cost estimate analysis should be performed on fly ash/quicklime vs cement-fly ash blended paste with high fly ash replacement if it is to be considered for environmental and encapsulation technology. The applicability of quicklime slaking in large amounts should also be explored if it is to be adopted in the production of paste for encapsulation technology.

REFERENCES

ACI (308-213) R-13. 2013. Report on Internally Cured Concrete Using Prewetted Absorptive Lightweight Aggregate. ACI committees 308, 213.

Antiohos, S., Papadakis, V., Maganari, K., and Tsimas, S. (2003). *The development of blended supplementary cementing materials consisting of high and low calcium fly ashes.* Paper presented at the Proceedings of the 11th International Congress on the Chemistry of Cement, Durban, South Africa.

Antiohos, S., Papageorgiou, A., and Tsimas, S. (2006). Activation of fly ash cementitious systems in the presence of quicklime. Part II: Nature of hydration products, porosity and microstructure development. *Cement and Concrete Research, 36*(12), 2123-2131.

Bach, T. T. H., Coumes, C. C. D., Pochard, I., Mercier, C., Revel, B., and Nonat, A. (2012). Influence of temperature on the hydration products of low pH cements. *Cement and Concrete Research, 42*(6), 805-817.

Bentz, D. P., Lura, P., and Roberts, J. W. (2005). Mixture proportioning for internal curing. *Concrete international*, *27*(02), 35-40.

Bhatty, J. I. (1986). Hydration versus strength in a portland cement developed from domestic mineral wastes — a comparative study. *Thermochimica Acta, 106*, 93-103.

Bouzoubaâ, N., Zhang, M. H., and Malhotra, V. M. (2001). Mechanical properties and durability of concrete made with high-volume fly ash blended cements using a coarse fly ash. *Cement and Concrete Research, 31*(10), 1393-1402.

Bullard, J. W., Jennings, H. M., Livingston, R. A., Nonat, A., Scherer, G. W., Schweitzer, J. S., Scrivener, K. L., and Thomas, J. J. (2011). Mechanisms of cement hydration. *Cement and Concrete Research, 41*(12), 1208-1223.

Castro, J., Keiser, L., Golias, M., and Weiss, J. (2011). Absorption and desorption properties of fine lightweight aggregate for application to internally cured concrete mixtures. *Cement and Concrete composites*, *33*(10), 1001-1008.

Day, R. L. (1981). Reactions between methanol and portland cement paste. *Cement and Concrete Research, 11*(3), 341-349.

Deboucha, W., Leklou, N., Khelidj, A., and Oudjit, M. N. (2017). Hydration development of mineral additives blended cement using thermogravimetric analysis (TGA): Methodology of calculating the degree of hydration. *Construction and Building Materials, 146*, 687-701.

Deschner, F., Winnefeld, F., Lothenbach, B., Seufert, S., Schwesig, P., Dittrich, S., Goetz-Neunhoeffer, F., and Neubauer, J. (2012). Hydration of Portland cement with high replacement by siliceous fly ash. *Cement and Concrete Research, 42*(10), 1389-1400.

Fourmentin, M., Faure, P., Gauffinet, S., Peter, U., Lesueur, D., Daviller, D., Ovarlez, G., and Coussot, P. (2015). Porous structure and mechanical strength of cement-lime pastes during setting. *Cement and Concrete Research, 77*, 1-8.

Gartner, E., Young, J., Damidot, D., and Jawed, I. (2002). Hydration of Portland cement. *Structure and performance of cements, 2*, 57-108.

Ghose, A., and Pratt, P. (1981). *Studies of the hydration reactions and microstructure of cement-fly ash pastes.* Paper presented at the Boston: Mat. Res. Soc. Effects of Fly-Ash Incorporation in Cement and Concrete: Proceedings Symposium N Annual Meeting (Diamond, S.(Ed.)). Boston, November.

Henkensiefken, R., Bentz, D., Nantung, T., and Weiss, J. (2009). Volume change and cracking in internally cured mixtures made with saturated lightweight aggregate under sealed and unsealed conditions. *Cement and Concrete Composites, 31*(7), 427-437.

Huang, S., Li, Z., and Cheng, J. (1986). Reaction dynamics in fly ash-Ca (OH) 2-H2O system. *J Chin Ceram Soc, 14*(1), 191-197.

Ioannidou, K., Masoero, E., Levitz, P., Pellenq, R.-M., and Del Gado, E. (2015). Hydration Kinetics and Gel Morphology of CSH. In *CONCREEP 10* (pp. 565-573).

Jennings, H. M., and Pratt, P. L. (1979). An experimental argument for the existence of a protective membrane surrounding portland cement during the induction period. *Cement and Concrete Research, 9*(4), 501-506.

Langan, B. W., Weng, K., and Ward, M. A. (2002). Effect of silica fume and fly ash on heat of hydration of Portland cement. *Cement and Concrete Research, 32*(7), 1045-1051.

Lawrence, P., Cyr, M., and Ringot, E. (2003). Mineral admixtures in mortars: effect of inert materials on short-term hydration. *Cement and Concrete Research, 33*(12), 1939-1947.

Li, D., Chen, Y., Shen, J., Su, J., and Wu, X. (2000). The influence of alkalinity on activation and microstructure of fly ash. *Cement and Concrete Research, 30*(6), 881-886.

Mehta, P., and Gjørv, O. (1982). Properties of portland cement concrete containing fly ash and condensed silica-fume. *Cement and Concrete Research, 12*(5), 587-595.

Moffatt, E. G., Thomas, M. D. A., and Fahim, A. (2017). Performance of high-volume fly ash concrete in marine environment. *Cement and Concrete Research, 102*, 127-135.

Monteagudo, S. M., Moragues, A., Gálvez, J. C., Casati, M. J., and Reyes, E. (2014). The degree of hydration assessment of blended cement pastes by differential thermal and thermogravimetric analysis. Morphological evolution of the solid phases. *Thermochimica Acta, 592*, 37-51.

Palou, M. T., Kuzielová, E., Žemlička, M., Boháč, M., and Novotný, R. (2016). The effect of curing temperature on the hydration of binary Portland cement. *Journal of Thermal Analysis and Calorimetry, 125*(3), 1301-1310.

Pane, I., and Hansen, W. (2005). Investigation of blended cement hydration by isothermal calorimetry and thermal analysis. *Cement and Concrete Research, 35*(6), 1155-1164.

Paulik, F., Paulik, J., and Arnold, M. (1992). Thermal decomposition of gypsum. *Thermochimica Acta, 200*, 195-204.

Pietersen, H. S., and Bijen, J. M. J. M. (1994). Fly Ash and Slag Reactivity in Cements: Tem Evidence and Application of Thermodynamic Modelling. In J. J. J. M. Goumans, H. A. van der Sloot, & T. G. Aalbers (Eds.), *Studies in Environmental Science* (Vol. 60, pp. 949-960): Elsevier.

Ramezanianpour, A. A. (2013). *Cement Replacement Materials: Properties, Durability, Sustainability*: Springer Berlin Heidelberg.

Rivera, J., Sánchez de Rojas, M., and Frías, M. (2001). *Properties of cement pastes containing calcined clay from waste ceramic tiles as pozzolana.* Paper presented at the 7th CANMET/ACI Int. Conference on Fly ash, silica fume, slag and natural pozzolans in concrete. Madras, India. Procceding.

Sakai, E., Miyahara, S., Ohsawa, S., Lee, S.-H., and Daimon, M. (2005). Hydration of fly ash cement. *Cement and Concrete Research, 35*(6), 1135-1140.

Scrivener, K., Snellings, R., and Lothenbach, B. (2016). *A practical guide to microstructural analysis of cementitious materials*: Crc Press.

Scrivener, K. L. (2004). Backscattered electron imaging of cementitious microstructures: understanding and quantification. *Cement and Concrete Composites, 26*(8), 935-945.

Scrivener, K. L., Füllmann, T., Gallucci, E., Walenta, G., and Bermejo, E. (2004). Quantitative study of Portland cement hydration by X-ray diffraction/Rietveld analysis and independent methods. *Cement and Concrete Research, 34*(9), 1541-1547.

Scrivener, K. L., and Pratt, P. (1983). Characterisation of Portland cement hydration by electron optical techniques. *MRS Online Proceedings Library Archive, 31*.

Shafiq, N. (2011). Degree of hydration and compressive strength of conditioned samples made of normal and blended cement system. *KSCE Journal of Civil Engineering, 15*(7), 1253.

Shi, C., and Day, R. L. (1995). Acceleration of the reactivity of fly ash by chemical activation. *Cement and Concrete Research, 25*(1), 15-21.

Song, S., Jiang, L., Jiang, S., Yan, X., and Xu, N. (2018). The mechanical properties and electrochemical behavior of cement paste containing nano-MgO at different curing temperature. *Construction and Building Materials, 164*, 663-671.

Standard Specification for Fly Ash and Other Pozzolans for Use With Lime for Soil Stabilization. (2011).

Stein, H. N., and Stevels, J. M. (1964). Influence of silica on the hydration of 3 CaO,SiO2. *Journal of Applied Chemistry, 14*(8), 338-346.

Taylor, H. F. W., Barret, P., Brown, P. W., Double, D. D., Frohnsdorff, G., Johansen, V., Ménétrier-Sorrentino, D., Odler, I., Parrott, L. J., Pommersheim, J. M., Regourd, M., and Young, J. F. (1984). The hydration of tricalcium silicate. *Matériaux et Construction, 17*(6), 457-468.

Thomas, C., Setién, J., Polanco, J. A., Cimentada, A. I., and Medina, C. (2018). Influence of curing conditions on recycled aggregate concrete. *Construction and Building Materials, 172*, 618-625.

Tonelli, M., Martini, F., Calucci, L., Geppi, M., Borsacchi, S., and Ridi, F. (2017). Traditional Portland cement and MgO-based cement: a promising combination? *Physics and Chemistry of the Earth, Parts A/B/C, 99*, 158-167.

Uchikawa, H., and Furuta, R. (1981). Hydration of C3S-pozzolana paste estimated by trimethylsilylation. *Cement and Concrete Research, 11*(1), 65-78.

Vedalakshmi, R., Sundara Raj, A., Srinivasan, S., and Ganesh Babu, K. (2003). Quantification of hydrated cement products of blended cements in low and medium strength concrete using TG and DTA technique. *Thermochimica Acta, 407*(1), 49-60.

Walenta, G., and Füllmann, T. (2004). Advances in quantitative XRD analysis for clinker, cements, and cementitious additions. *Powder Diffraction, 19*(1), 40-44.

Zeng, Q., Li, K., Fen-chong, T., and Dangla, P. (2012). Determination of cement hydration and pozzolanic reaction extents for fly-ash cement pastes. *Construction and Building Materials, 27*(1), 560-569.

Zhang, J., and Scherer, G. W. (2011). Comparison of methods for arresting hydration of cement. *Cement and Concrete Research, 41*(10), 1024-1036.

Zhang, M. H., and Canmet. (1995). Microstructure, crack propagation, and mechanical properties of cement pastes containing high volumes of fly ashes. *Cement and Concrete Research, 25*(6), 1165-1178.

APPENDIX

Version 6.42

Holcim — NSF — Material Certification Report

| Material: | Portland Cement | Test Period: | 14-Sep-2015 |
| Type: | I-II(MH) | To: | 15-Sep-2015 |

Certification

This Holcim cement meets the specifications of ASTM C150 for Type I-II(MH) cement,
and complies with AASHTO M85 specifications for Type I-II(MH) cement.

General Information

Supplier:	Holcim (US) Inc.	Source Location:	Holly Hill Plant
Address:	2173 Gardiner Boulevard		2173 Gardiner Boulevard
	Holly Hill, SC 29059		Holly Hill, SC 29059
Telephone:	803-496-2995	Contact:	Scott Poaps
Date Issued:	15-Dec-2015		

The following information is based on average test data during the test period.
The data is typical of cement shipped by Holcim; individual shipments may vary.

Tests Data on ASTM Standard Requirements

Chemical Item	Limit[A]	Result	Physical Item	Limit[A]	Result
SiO_2 (%)	-	20.4	Air Content (%)	12 max	6
Al_2O_3 (%)	6.0 max	4.8	Blaine Fineness (m^2/kg)	260-430	393
Fe_2O_3 (%)	6.0 max	3.3			
CaO (%)	-	63.8			
MgO (%)	6.0 max	1.6	Autoclave Expansion (%) (C151)	0.80 max	0.05
SO_3 (%)	3.0 max[B]	3.1	Compressive Strength MPa (psi):		
Loss on Ignition (%)	3.0 max	1.6			
Insoluble Residue (%)	0.75 max	0.23	3 days	10.0 (1450) min	29.0 (4210)
CO_2 (%)	-	1.1	7 days	17.0 (2470) min	34.8 (5040)
Limestone (%)	5.0 max	2.6			
$CaCO_3$ in Limestone (%)	70 min	92	Initial Vicat (minutes)	45-375	117
Inorganic Processing Addition (%)	5.0 max	0.0			
Potential Phase Compositions[C]:			Mortar Bar Expansion (%) (C1038)		0.006
C_3S (%)	-	54			
C_2S (%)	-	17	Heat of Hydration: kJ/kg (cal/g)[D]	-	305 (73)
C_3A (%)	8 max	7	7 Days (for informational purposes)		
C_4AF (%)	-	10			
$C_3S + 4.75C_3A$ (%)	100 max	87.3			

Tests Data on ASTM Optional Requirements

Chemical Item	Limit[A]	Result	Physical Item	Limit[A]	Result
Equivalent Alkalies (%)	0.60 max	0.53			

Notes

[A] Dashes in the limit / result columns mean Not Applicable.

[B] It is permissible to exceed the specification limit provided that ASTM C1038 Mortar Bar Expansion does not exceed 0.020 % at 14 days.

[C] Adjusted per Annex A1.6 of ASTM C150 and AASHTO M85.

[D] Test result represents most recent value and is provided for information only. Analysis of Heat of Hydration has been carried out by CTLGroup, Skokie, IL. This data may have been reported on previous mill certificates.

Silo 18
9/14/2015
Grind 257-259

Additional Data

Inorganic Processing Addition Data		Base Cement Phase Composition	
Item	Result[A]	Item	Result
Type	-	C_3S (%)	56
Amount (%)	-	C_2S (%)	18
SiO_2 (%)	-	C_3A (%)	7
Al_2O_3 (%)	-	C_4AF (%)	10
Fe2O3 (%)	-		
CaO (%)	-		
SO_3 (%)	-		

Figure A.1: Cement mill report.

RJ Lee Group, Inc.

Sample: 10408505

(Lime)

- Analysis Date: 06-07-17
- Median: 8.6039µm
- Diameter on %: (1) 10.00% - 1.5898µm
  (2) 50.00% - 8.6039µm

  (3) 90.00% - 60.0643µm
- Mean: 20.9884µm
- Distribution Base: Volume
- Form of Distribution: Standard
- Run Number Average of: 3 Runs
- Dispersant: Isopropyl alcohol (IPA)
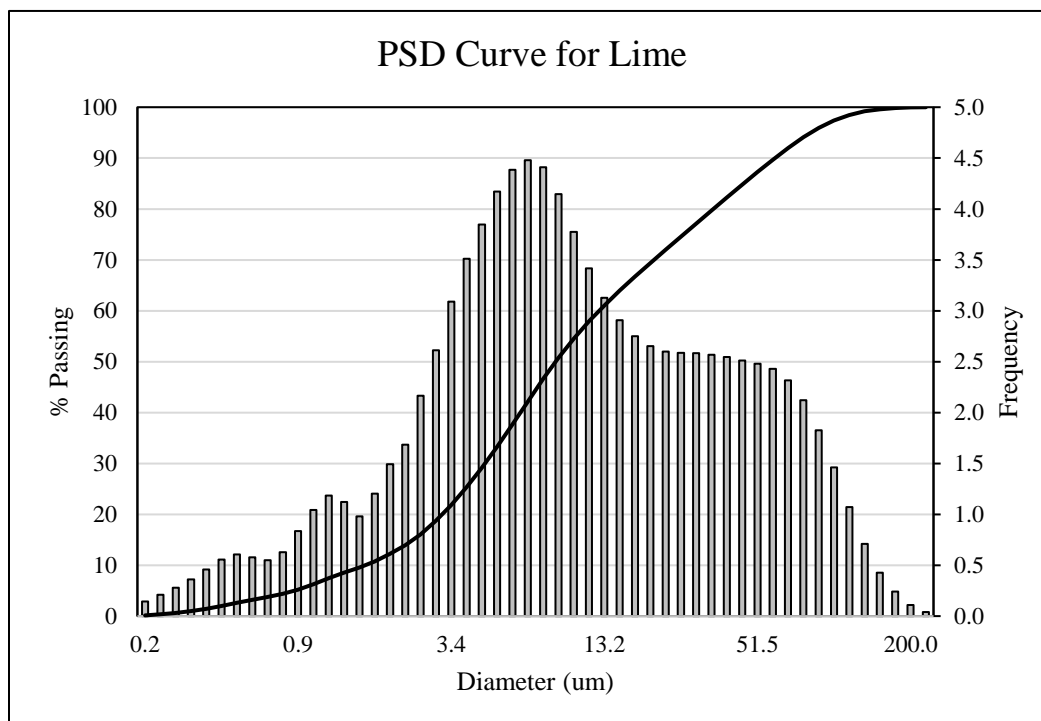
Figure A.2 PSD curve for Lime

Figure A3. X-ray diffraction pattern for sample "Lime" (RJ Lee Group Sample 10408505), with degrees 2Θ along the x-axis and intensity (counts) along the y-axis (top). Corresponding legend showing the matching patterns (bottom).
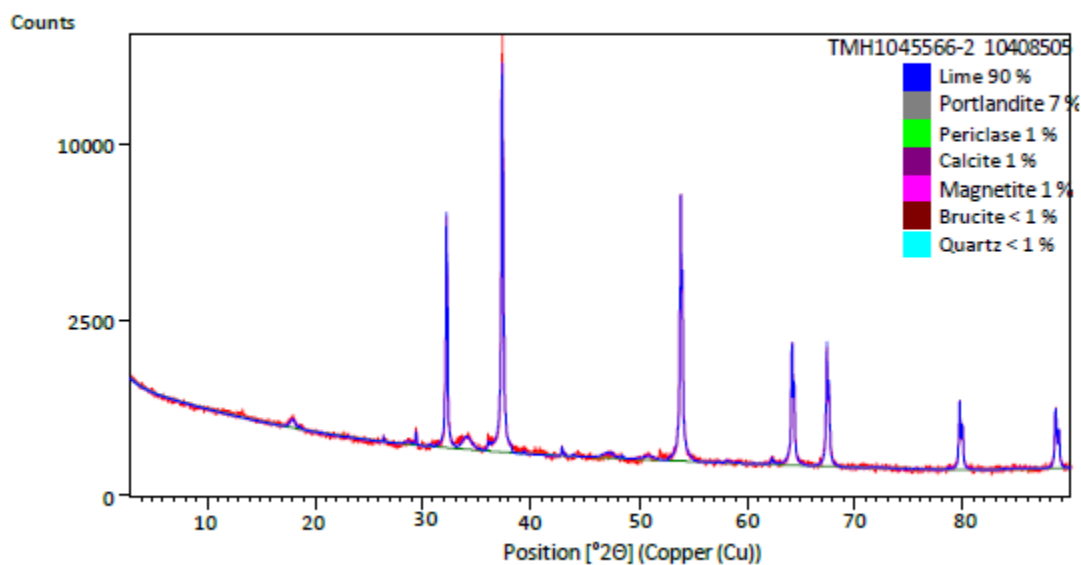
Figure A3: XRD Diffraction pattern for lime

Table A.1: XRD diffraction summary for Lime

Approximate Composition Phase		Concentration (Weight %)
Lime	CaO	90
Portlandite	Ca(OH)$_2$	7
Calcite	CaCO$_3$	1
Magnetite	Fe$_3$O$_4$	1
Periclase	MgO	1
Brucite	Mg(OH)$_2$	< 1
Quartz	SiO$_2$	< 1
Unknown(s)	-	Trace

Table A.2 Specific gravity test 1 for fly ash

	Belews Creek Fly ash Test 1	
	PYCNOMETER 1C	
Mp	Mass of Pycnometer (g)	107.79
Vp	Volume of Pycnometer (mL)	249.64
	Pan ID:	#1
	Pan Empty Mass (g):	469.4
	Pan+Dry Soil Mass (g):	520
Ms	Mass of Soil Tested (g)	50.60
Mpws	Pycno+Water+Soil Mass (g):	387.2
	Test Temperature (°C)	22.0
	Density Correction	0.99777
	Temperature Coefficient	0.99957
Mpw,t	Pycno+Water at Test Temp. (g)	356.87
Gt	Specific Gravity at Test Temp	2.50
G20	Specific Gravity at 20°C	**2.49**

Table A.2 Specific gravity test 2 for fly ash

	Test 2	
	PYCNOMETER 1S	
Mp	Mass of Pycnometer (g)	108.15
Vp	Volume of Pycnometer (mL)	249.49
	Pan ID:	M5A
	Pan Empty Mass (g):	257
	Pan+Dry Soil Mass (g):	308.2
Ms	Mass of Soil Tested (g)	51.20
Mpws	Pycno+Water+Soil Mass (g):	388.4
	Test Temperature (°C)	22.0
	Density Correction	0.99777
	Temperature Coefficient	0.99957
Mpw,t	Pycno+Water at Test Temp. (g)	357.08
Gt	Specific Gravity at Test Temp	2.57
G20	Specific Gravity at 20°C	**2.57**

Average S.G for fly ash = 2.53

Belews Creek Fly ash

- Analysis Date: 09-03-18
- Median: 16.47 µm
- Diameteron%: (1) 10.00% - 4.6312 µm
     (2) 50.00% - 16.4768 µm

     (3) 90.00% - 58.5835 µm
- Mean: 26.102µm
- Distribution Base: Volume
- Form of Distribution: Standard
- Run Number Average of: 3 Runs
- Dispersant: Water
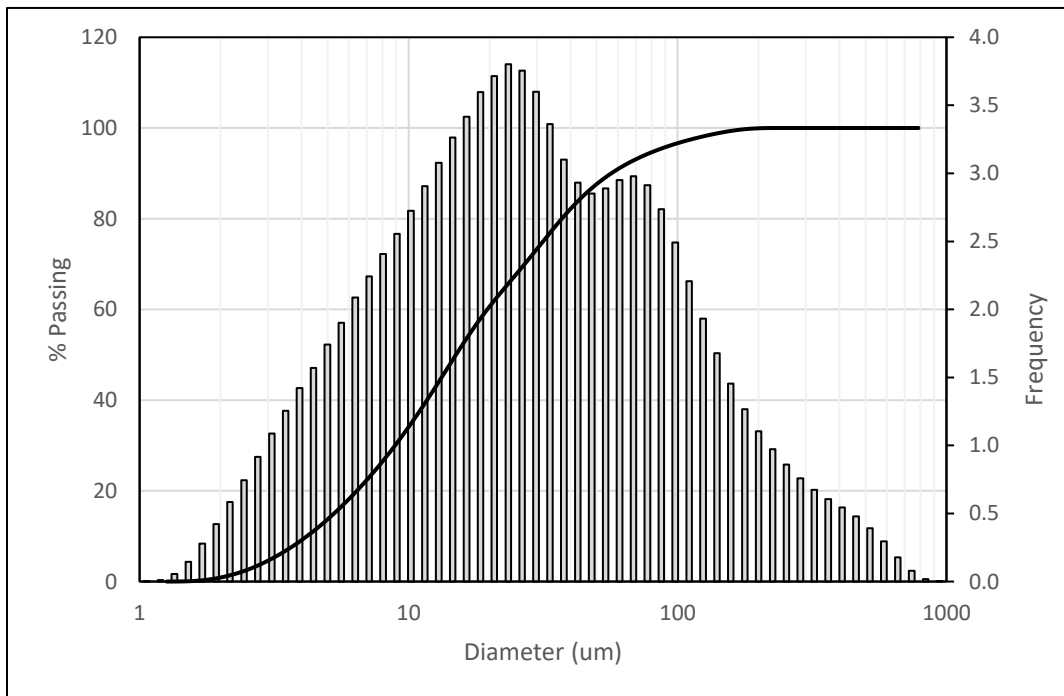
Figure A.4: PSD curve for Fly ash

DTG and TGA curves for cement-fly ash-quicklime blended paste
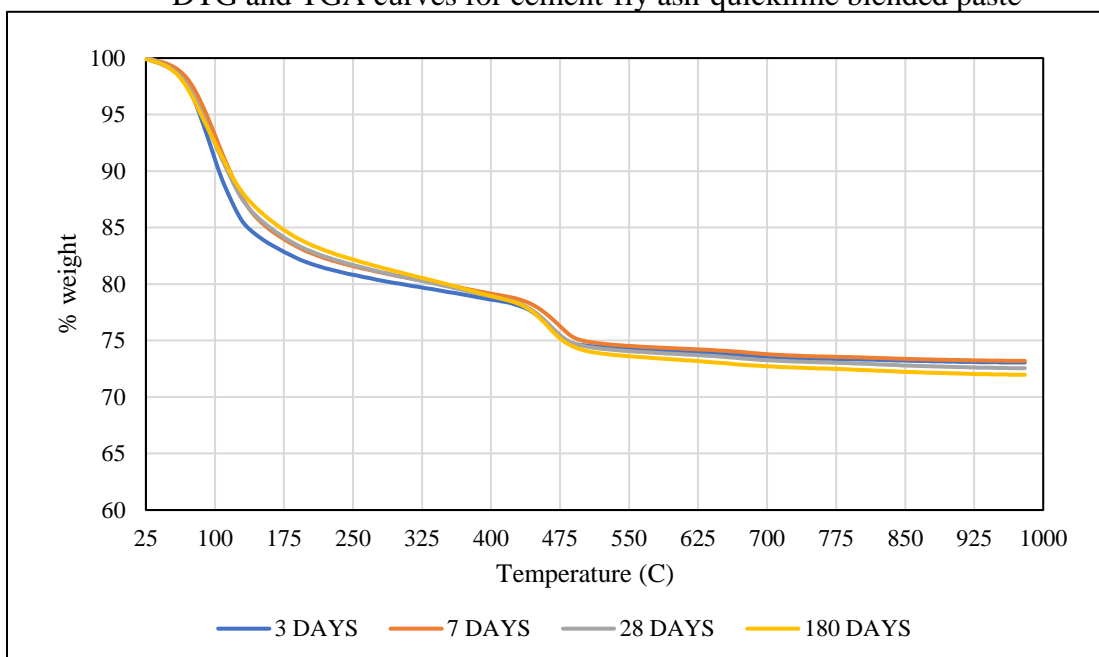
Figure A5: Percentage weight loss for paste P with time
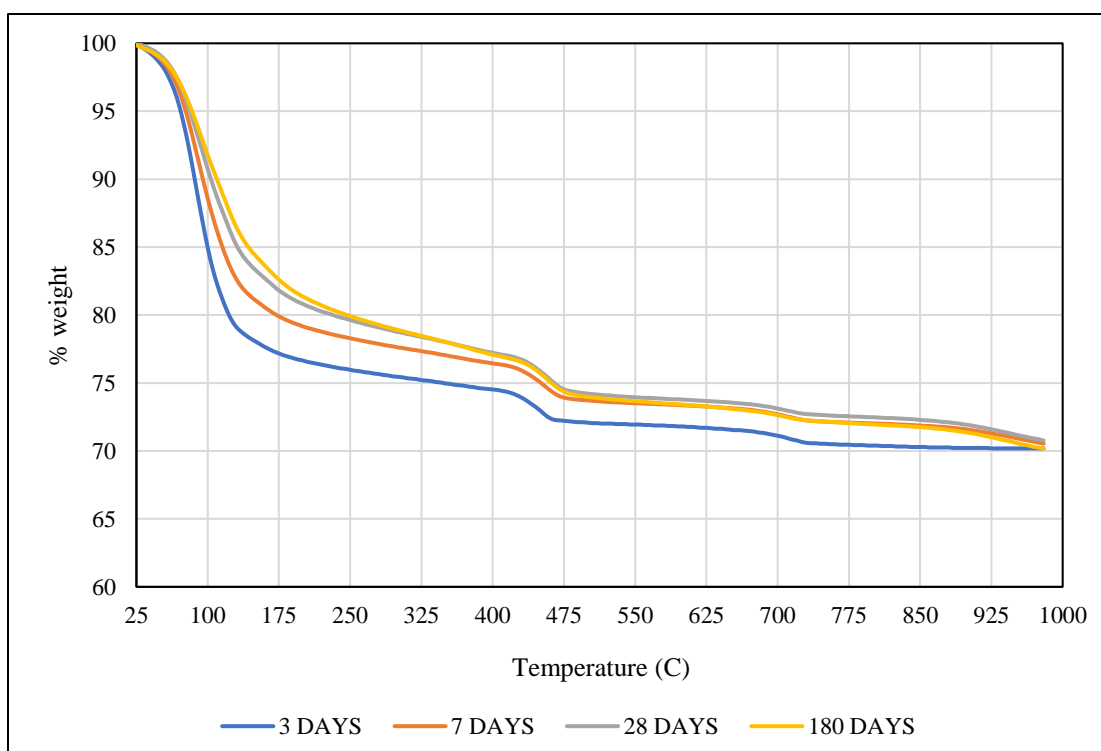
Figure A6: Percentage weight loss for paste P20FA with time

Figure A7: Percentage weight loss for paste P40FA with time
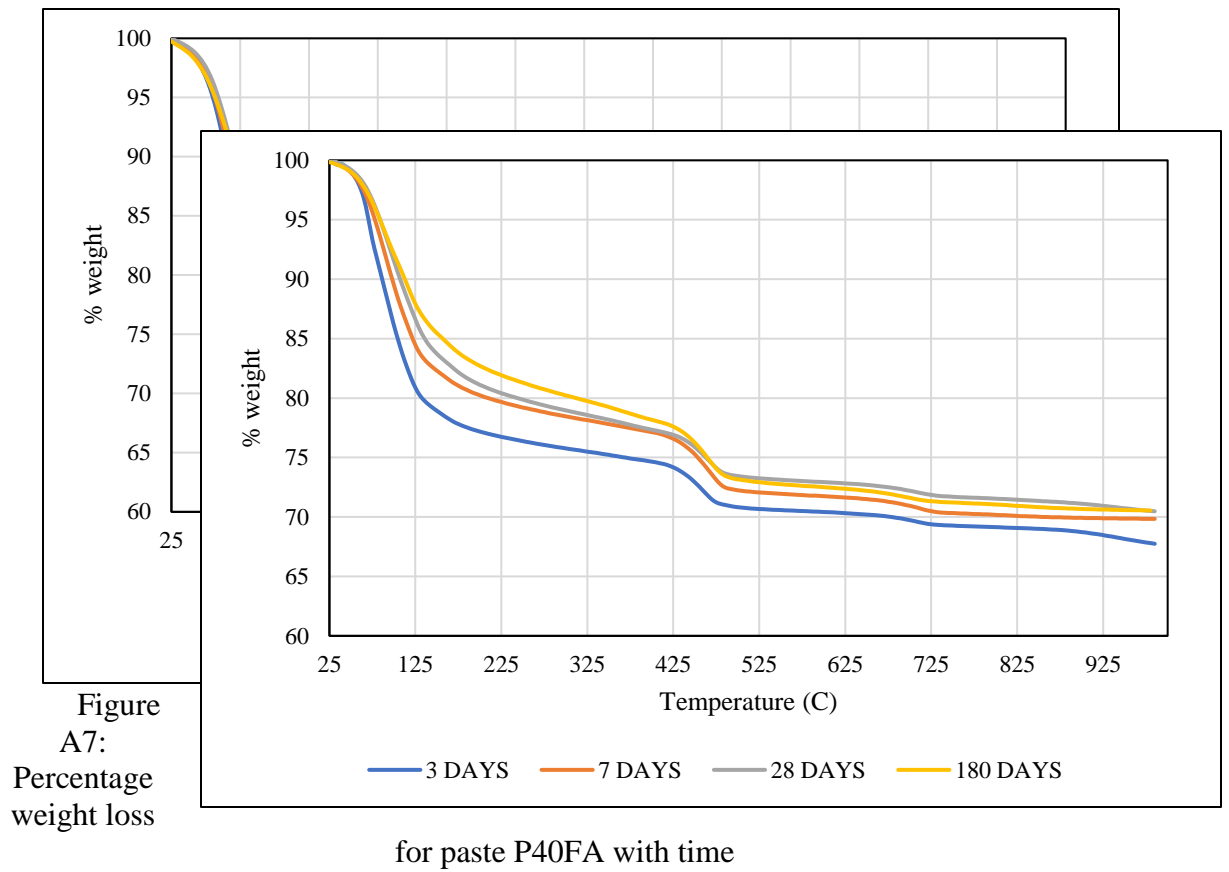
Figure A8: Percentage weight loss for paste P95FA with time
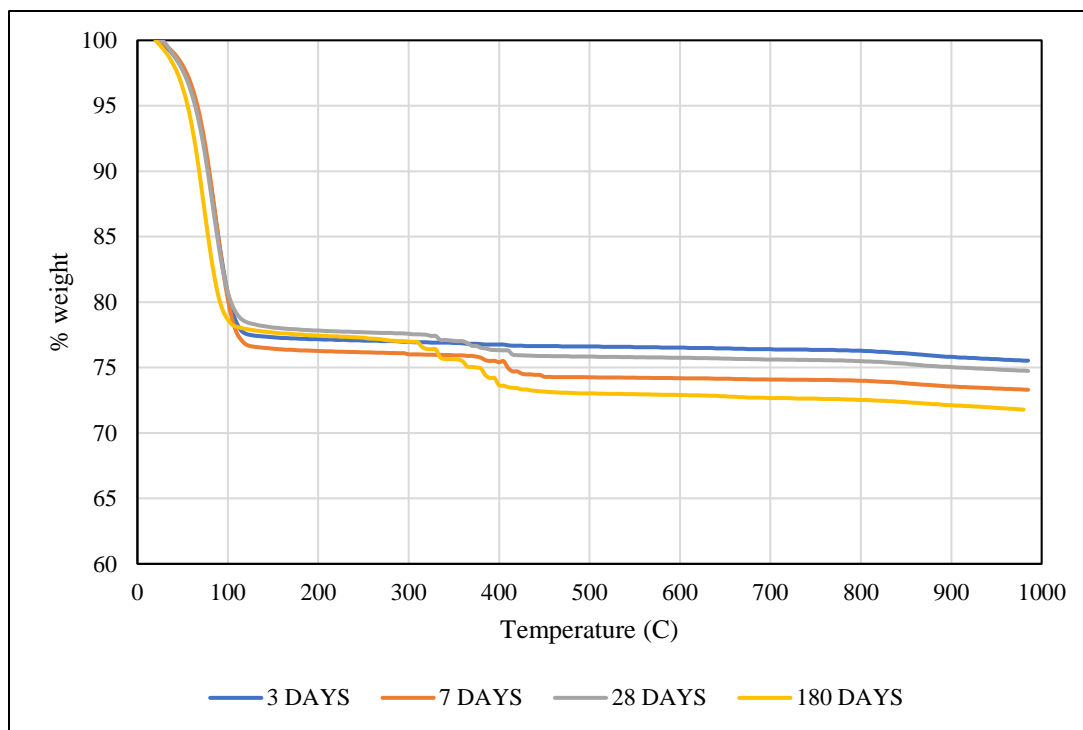
Figure A9: Percentage weight loss for paste P-QL with time
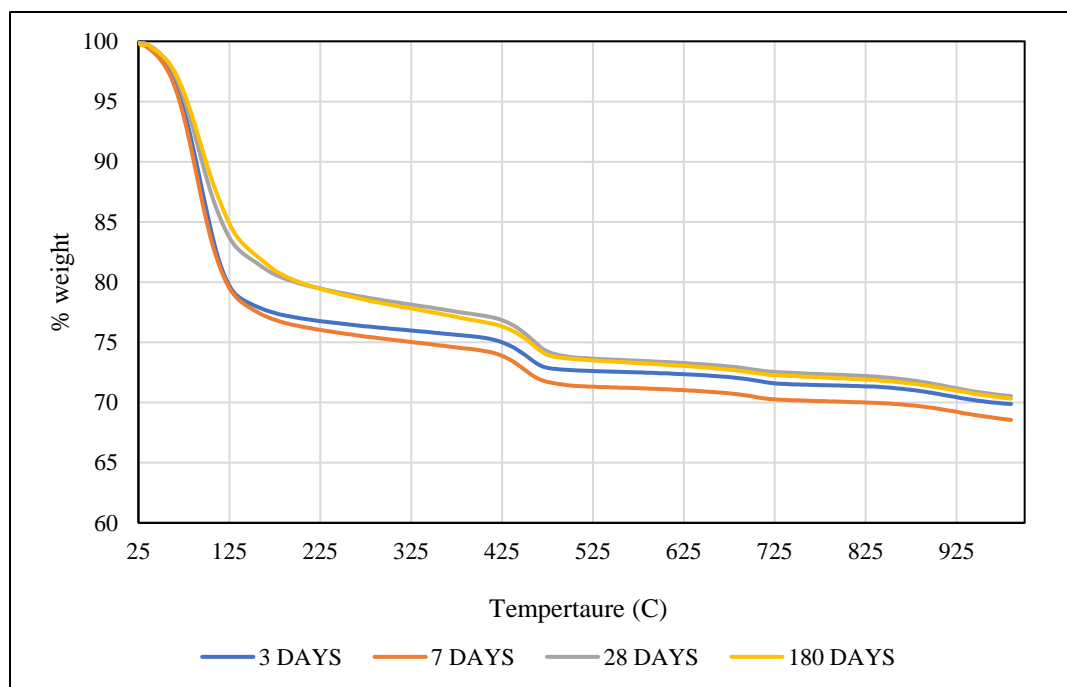
Figure A10: Percentage weight loss for paste P20FA-QL with time
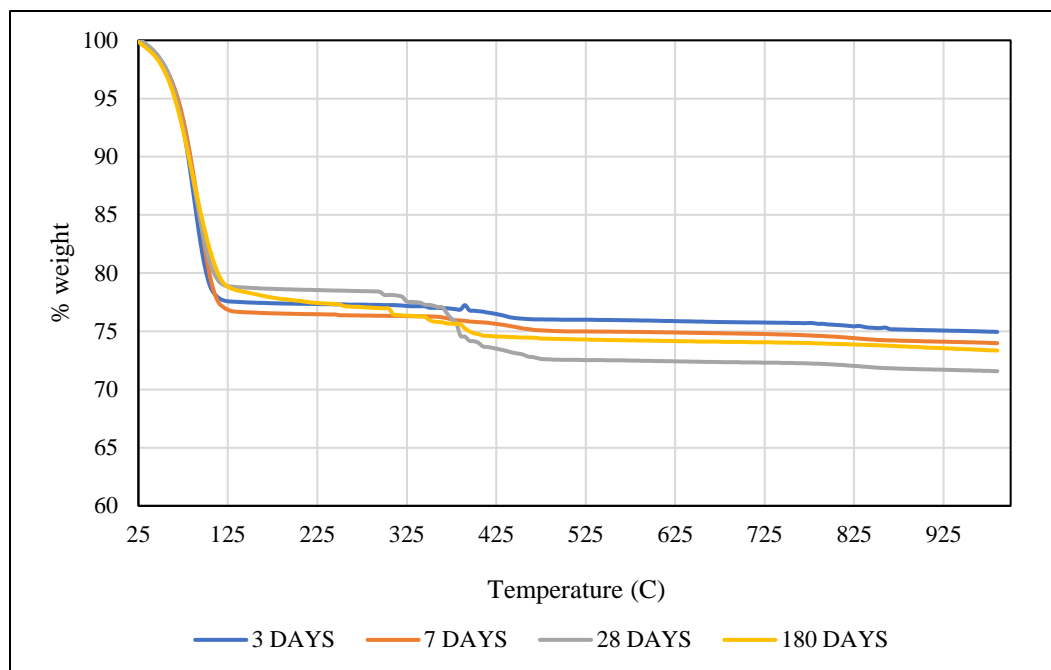
Figure A11: Percentage weight loss for paste P40FA-QL with time
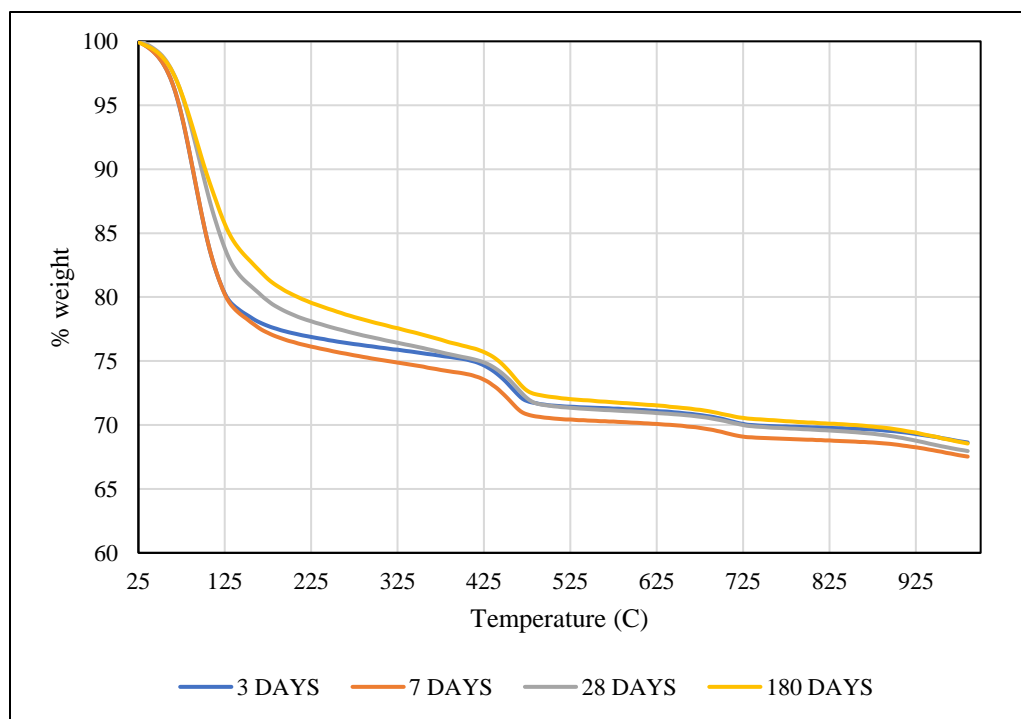
Figure A12: Percentage weight loss for paste P95FA-QL with time
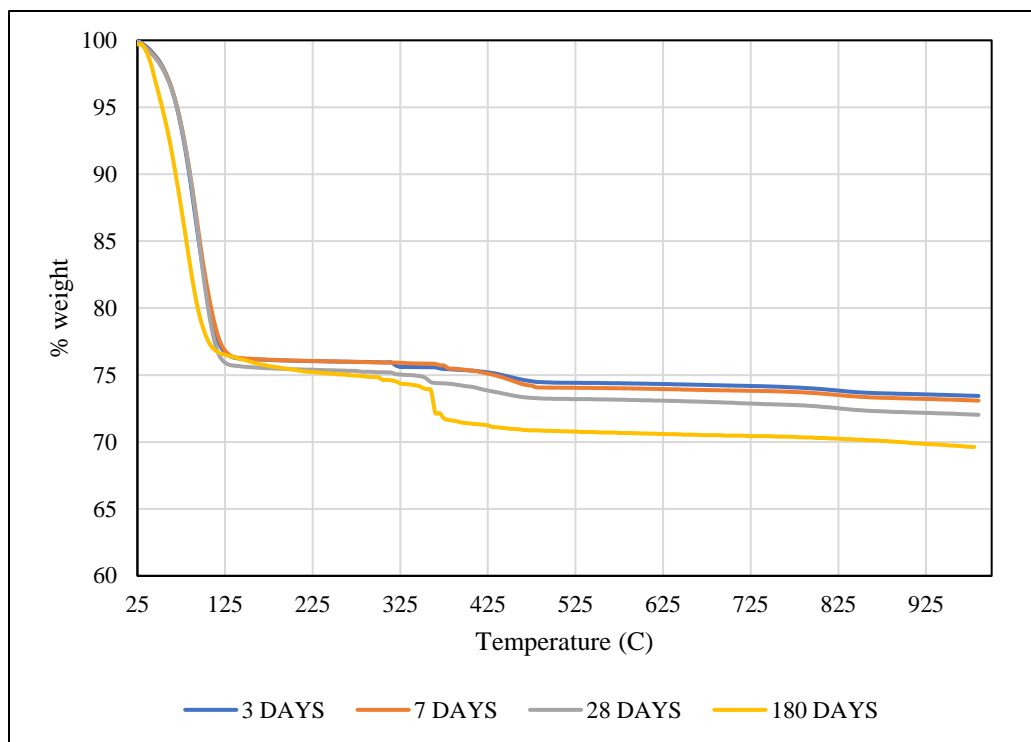
Figure A13: Percentage weight loss for paste P20FA-QL-EM with time
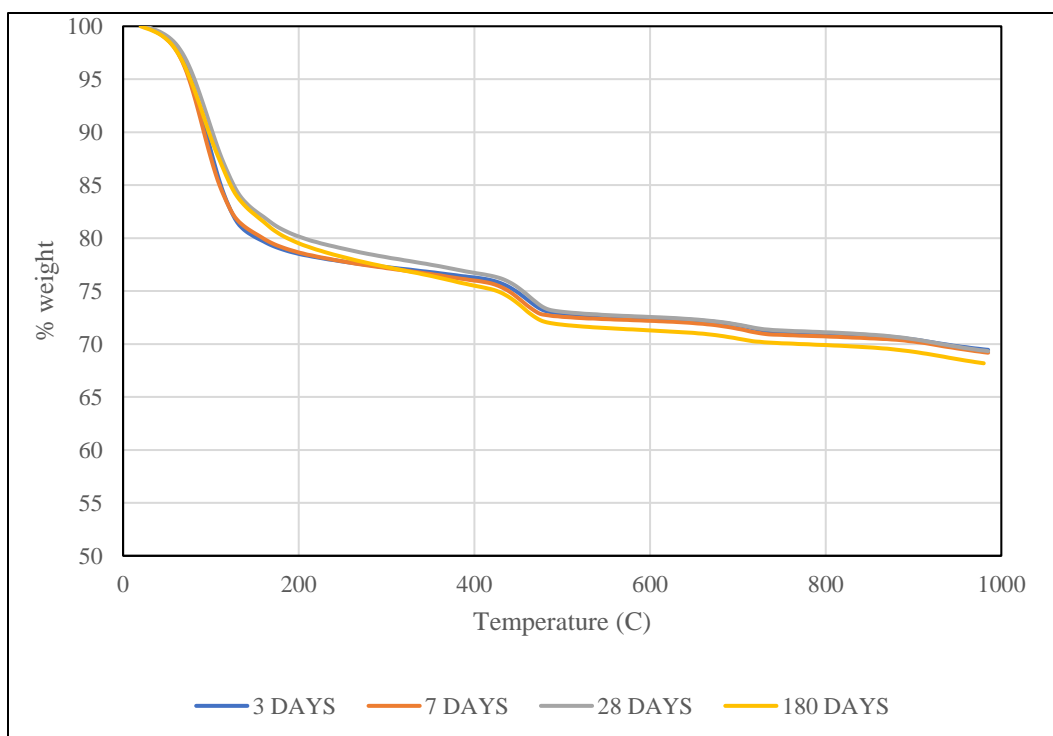
Figure A14: Percentage weight loss for paste P95FA-QL-EM with time
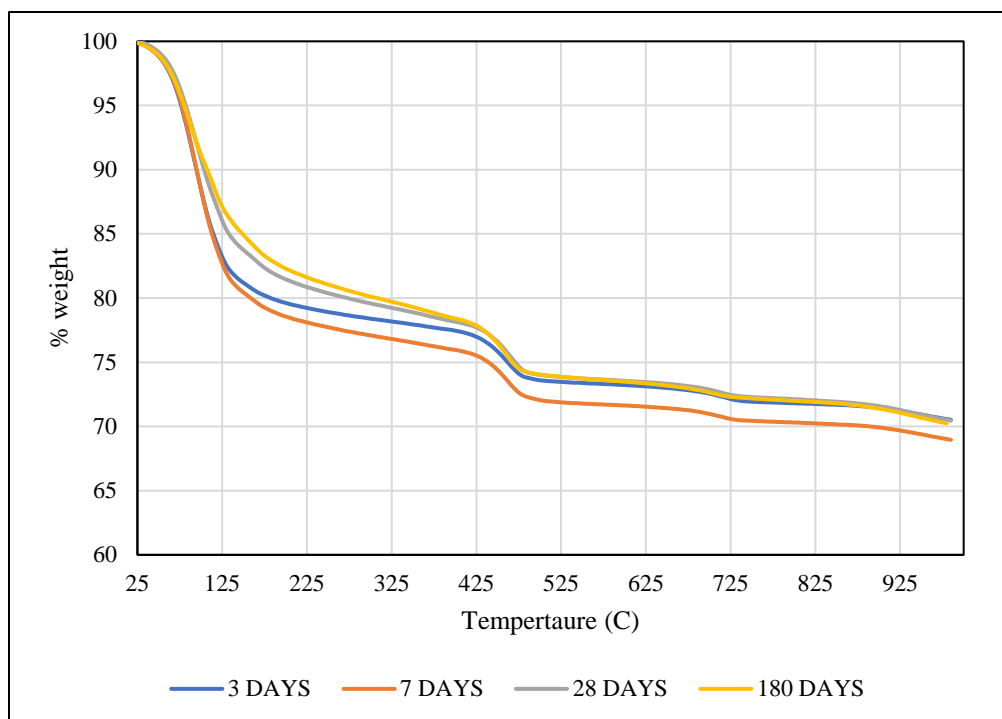
Figure A15: Percentage weight loss for paste P20FA-QL-EM-SL with time
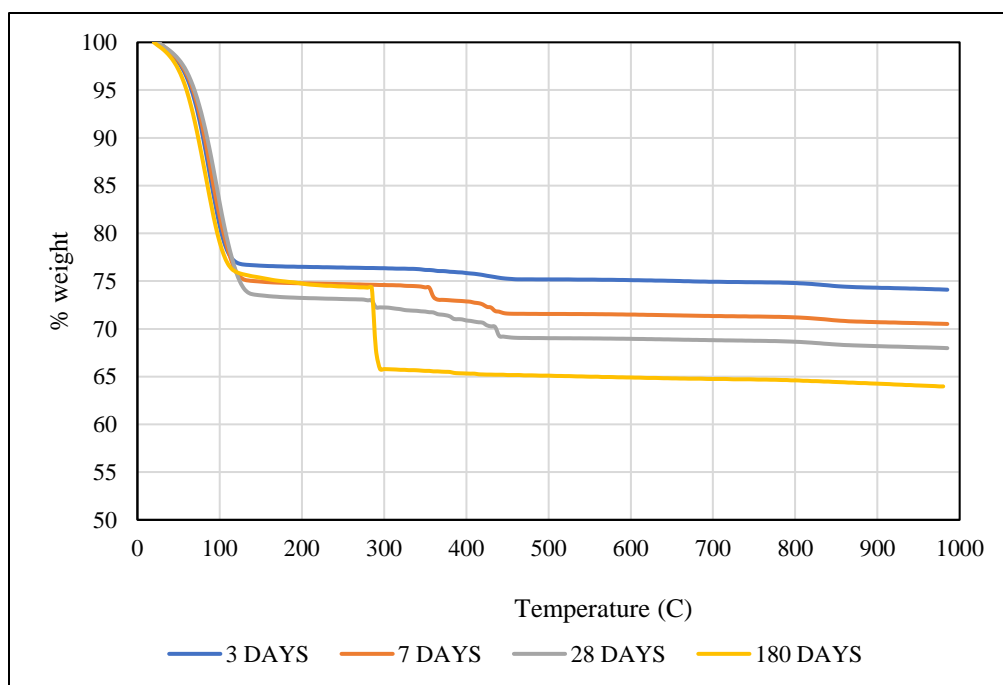
Figure A16: Percentage weight loss for paste P95FA-QL-EM-SL with time
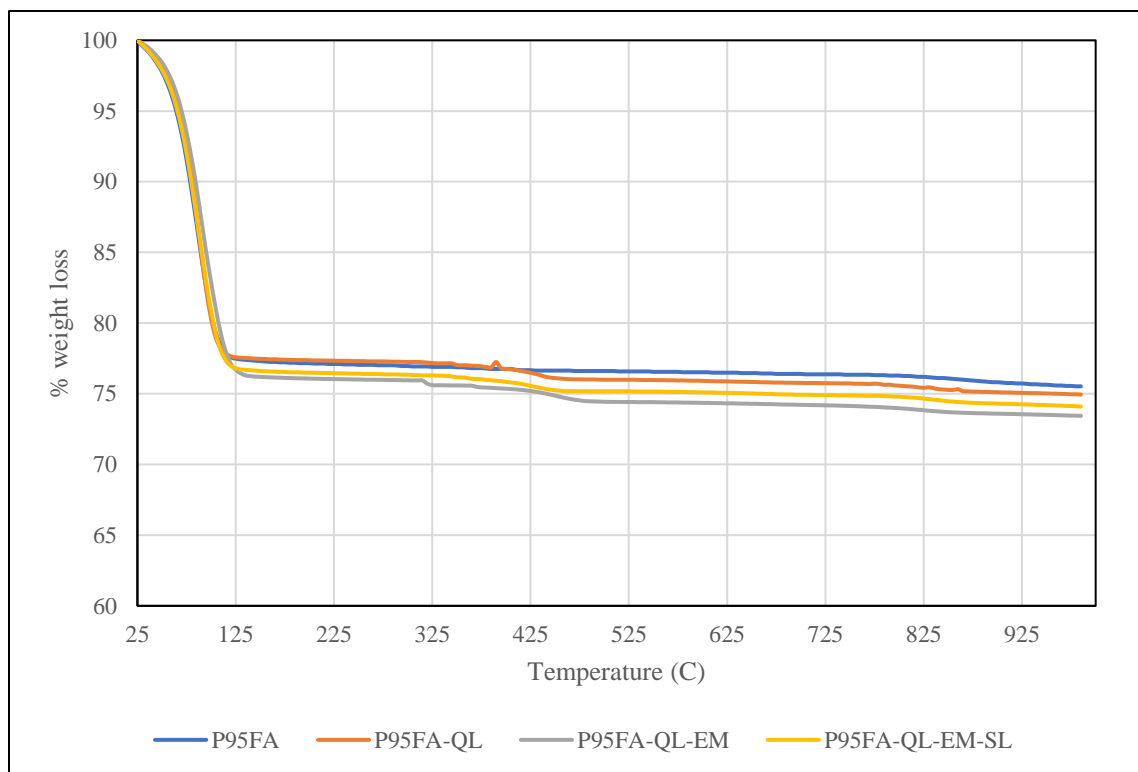
Figure A17: Percentage weight loss for 95% fly ash blended paste at 3 days.
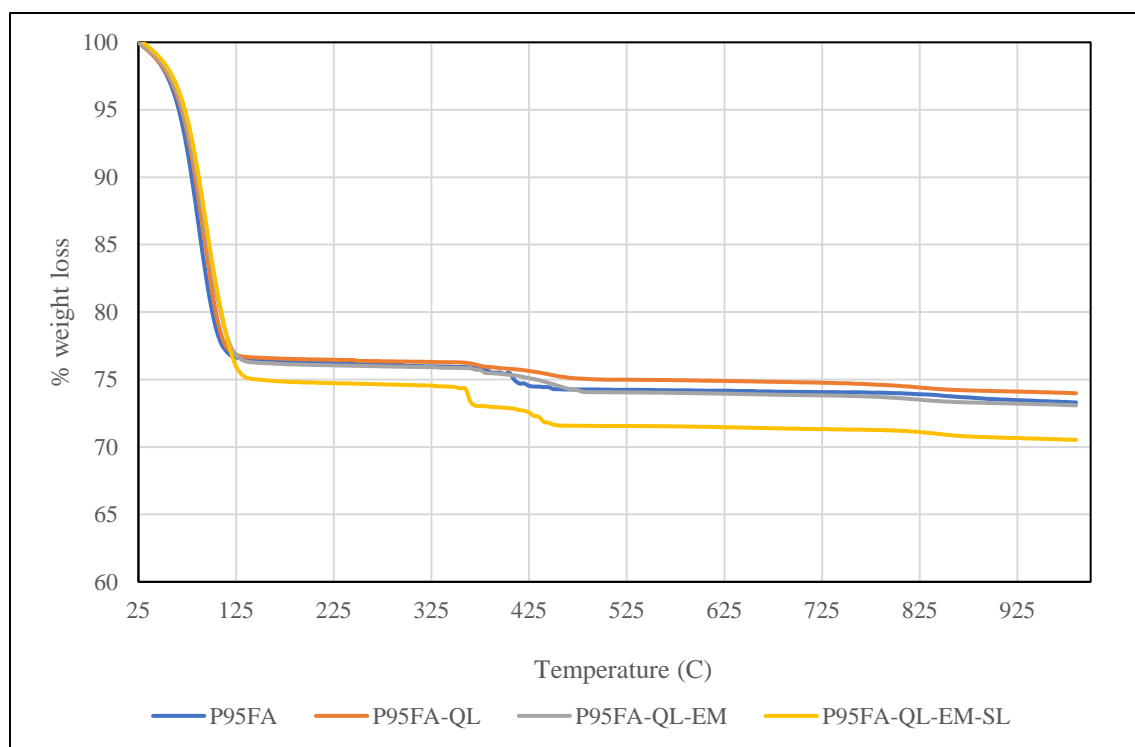
Figure A18: Percentage weight loss for 95% fly ash blended paste at 7 days.
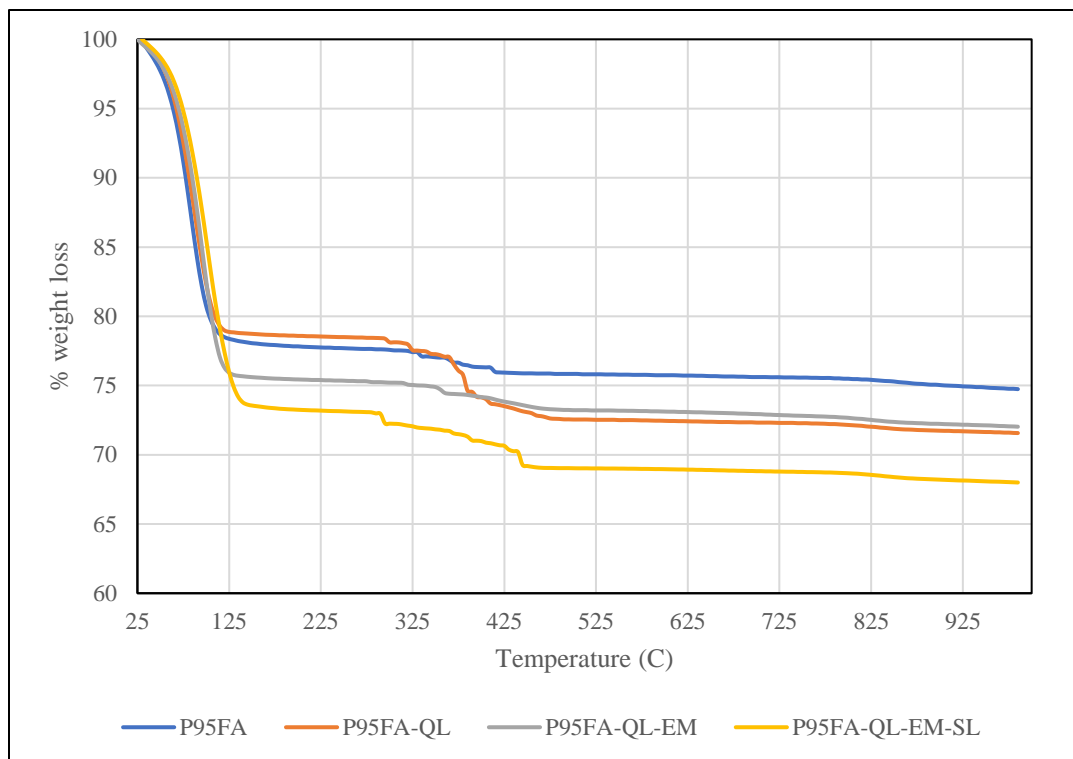
Figure A19: Percentage weight loss for 95% fly ash blended paste at 28 days.
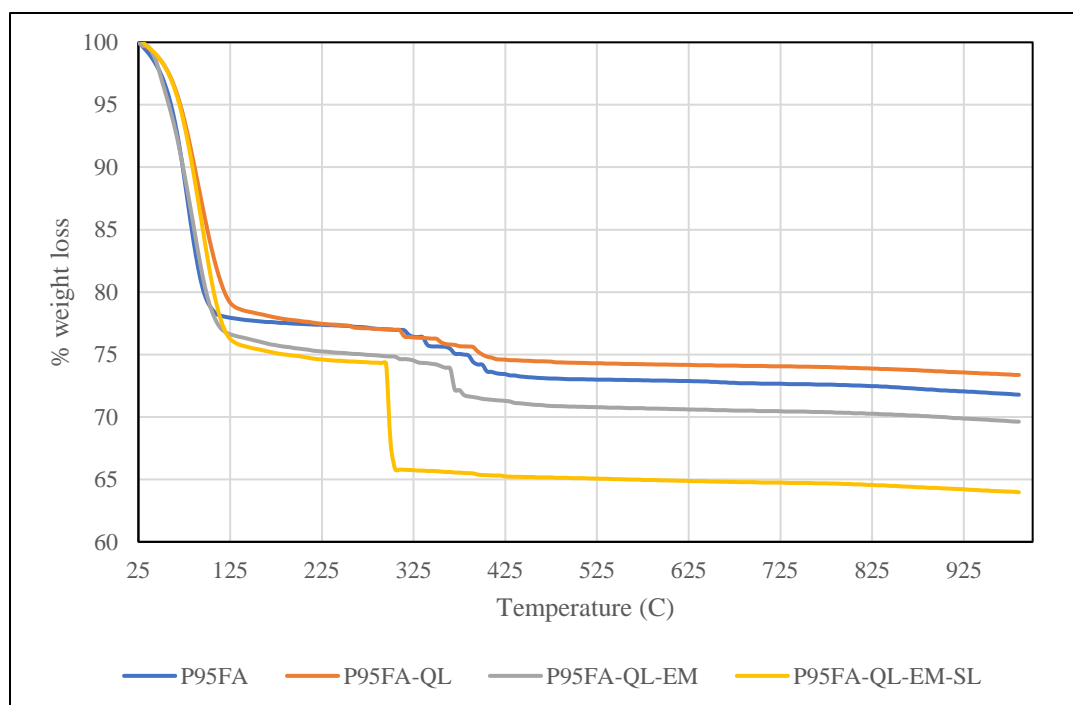
Figure A20: Percentage weight loss for 95% fly ash blended paste at 180 days.
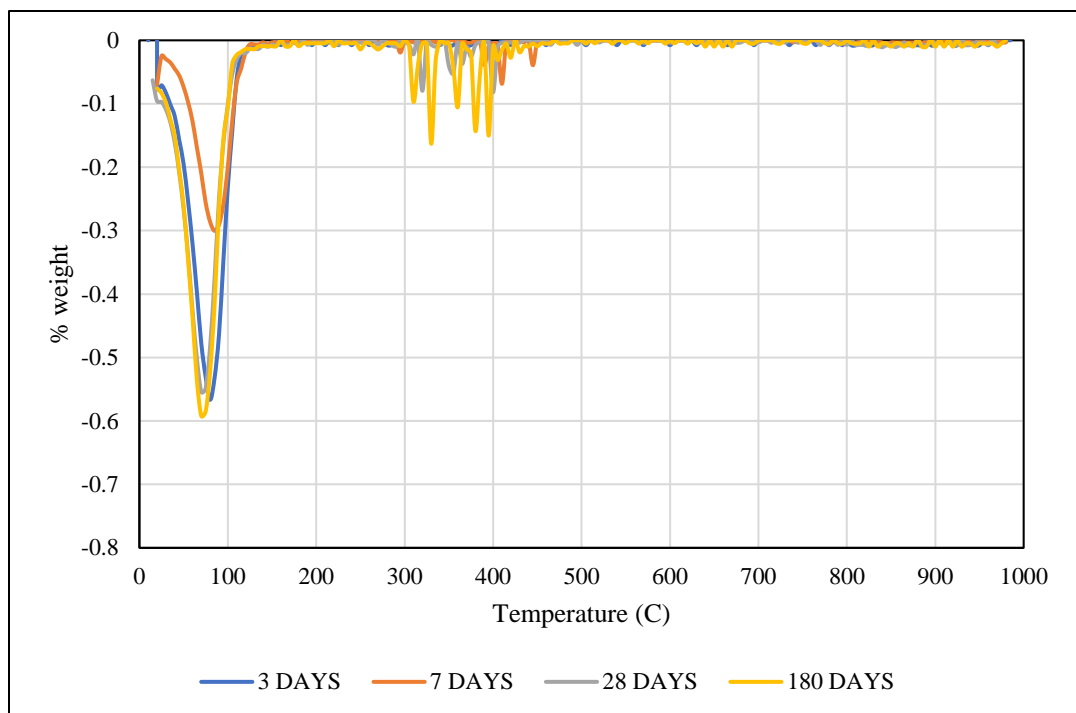
Figure A21: DTG curves for paste P20FA with time
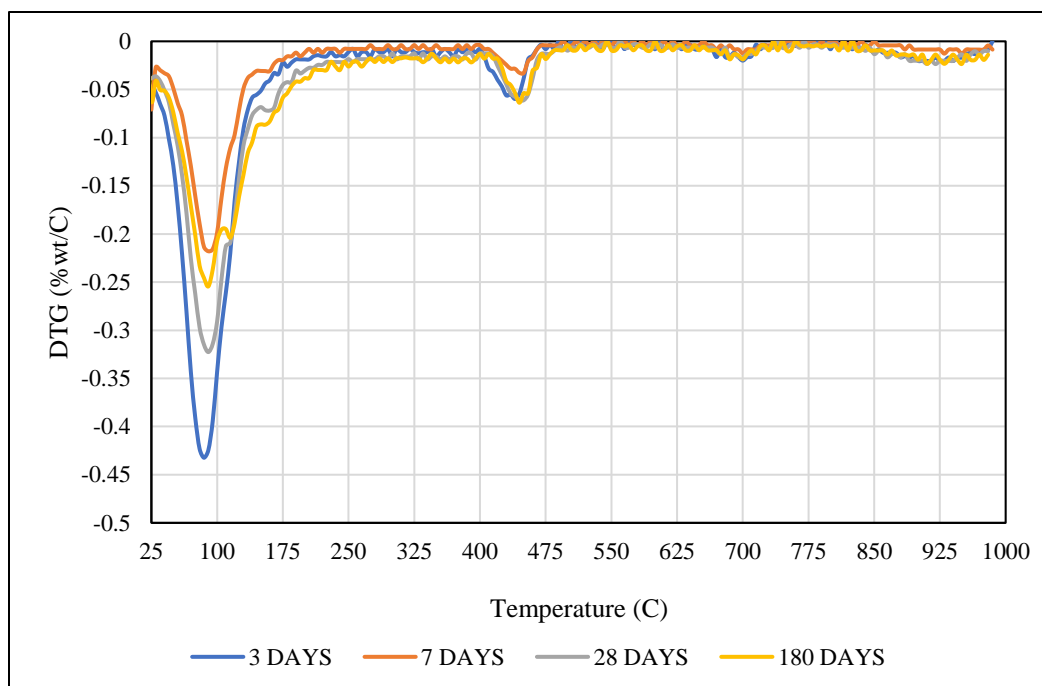
Figure A22: DTG curves for paste P40FA with time
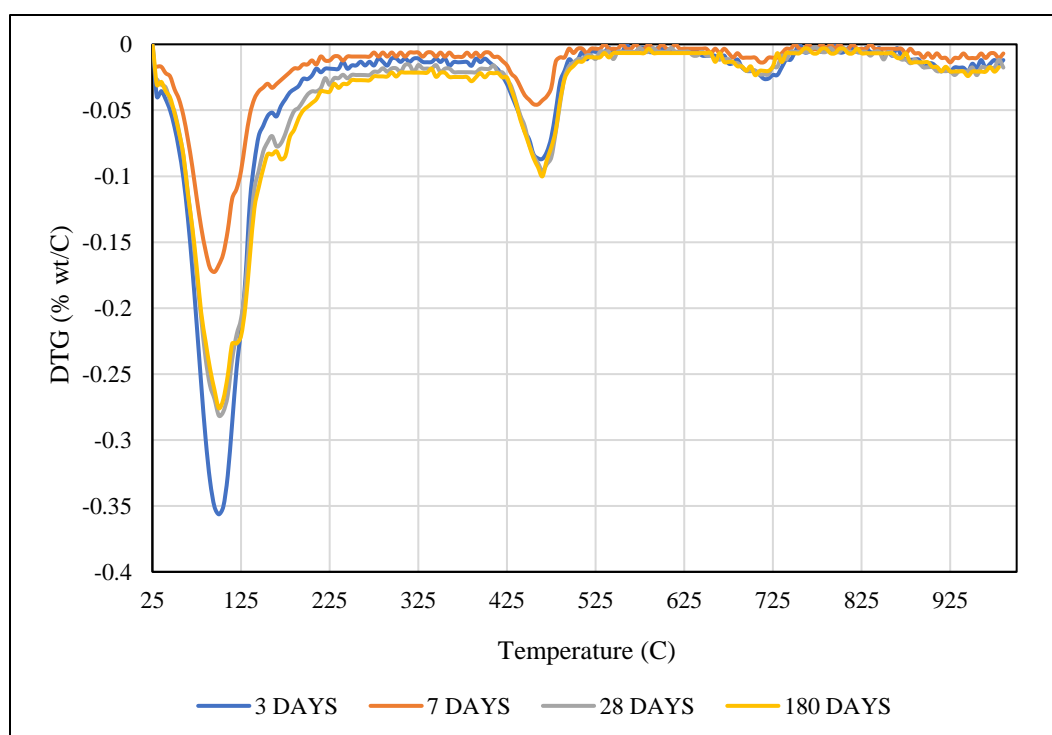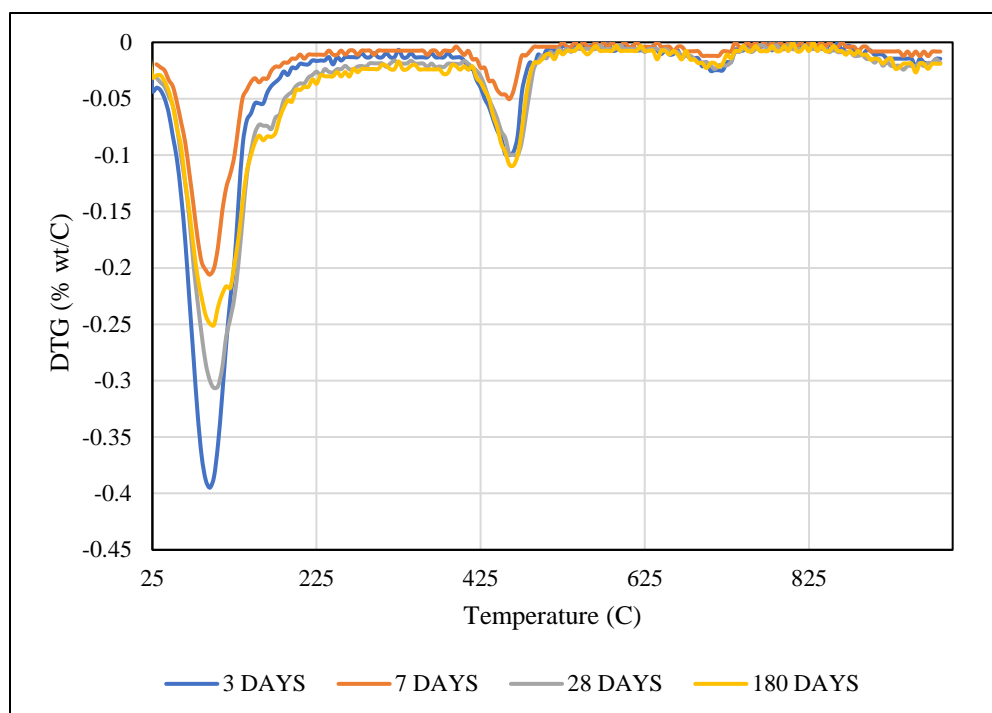
Figure A23: DTG curves for paste P95FA with time
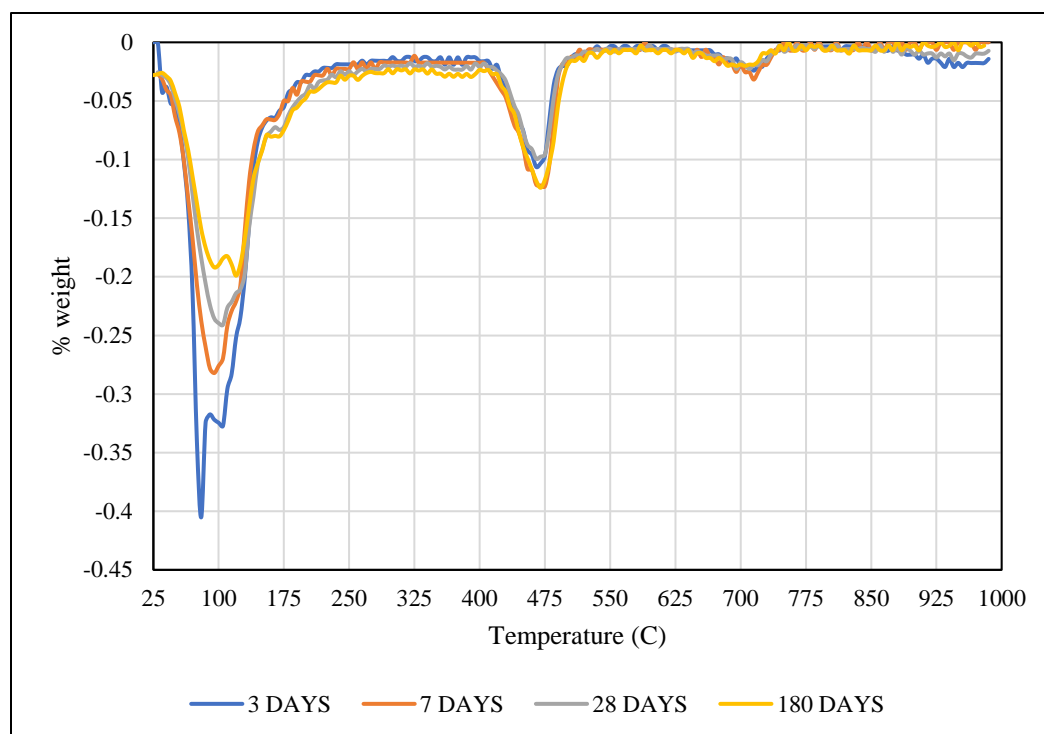
Figure A24: DTG curves for paste P-QL with time
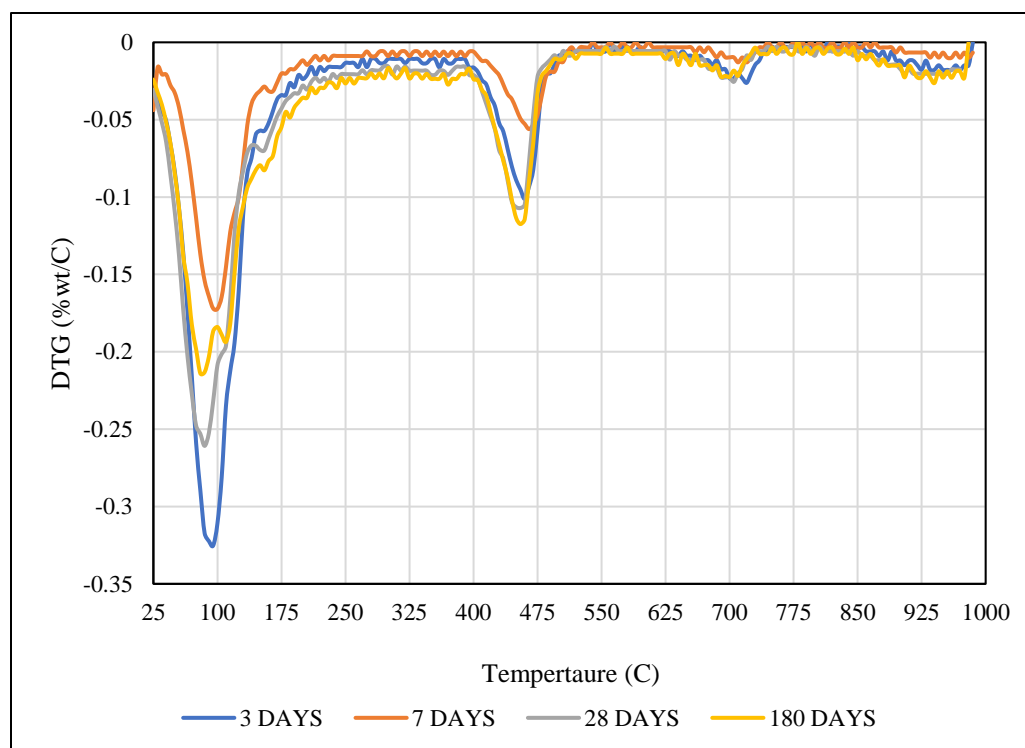
Figure A25 DTG curves for paste P20FA-QL with time
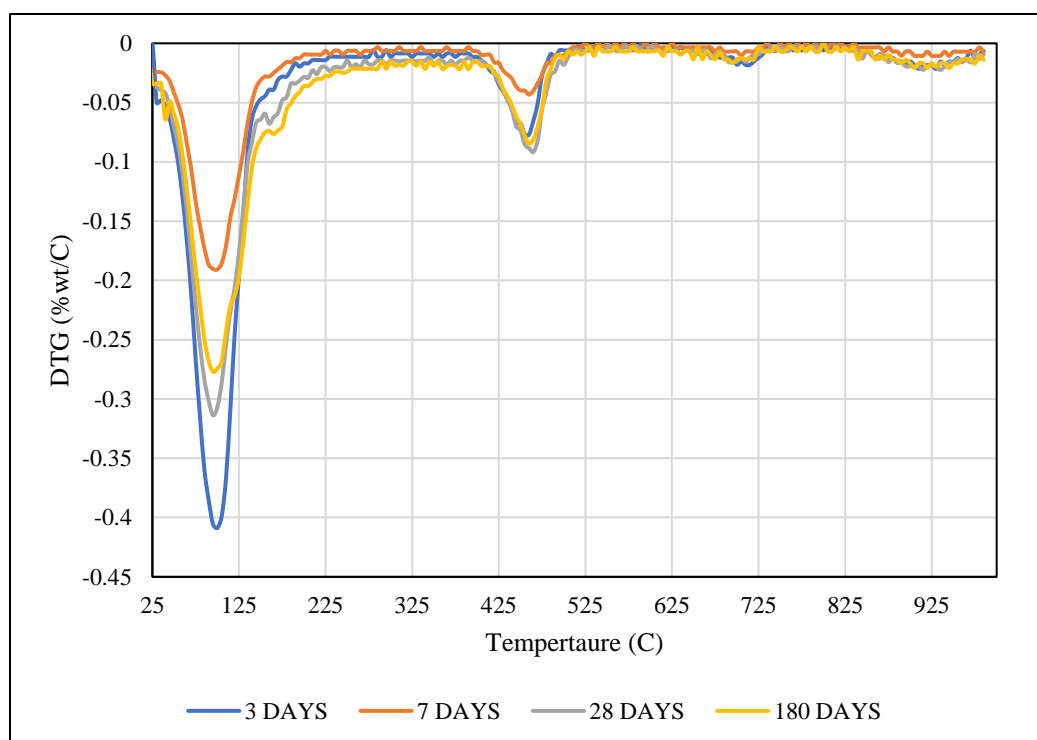
Figure A26: DTG curves for paste P40FA-QL with time
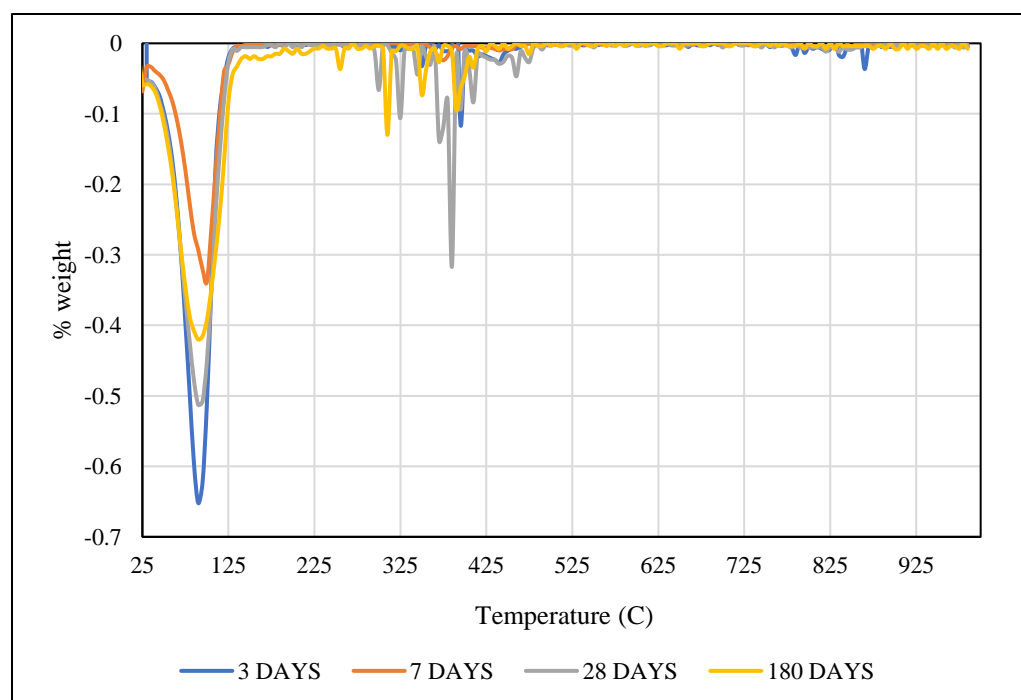
Figure A27: DTG curves for paste P95FA-QL with time
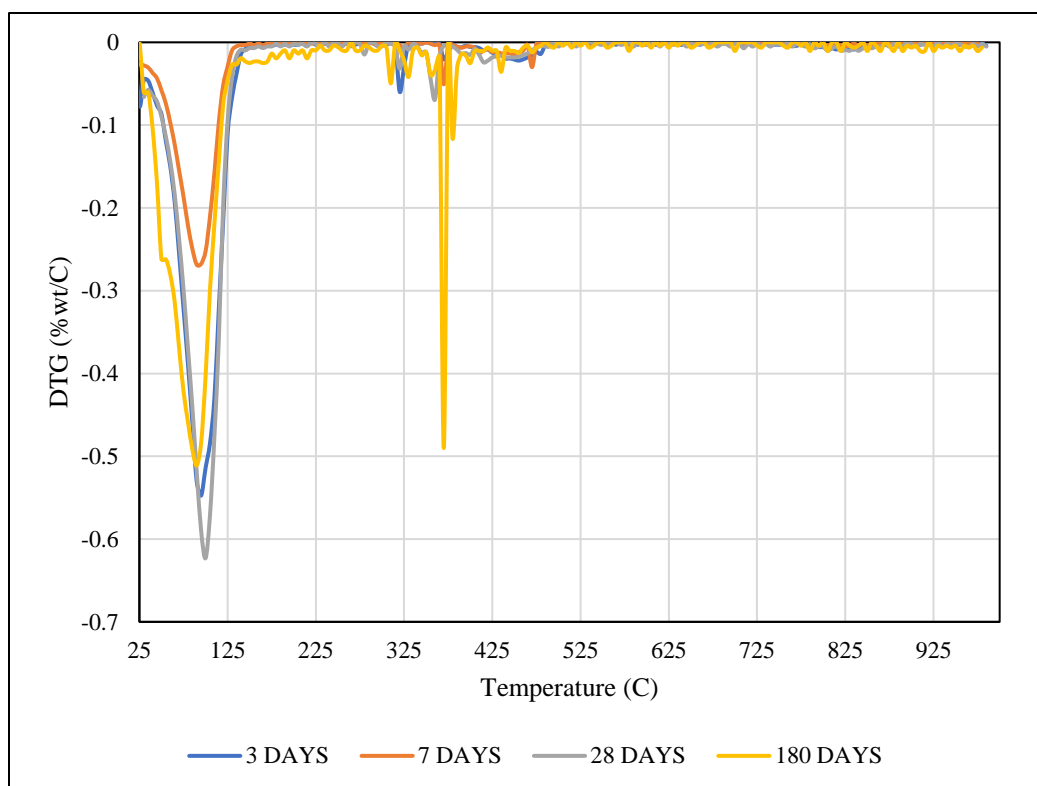
Figure A29: DTG curves for paste P20FA-QL-EM with time

Figure A30: DTG curves for paste P95FA-QL-EM with time

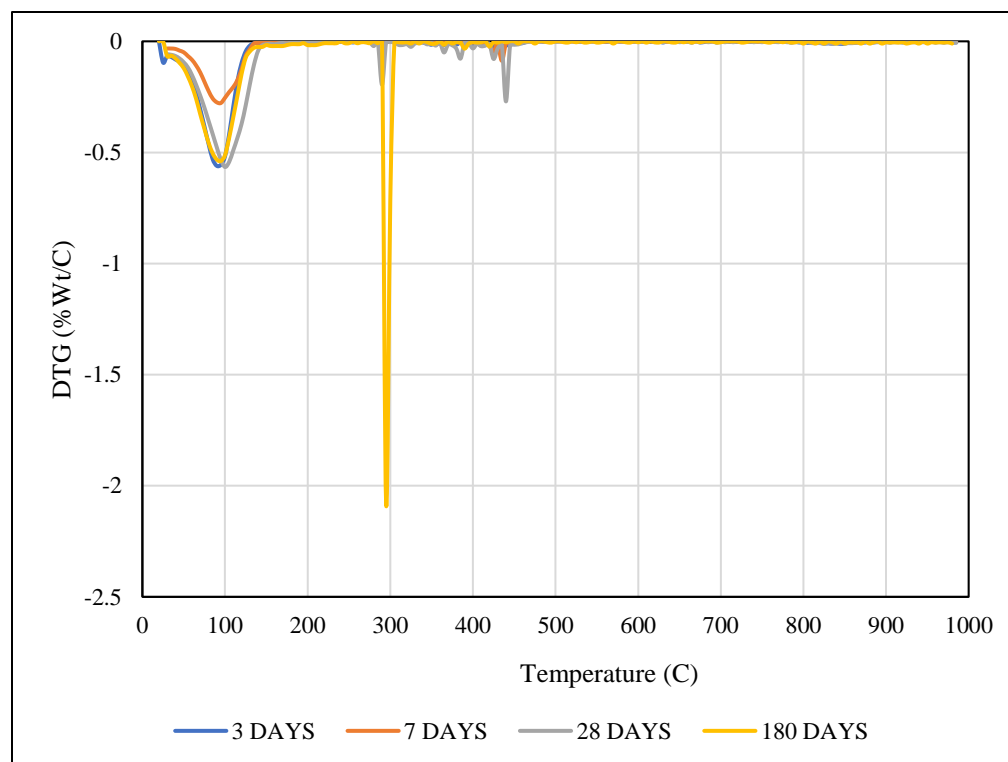Figure A31: DTG curves for paste P20FA-QL-EM-SL with time

Figure A32: DTG curves for paste P95FA-QL-EM-SL with

Mass Balance Analysis of Blended Paste

The weight for all freshly prepared cement-fly ash-quicklime blended paste casted in 50 x 100 mm cylinders was recorded prior to curing. This was done to properly characterize the sealed curing technique used in this study and also to see how much of the actual mix water was available for hydration reactions. For each blended paste mix, the weight of ten 50 x 100 mm cylinders were measured at curing intervals of 3, 7, 28 and 180 days and compared to their initial weights prior to curing. For mixes containing fly ash replacement of 40% and 95%, bleeding water was noticed above paste especially after 3, 7 and 28 days. (Figure A.1). This can be attributed the dilution effect of fly ash blends due its pozzolanic nature as confirmed by Sakai et al. (2005). Figure A.2 and Figure A.3 shows the percentage change in weight paste as a function of time for cement/fly ash and cement-fly ash-quicklime pastes respectively.

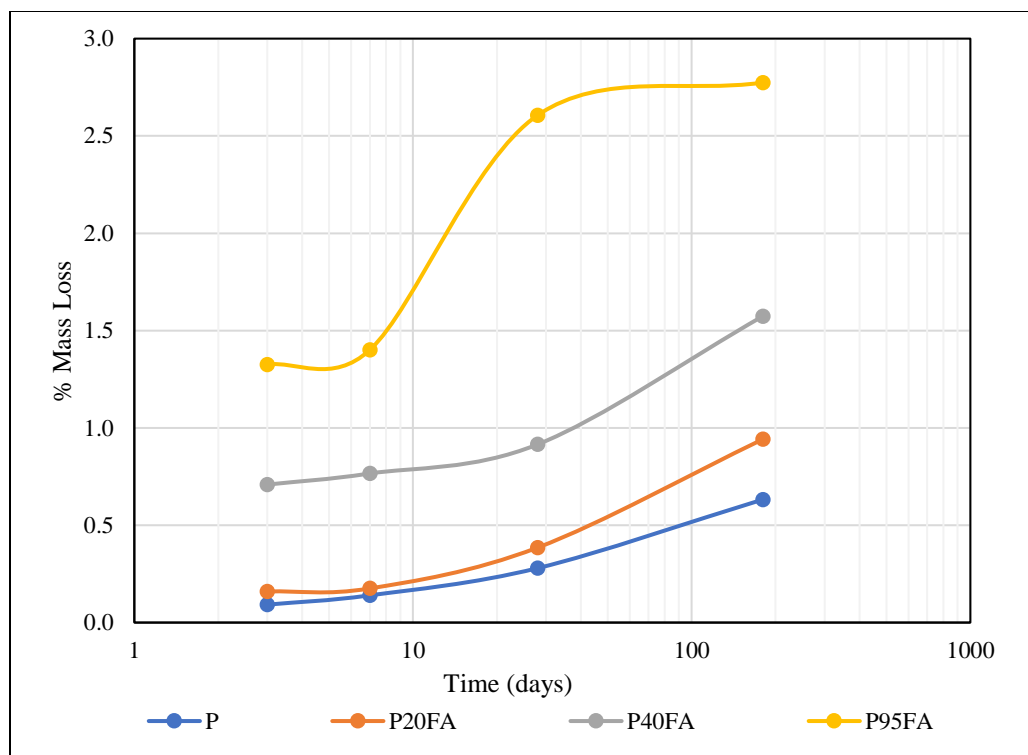Figure A33: P95FA with bleeding water at 28 days.

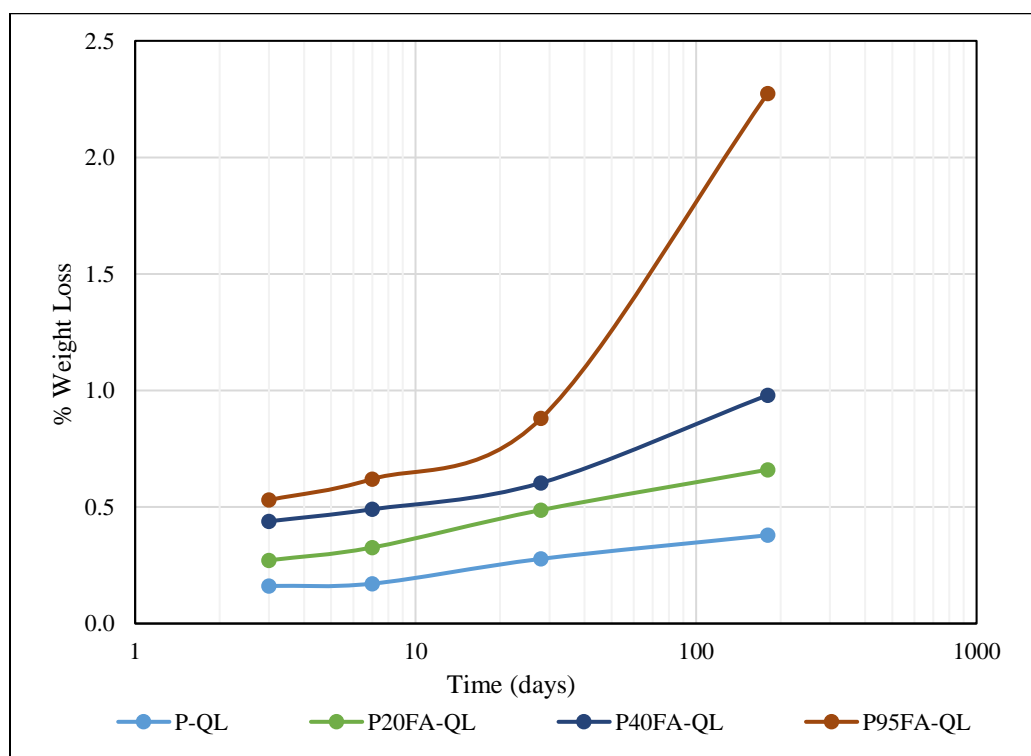Figure A34: Percentage weight loss vs time for cement-fly ash blended paste

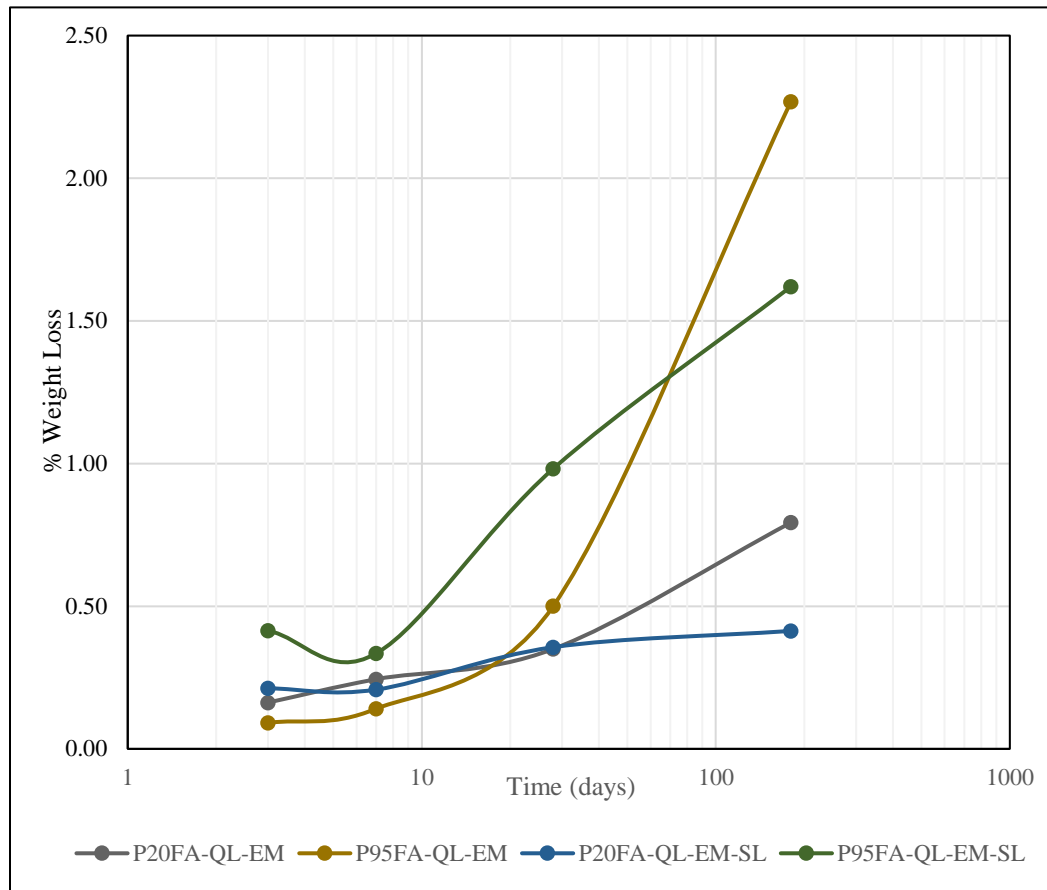Figure A35: Percentage weight loss vs time for cement-fly ash-quicklime blended paste

Figure A36: Percentage weight loss vs time for cement-fly ash-quicklime blended paste with additional water

For ideal system, it is expected that weight of the paste matrix would remain relatively constant with time under sealed curing conditions as autogenous shrinkage associated with hydration reactions only causes a change in volume. Autogenous shrinkage is due to the volume of the hydrates being less than the initial volume of individual reactants within the paste matrix. However, this was not the case, as weight loss with time was noticed for blended paste especially for blended paste with increasing fly ash replacement. This increased weight loss for the blended paste mixes could possibly be due to evaporation of the bleeding water, as the relative humidity of the room was not controlled.